Stabilizer circuit verification

Vadym Kliuchnikov, Michael Beverland, Adam Paetznick September 19, 2023

Abstract

The ubiquity of stabilizer circuits in the design and operation of quantum computers makes techniques to verify their correctness essential. The simulation of stabilizer circuits, which aims to replicate their behavior using a classical computer, is known to be efficient and provides a means of testing correctness. However, simulation is limited in its ability to examine the exponentially large space of possible measurement outcomes. We propose a comprehensive set of efficient classical algorithms to fully characterize and exhaustively verify stabilizer circuits with Pauli unitaries conditioned on parities of measurements. We introduce, as a practical characterization, a general form for such circuits and provide an algorithm to find a general form of any stabilizer circuit. We then provide an algorithm for checking the equivalence of stabilizer circuits. When circuits are not equivalent our algorithm suggests modifications for reconciliation. Next, we provide an algorithm that characterizes the logical action of a (physical) stabilizer circuit on an encoded input. All of our algorithms provide relations of measurement outcomes among corresponding circuit representations. Finally, we provide an analytic description of the logical action induced by measuring a stabilizer group, with application in correctness proofs of code-deformation protocols including lattice surgery and code switching.

Contents

1	Motivation and main results	3					
3	Mathematical preliminaries 2.1 Pauli and Clifford unitaries, stabilizer codes and Bell states 2.2 Stabilizer circuits, quantum instruments and Choi states 2.3 Encoding circuits, unencoding circuits and logical action 2.4 Bipartite normal form of a stabilizer state 2.5 Linear algebra notation Algorithmic preliminaries	6 7 9 11 12					
	3.1 Stabilizer circuit parameters	13 13 13 16 18					
4	General form for stabilizer circuits	21					
5	Outcome-complete stabilizer circuit simulation 5.1 Solution with outcome-specific algorithm as a subroutine	27 28 29 31					
6	Computing a general form of a stabilizer circuit 6.1 Bipartite normal form of a family of stabilizer states	33 35 38					
7	Stabilizer circuit verification 7.1 Relating (un)encoding circuits	41 42 44					
8	Logical action of stabilizer circuits 8.1 General form circuit for logical action 8.2 Logical action verification	50 50 54					
9	Logical action of code deformation circuits (analytic) 9.1 Example: lattice surgery for repetition codes	57 59 62 63					
A	Additional mathematical material	7 2					
В	Additional algorithmic material						
\mathbf{C}	Bulk deallocation of qubits in stabilizer simulation algorithms						
D	Pauli propagation	87					
\mathbf{E}	Common symplectic basis of two stabilizer groups	87					
\mathbf{F}	Equations for common symplectic basis example	89					

1 Motivation and main results

It is widely appreciated that future generations of large-scale quantum computers will require Quantum Error Correction (QEC) techniques to correct hardware faults. However it is less well appreciated that techniques to identify and correct **software** faults will also be necessary. At scale, quantum computers will be extremely complex systems. They will require testing and debugging of high-level quantum algorithms, intermediate-level instruction sets, and low-level physical circuits. Moreover, at each level, exploration of new approaches and optimization of existing approaches is ongoing. Classically tractable techniques to test quantum circuits are needed now to enable this design and research process. While several methods have been proposed to verify universal quantum circuits [49, 16, 47, 40, 48, 45, 5, 33, 17, 46, 43], this problem is QMA complete [36] and so these approaches are expected to break down for large circuits. We seek efficient verification methods for important but non-universal quantum circuits.

One extensively studied approach for testing and debugging quantum circuits involves quantum simulation, i.e., replicating the behavior of a quantum circuit by using a classical computer. Simulation of general quantum circuits is widely believed to be intractable. Fortunately, efficient simulation is possible for an important subclass known as stabilizer circuits [27, 1]. Testing via simulation is simple: simulate a stabilizer circuit and check if the observed outcomes match expectations. This method of testing has a substantial drawback; measurement outcomes of a quantum circuit are non-deterministic. Moreover, gates in a circuit may depend on those outcomes so that the gate sequence itself is non-deterministic, requiring an exponential number of simulations to prove that results hold for all pathways through a circuit.

For limited classes of stabilizer circuits, such as sequences of Clifford unitaries and deterministic measurements, random outcomes do not appear and a single simulation captures the full behavior. Increasingly, however, stabilizer circuits proposed for large-scale quantum computers rely on interpreting random outcomes. Leading approaches for operations on encoded qubits prescribe an intermediate-level instruction set entirely based on measurements with random outcomes [34, 12, 35, 21, 39]. New high-performing codes are defined by low-level sequences of measurements that also have random outcomes, even in the absence of errors [31, 30, 19, 2, 24, 25, 41]. Some types of physical qubits such as those based on photons [14] or Majorana wires [15] rely on measurements rather than unitaries as entangling operations.

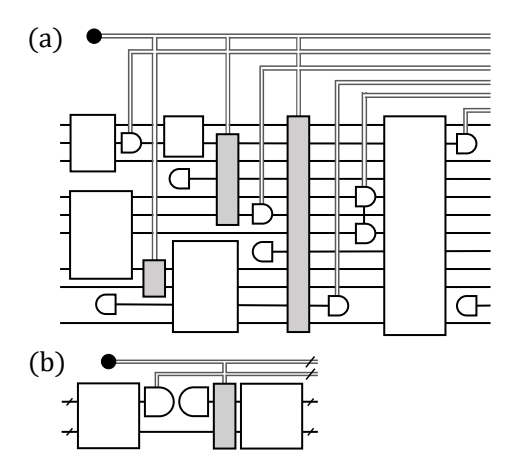


Figure 1.1: (a) Stabilizer circuits in this work are built from: allocations and deallocations of zero-state qubits (starting and ending wires next to G- and G-like symbols), allocations of random bit outcomes (black circle), Clifford unitaries (white rectangles), non-destructive Pauli measurements (G-like symbol with continued wire), Pauli unitaries conditioned on parities of earlier measurement and random bit outcomes (gray rectangles).

(b) General form circuit. For any stabilizer circuit, there is a general form circuit (as depicted) that matches the action on any input state for every possible path through the circuit. This forms the basis of our algorithms.

In this work we introduce classical tests of stabilizer circuits for all input states and outcome bit strings. We choose the definition of stabilizer circuits in Fig. 1.1(a) for complexity-theoretic reasons as discussed later in this section. In Section 4 we prove one of our central results: a general form circuit illustrated in Fig. 1.1(b) captures the action of any stabilizer circuit. We leverage this to build the algorithms in Fig. 1.2 to efficiently solve the following problems.

1. What is the action of a stabilizer circuit?

We would like to have a compact description for any stabilizer circuit that characterizes its action on the input qubits given any circuit outcome. This is directly achieved by our general form algorithm (Fig. 1.2) which provides an equivalent general form circuit, which for any outcome of the original circuit has the same action on every input state for a corresponding outcome of the general form circuit. We find the general form much easier interpret and compose than the typical characterization of quantum channels in terms of Choi states.

2. Do two stabilizer circuits have the same action?

To verify that a circuit achieves a desired goal requires more still - we need to compare against a reference circuit. Given two stabilizer circuits, and a *specific* outcome bitstring for each, verifying that circuits have the same action be accomplished using existing methods. One option is to perform stabilizer simulation of Choi circuits and then compare the output stabilizer states [22]. A second option is to write ZX diagrams for the Choi circuits and reduce them to a simplified pair of rGS-LC diagrams [9].

However, the action of both the circuit and the reference will depend on their respective outcomes. We would like to know if two circuits are have the same action for **all** outcomes, and if they do, which outcomes of the two circuits correspond to the same action. By comparing general forms, our verification algorithm (Fig. 1.2) achieves this while existing methods do not.

3. What is the action of a logical operation circuit on the encoded qubits?

Often a circuit is constructed in order to implement some logical operation on encoded information which can be used to protect against the effects of noise. To characterize such a circuit we need to identify its **logical action**. We propose doing so with our logical action algorithm (Fig. 1.2) to find a general form circuit equivalent to the action on the encoded information.

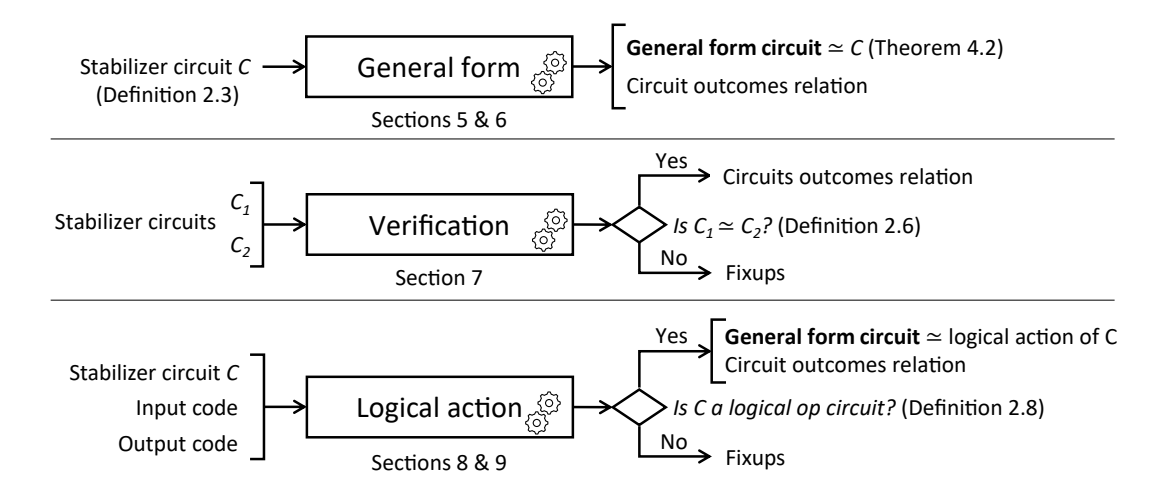


Figure 1.2: Algorithms to test stabilizer circuits for all input states and outcome bit strings.

Let us briefly sketch how the algorithms in Fig. 1.2, which solve these three problems, work. The general form algorithm (Section 6) combines two key ingredients: an enhanced stabilizer simulation of Choi states, and a generalization of a bipartite norm form for stabilizer states [7]. General form circuits are then used as the basis of the verification and logical action algorithms. Our verification algorithm (Section 7) maps both input circuits to general forms, and checks if those general forms are equivalent. The general form is not unique; the bulk of the algorithm involves checking the equivalence of the general form circuits and computing the relation between circuit outcomes. The logical action algorithm (Section 8) first forms a

composite by sandwiching the input circuit with encoding and unencoding circuits of the input and output codes, respectively. It then obtains a general form for the composite circuit, which characterizes the logical action. Validating that the circuit is indeed a logical operation uses the relation between outcomes of the composite circuit and its general form.

As noted above, a key ingredient of our work is an enhanced version of stabilizer simulation. The stabilizer simulation problem solved in the existing literature is, roughly, to find the probability of a specific subset of outcome bitstrings of a circuit and to provide an efficient description of the output state [1, 23, 6, 28, 10]. We formalize this problem in Section 3.5 as outcome-specific stabilizer simulation. By considering the Choi states of a stabilizer circuit, outcome-specific simulation can be used to efficiently characterize the circuit action over all possible input states.

Dealing with all possible measurement outcomes requires more care. Pauli operations controlled on random bits along with the probabilistic outcomes of quantum measurements cause each circuit simulation to take a different pathway. Accordingly, we introduce the **outcome-complete** stabilizer simulation problem, and show that it can be efficiently reduced to the outcome-specific stabilizer simulation. In Section 5, we show that outcome-complete stabilizer simulation can be performed by using any outcome-specific stabilizer simulation as a subroutine which is called many times. We also find a new algorithm to solve the outcome-complete case which is more efficient than using outome-specific subroutines.

Our outcome-complete simulation algorithm and the three algorithms in Fig. 1.2 are computationally efficient in that their run times scale polynomially with the parameters of the input circuits. Throughout this paper we present detailed fine-grained analyses of the run time of each algorithm. Here it is convenient to consider families of circuits with growing maximum width n and depth D, and where all stabilizer operations appear with constant non-zero density. Then, the run time of the aforementioned algorithms for outcome-complete stabilizer simulation, general form, verification and logical action, are all $O(n^3D^2)$. For context, previously known outcome-specific simulations have complexity $O(n^3D)$ and using them for outcome-complete simulation results in an $O(n^4D^2)$ run time.

In some important special cases, the general form can be used to **analytically** characterize the logical action. In Section 9 we consider the logical action of circuits which measure the generators of a stabilizer code when the initial state is encoded in a different stabilizer code (code deformation). We find a general form and outcome relation for the logical action, expressed in terms of a common symplectic basis of the two stabilizer groups. This basis may be of independent interest. We illustrate our analytic results with an example of logical XX measurement on two copies of the repetition code via lattice surgery.

Lastly, our techniques require a restriction on the classical conditions of stabilizer circuits: we only allow Pauli unitaries conditioned on previous outcome parities (Fig. 1.1(a)). This restriction is motivated by the computational complexity of simulation; efficient simulation is necessary for efficient characterization. As a consequence of the Gottesman-Knill theorem [27], a broader class of stabilizer circuits than we consider, that also includes Clifford gates conditioned on previous outcomes, can be sampled efficiently. Characterization requires a notion of simulation stronger than sampling, one that can determine the probability distribution of circuit outcomes. Somewhat surprisingly, this stronger simulation of stabilizer circuits is #P-hard [38]. Pauli gates conditioned on the AND of previous outcomes can encode arbitrary Boolean function evaluation. Limiting to Pauli gates conditioned on parities admits a reformulated Gottesman-Knill theorem that can be leveraged into an efficient algorithm for characterization.

Despite the restriction to partity conditions, circuits from this set describe important components of high-level quantum algorithms, such as QROM lookups [8]. They also include intermediate-level implementations that, for example, transform algorithms according to architectural constraints [12]. Of course, such circuits also describe the vast majority of logical operations in existing QEC schemes. We propose that future design of quantum circuits should adhere to this restriction, where possible, in order to permit characterization and verification.

2 Mathematical preliminaries

Here we review some relevant mathematical concepts and specify notation.

2.1 Pauli and Clifford unitaries, stabilizer codes and Bell states

The **Pauli unitaries** on n qubits are $i^k\{I, X, Y, Z\}^{\otimes n}$ for k = 0, 1, 2, 3, where I, X, Y, Z are the single-qubit Pauli matrices. We call any group of Pauli operators **a Pauli group**, while the set of all Pauli unitaries on n qubits forms a group known as **the Pauli group** \mathcal{P}_n . We also find it useful to label the subset of Hermitian Pauli unitaries $\pm \{I, X, Y, Z\}^{\otimes n}$, which we call the **Pauli observables**.

A stabilizer group is a group of commuting Pauli observables not containing -I. We say a state is stabilized by a set of Pauli observables if it is a +1 eigenstate of all elements of the set. A stabilizer code is a sub-space of a Hilbert space consisting of all vectors which are stabilized by a stabilizer group S. A stabilizer state is a state on n qubits which is stabilized by a set of n independent Pauli observables.

For any two Pauli unitaries, we write that $[\![P,Q]\!]=0\in\mathbb{F}_2$ if P,Q commute and $[\![P,Q]\!]=1\in\mathbb{F}_2$ otherwise:

$$PQ = (-1)^{[\![P,Q]\!]}QP = (-1)^{[\![Q,P]\!]}QP.$$

We will find use for the following identity,

$$e^{i\frac{\pi}{4}P}Qe^{-i\frac{\pi}{4}P} = (iP)^{[\![P,Q]\!]}Q.$$
 (1)

For any subgroup G of the n-qubit Pauli group \mathcal{P}_n , we define G^{\perp} as

$$G^{\perp} = \{ P \in \mathcal{P}_n : [\![P, g]\!] = 0, \forall g \in G \}.$$

Note that G^{\perp} is a group because $\llbracket PQ,R \rrbracket = \llbracket R,PQ \rrbracket = \llbracket P,R \rrbracket + \llbracket Q,R \rrbracket$.

An *n*-qubit Clifford unitary is any *n*-qubit unitary C such that $\forall P \in \mathcal{P}_n : CPC^{\dagger} \in \mathcal{P}_n$. We refer to CPC^{\dagger} as the **image** of P under C and $C^{\dagger}PC$ as the **preimage** of P under C.

For computational basis states we define

$$(|a_1\rangle \otimes \ldots \otimes |a_{i-1}\rangle \otimes |a_{i+1}\rangle \otimes \ldots \otimes |a_n\rangle) \otimes_i |b\rangle = |a_1\rangle \otimes \ldots \otimes |a_{i-1}\rangle \otimes |b\rangle \otimes |a_{i+1}\rangle \ldots \otimes |a_n\rangle.$$

We then extend \otimes_j to a linear map from $\mathbb{C}^{2^{n-1}} \times \mathbb{C}^2$ into \mathbb{C}^{2^n} by linearity. Similarly we define \otimes_j from n-1 and 1 qubit linear operators into n qubit linear operators as

$$(A \otimes_j B)(|\phi\rangle \otimes_j |\psi\rangle) = (A|\phi\rangle) \otimes_j (B|\psi\rangle).$$

We define the **controlled-Pauli operator** for any commuting Pauli observables P_1, P_2 as:

$$\Lambda(P_1, P_2) = \frac{I + P_1}{2} + \frac{I - P_1}{2} \cdot P_2. \tag{2}$$

The requirement that $[\![P,Q]\!]=0$ ensures that the matrix defined by the equation above is unitary and Hermitian. We will make use of the following relations:

$$\left(\Lambda(P_1, P_2)\right)^{\dagger} = \Lambda(P_1, P_2),\tag{3}$$

$$\Lambda(P_1, P_2) = \Lambda(P_2, P_1),\tag{4}$$

$$\Lambda(P_1, P_2)|\psi\rangle = |\psi\rangle \text{ if } P_1|\psi\rangle = |\psi\rangle \text{ or } P_2|\psi\rangle = |\psi\rangle, \tag{5}$$

$$\Lambda(P_1, P_2) \ Q \ \Lambda(P_1, P_2) = P_1^{[\![P_2, Q]\!]} \ Q \ P_2^{[\![P_1, Q]\!]}, \tag{6}$$

where any operator P raised to the power zero is interpreted as the identity.

We say that a stabilizer code on n qubits and with k logical qubits is specified by an n qubit Clifford unitary C, if images $CZ_1C^{\dagger}, \ldots, CZ_{n-k}C^{\dagger}$ are generators of the code's stabilizer group,

 $CZ_{n-k+1}C^{\dagger}, \ldots, CZ_nC^{\dagger}$ are representatives of logical Z operators for logical qubits $1, \ldots, k$ and $CX_{n-k+1}C^{\dagger}, \ldots, CX_nC^{\dagger}$ are representatives of logical X operators for logical qubits $1, \ldots, k$. We call such C an **encoding unitary** of the stabilizer code. Note that C is not unique; images $CX_1C^{\dagger}, \ldots, CX_{n-k}C^{\dagger}$ are arbitrary. We say that such code is $[\![\mathbf{n}, \mathbf{k}, \mathbf{C}]\!]$ **code**. Code $[\![\mathbf{n}, \mathbf{k}, C]\!]$ is a subspace of code $[\![\mathbf{n}, \mathbf{k}', C']\!]$ if stabilizer group of $[\![\mathbf{n}, \mathbf{k}', C']\!]$ is a subgroup of $[\![\mathbf{n}, \mathbf{k}, C]\!]$. We say that a state is **encoded in** $[\![\mathbf{n}, \mathbf{k}, C]\!]$ **with syndrome** s if the state is stabilized by $(-1)^{s_1}CZ_1C^{\dagger}, \ldots, (-1)^{s_{n-k}}CZ_{n-k}C^{\dagger}$. Syndrome s is given by n-k dimensional binary vector.

A symplectic basis of a Pauli group is a choice of generators that mimics the commutation relations of pairwise X and Z operators. Such a basis is useful for selecting X and Z images of a Clifford unitary.

Definition 2.1 (Symplectic basis). A sequence of 2m Pauli operators form a symplectic basis if they have the same commutation relations as $X_1, Z_1, \ldots, X_m, Z_m$.

The 2n-qubit **Bell state** is defined as

$$|\mathrm{Bell}_n\rangle = \frac{1}{\sqrt{2}^n} \sum_{k \in \{0,1\}^n} |k\rangle \otimes |k\rangle.$$
 (7)

The two-qubit Bell state $|\text{Bell}_1\rangle$ is stabilized by $X \otimes X, -Y \otimes Y, Z \otimes Z$ Using the notation $Y^* = -Y$ for element-wise complex conjugation of a matrix, the stabilizers of $|\text{Bell}_n\rangle$ are $P^* \otimes P^* = P \otimes P^*$ for all Pauli matrices $P \in \{I, X, Y, Z\}^{\otimes n}$. This stabilizer group is generated by $Z_j \otimes Z_{n+j}$ and $X_j \otimes X_{n+j}$ for j = 1, ..., n. Recall also that for any n-qubit unitary we have $(U \otimes I_n)|\text{Bell}_n\rangle = (I_n \otimes U^T)|\text{Bell}_n\rangle$, where U^T is the transpose of U.

We use n(U) to denote the number of qubits n for which a unitary U is defined, supp(U) to denote the set of qubits on which U acts non-trivially, and |U| to denote the size of supp(U).

It can be useful to build a Clifford unitary from a Pauli measurement as follows.

Proposition 2.2 (Measurement as unitary). Let $|\psi\rangle$ be a state stabilized by a Pauli observable $(-1)^bQ$ for $b \in \{0,1\}$, and let P be a Pauli observable that anti-commutes with Q. The probability of outcome zero of measuring P is 1/2. For measurement outcome r, the resulting state is $Q^{r+b}e^{i\frac{\pi}{4}(iQP)}|\psi\rangle$.

Proof. The probability of outcome zero is equal to the probability of outcome one because:

$$\langle \psi | \frac{I+P}{2} | \psi \rangle = \langle \psi | (-1)^b Q \frac{I+P}{2} (-1)^b Q | \psi \rangle = \langle \psi | \frac{I-P}{2} | \psi \rangle.$$

For outcome r, the state is equal to $(I+(-1)^rP)/\sqrt{2}|\psi\rangle$ and proportional to

$$Q^{r+b}e^{i\frac{\pi}{4}(iQP)}|\psi\rangle = \frac{Q^{r+b}}{\sqrt{2}}|\psi\rangle - \frac{Q^{r+b}QP}{\sqrt{2}}|\psi\rangle = \frac{(-1)^{b(r+b)}}{\sqrt{2}}|\psi\rangle + \frac{(-1)^{b+r+b(r+b+1)}P}{\sqrt{2}}|\psi\rangle,$$

where we used that $Q^{r+b}|\psi\rangle = (-1)^{b(r+b)}|\psi\rangle$ and $Q^{r+b}P = (-1)^{r+b}PQ^{r+b}$.

We include additional useful mathematical material in Appendix A.

2.2 Stabilizer circuits, quantum instruments and Choi states

Here we introduce several definitions that help to classify quantum circuits and identify sets of circuits which can be considered equivalent. We are particularly interested in a particular subclass of circuits which we define as follows.

Definition 2.3 (Stabilizer circuit). A **stabilizer circuit** is any sequence of the following elementary operations, that we call **stabilizer operations**,

• allocations of qubits initialized to zero states,

- allocation of classical random bits distributed as fair coins,
- Clifford and Pauli unitaries,
- non-destructive Pauli measurements,
- deallocation of qubits in zero states,
- Pauli unitaries conditioned on the parity of sets of measurement outcomes and classical random bits from earlier in the sequence.

Any stabilizer circuit starts with qubits in an arbitrary state that we call **input qubits**. Qubits that remain after executing the circuit are **output qubits**. We call the sequence of all measurement outcomes and classical random bits allocated by the circuit the **circuit outcome vector**.

Note that destructive Pauli measurements, while not explicitly in this list, can be formed by following a single-qubit non-destructive Pauli Z measurement with a conditional Pauli unitary and a de-allocation of that qubit.

It is classically efficient to calculate the state output by a stabilizer circuit for a particular input stabilizer state and a given circuit outcome vector [27, 1]. Note that due to the inclusion of destructive qubit measurements and qubit allocations, a stabilizer circuit can have a different number of input and output qubits. We find it convenient to explicitly include the allocation of classical bits in our definition, although the same effect could be created by allocating a qubit to the zero state and then immediately measuring it in the X basis.

We classify circuit outcomes into different types. We call an outcome **input dependent**, if the probability it is zero (conditioned on any previous outcomes) depends on the circuit input. We distinguish two classes of outcomes which are not input dependent: **random** and **redundant**. We call an outcome redundant if the probability that it is zero is either zero or one (conditioned on any sequence of previous outcomes), and we call the outcome random otherwise.

The **action** of any stabilizer circuit (and indeed a much broader class of quantum channels) can be faithfully captured by a **quantum instrument** [44, 18], defined as follows.

Definition 2.4 (Quantum instrument). A quantum instrument consists of a set R and an associated set of completely positive non-zero maps $\{Q_r : r \in R\}$ where $\sum_{r \in R} Q_r$ is a trace preserving map. The quantum instrument maps a density matrix ρ to a joint quantum-classical state $\{r, \rho_r\}$, where $p_r = \text{Tr}(Q_r[\rho])$ is the probability of observing the outcome r and $\rho_r = Q_r[\rho]/p_r$ is the output state conditioned on observing that outcome.

The action of a stabilizer circuit is formally identified by assigning a label r to each of the possible sets of outcomes (measurements and random classical bits) that can be observed when running the circuit, and specifying the map Q_r that is enacted on the input qubits when r is observed. In our context, the instrument is defined by a stabilizer circuit in which all outcomes are retained. For each r, the map therefore has the form $Q_r(\rho) = Q_r \rho Q_r^{\dagger}$ for linear operator Q_r . We refer to a quantum instrument defined by a stabilizer circuit as a **stabilizer instrument**. We also refer to Q_r as the linear map enacted by the instrument for outcome r.

We can classify sets of stabilizer circuits by identifying whether or not they have equal action. In certain cases it can be useful not just to identify if the actions of two stabilizer circuits are equal, but to consider a more general notion of equivalence. Informally, we consider two quantum instruments to be equivalent if their actions are equal up to a regrouping and relabeling of their outcomes. We make this more formal with the following two definitions.

Definition 2.5 (Outcome compression map). Consider an instrument consisting of a set of outcomes R and completely positive maps $\{Q_r : r \in R\}$. Define a new quantum instrument with a set of outcomes S and completely positive maps $\{Q'_s : s \in S\}$, where each element of s consists of a disjoint subset of elements of R, such that S forms a partition of R and $Q_r = \alpha_{r,r'}Q_{r'}$ if and only if r, r' in S, and Q'_s is then defined as $Q'_s = \sum_{r \in s} Q_r$. The map from R to S, that maps element r to s such that r is in s is called the **outcome compression map**. The map that takes instrument Q and outputs instrument Q' is called the **compression map**.

Definition 2.6 (Quantum instrument equivalence). Consider two quantum instruments, which after the application of the compression map have sets of outcomes R and R' and completely positive maps $\{Q_r : r \in R\}$, and $\{Q'_r : r \in R'\}$. We say that the instruments are **equivalent** if there is a bijection $f : R \to R'$ such that for all $r \in R$, $Q_r = Q'_{f(r)}$.

Note that if for two quantum instruments $\{Q_r : r \in R\}$, and $\{Q'_r : r \in R'\}$ there is bijection $f: R \to R'$ such that for all $r \in R$, $Q_r = Q'_{f(r)}$, then theses quantum instruments are equivalent. We also find it useful to define the Choi states.

Definition 2.7 (Choi states). Consider a quantum instrument with the set R and completely positive maps $\{Q_r : r \in R\}$, where $Q_r(\rho) = Q_r \rho Q_r^{\dagger}$ for some linear operator Q_r from $n_{\rm in}$ qubits into $n_{\rm out}$ qubits. Then, the Choi state given r is the $(n_{\rm out} + n_{\rm in})$ -qubit state

$$(Q_r \otimes I)|\mathrm{Bell}_{n_{\mathrm{in}}}\rangle = \frac{1}{\sqrt{2}^{n_{\mathrm{in}}}} \sum_{k \in \{0,1\}^{n_{\mathrm{in}}}} \underbrace{Q_r|k\rangle}_{n_{\mathrm{out}}} \otimes \underbrace{|k\rangle}_{n_{\mathrm{in}}}.$$

As noted above, the condition $Q_r(\rho) = Q_r \rho Q_r^{\dagger}$ is satisfied for any stabilizer instrument. Furthermore, each Choi state of a stabilizer instrument is a stabilizer state, allowing it to be efficiently represented (by providing a set of generators of it's stabilizer group).

Given a circuit \mathcal{C} for a quantum instrument, a Choi state can be prepared by initializing an appropriate number of Bell pairs and then applying \mathcal{C} to the first half of each pair, as illustrated in Fig. 2.1. We call this the **Choi circuit** Choi(\mathcal{C}) of \mathcal{C} . While the circuit \mathcal{C} has $n_{\rm in}$ input qubits and $n_{\rm out}$ output qubits, the corresponding Choi circuit has zero input qubits and $(n_{\rm out} + n_{\rm in})$ output qubits.

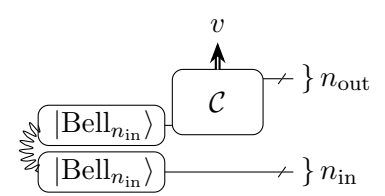


Figure 2.1: The Choi circuit Choi(C) of a circuit C with n_{in} input qubits, n_{out} output qubits and outcome vector v. We use the labels " n_{in} " and " n_{out} " to indicate multi-qubit registers of n_{in} , n_{out} qubits, and a double wire for a multi-bit classical register. The first operation in the circuit initializes qubits into a n_{in} -qubit Bell state (defined in Eq. (7)).

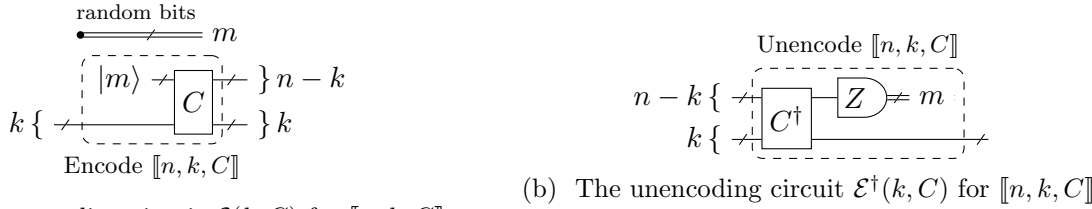
While the Choi state fully specifies the action of the circuit for the fixed outcome vector, it does not typically provide a very intuitive operational interpretation of the action. In Section 4 we describe a circuit-based representation of the action which provides a more natural interpretation. It will be fruitful to analyze Choi states as bipartite states with respect to bipartition of $(n_{\text{out}} + n_{\text{in}})$ qubits into first n_{out} and last n_{in} qubits. We discuss properties of stabilizer states related to such a bipartition in the next subsection.

2.3 Encoding circuits, unencoding circuits and logical action

We make frequent use of small explicit circuits that take an input state and encode into, or unencode out of a quantum error correcting code (see Fig. 2.2). For each, we provide an explicit encoding Clifford unitary C, which along with an integer k defines a stabilizer code that we call [n, k, C] as described in Section 2.1. Specifically, the stabilizer generators are CZ_iC^{\dagger} for $i \in [n-k]$, and $CZ_{n-k+j}C^{\dagger}$, $CX_{n-k+j}C^{\dagger}$ are the jth logical qubits' Z and X operators for $j \in [k]$.

When we write $\mathcal{E}(k,C)$ or "encode [n,k,C]", we mean the circuit in Fig. 2.2(a) and when we write $\mathcal{E}^{\dagger}(k,C)$ or "unencode [n,k,C]", we mean the circuit in Fig. 2.2(b). Note that the circuit $\mathcal{E}(k,C)$ encodes with respect to a bitstring m, which is typically generated as random bits. The

circuit encodes in the stabilizer code with generators $(-1)^{m_i}CZ_iC^{\dagger}$ for $i \in [n-k]$. Similarly, the circuit $\mathcal{E}^{\dagger}(k,C)$ unencodes any stabilizer code with generators given by $(-1)^{m_i}CZ_iC^{\dagger}$ for $i \in [n-k]$ for some $m_i = 0, 1$, and outputs the syndrome as the circuit's outcome vector m.



(a) The encoding circuit $\mathcal{E}(k,C)$ for [n,k,C]

Figure 2.2: A unitary C and integers n, k define encoding and unencoding circuits for [n, k, C]. In this and other circuit diagrams, measuring Z on an (n-k)-qubit register implies destructively measuring each qubit in the Z basis and recording the results as an (n-k)-bit vector m.

We can use encoding and unencoding circuits to formally define the concept of a logical operation circuit and its logical action as follows.

Definition 2.8 (Logical operation circuit). A stabilizer circuit C is a logical operation circuit with input code $[n_{in}, k_{in}, C_{in}]^1$ and output code $[n_{out}, k_{out}, C_{out}]$ if applying circuit C to any input state encoded in $[n_{in}, k_{in}, C_{in}]$ results in an output state encoded in $[n_{out}, k_{out}, C_{out}]$.

Definition 2.9 (Logical action). Given a logical operation circuit (*Definition 2.8*) C with input code $[n_{in}, k_{in}, C_{in}]$ and output code $[n_2, k_{out}, C_{out}]$ its **logical action** is the action of the circuit given in Fig. 2.3 when input code syndrome s_{in} is zero.

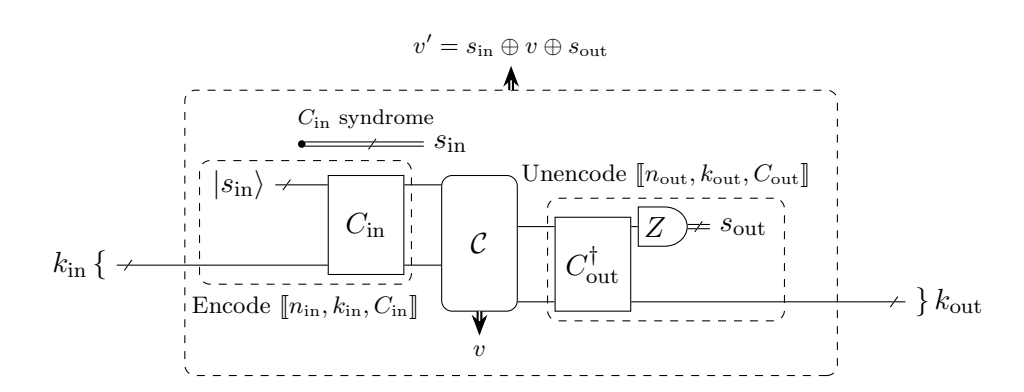


Figure 2.3: The circuit $\mathcal{E}(k_{\rm in}, C_{\rm in}) \circ \mathcal{C} \circ \mathcal{E}^{\dagger}(k_{\rm out}, C_{\rm out})$ with outcome vector v' used for defining the logical action of a logical operation circuit \mathcal{C} with outcome vector v, input code $[n_{\rm in}, k_{\rm in}, C_{\rm in}]$ and output code $[n_{\rm out}, k_{\rm out}, C_{\rm out}]$.

Note that according to our definition of a logical operation circuit and its logical action, the outcome $v' = 0^{n_{\rm in}-k_{\rm in}} \oplus v \oplus 0^{n_{\rm out}-k_{\rm out}}$ when $s_{\rm in} = 0^{n_{\rm in}-k_{\rm in}}$ and so the outcome vector of the circuit in Fig. 2.3 and the outcome vector v of its sub-circuit \mathcal{C} are directly related.

It can be useful to explicitly define a map from logical operator representatives to elements of the logical Pauli group of a stabilizer code. Recall, that given a code [n, k, C] with stabilizer group S, n-qubit Pauli unitary P is in S^{\perp} if and only if preimage $C^{\dagger}PC = Z^a \otimes Q$ for some Pauli unitary Q from \mathcal{P}_k and bit string a from \mathbb{F}_2^{n-k} . Using this fact, we define $\mathcal{L}_{(k,C)}: S^{\perp} \to \mathcal{P}_k$ and $\mathcal{G}_{(k,C)}: S^{\perp} \to \mathbb{F}_2^{n-k}$ via the following equation:

$$C^{\dagger}PC = Z^{\mathcal{G}_{(k,C)}} \otimes (\mathcal{L}_{(k,C)}(P)). \tag{8}$$

¹When considering a code [n, k, C] we assume that we are given integers n, k and fixed Clifford unitary C

It is also useful to note that upon syndrome $s \in \mathbb{F}_2^{n-k}$ the unencoding circuit $\mathcal{E}^{\dagger}(k,C)$ implements a linear map:

$$\mathcal{E}^{\dagger}(k,C): P \xrightarrow{\text{outcome } s} (-1)^{\langle s,\mathcal{G}_{(k,C)}\rangle} \mathcal{L}_{(k,C)}(P).$$
 (9)

2.4 Bipartite normal form of a stabilizer state

Bipartite entanglement of stabilizer states is useful for reconstructing the action of a Clifford channel given the Choi state of the channel. This connection is first clarified in Section 4 and used for algorithmic purposes in Section 6. We find it useful to restate a result from [29] (which is a special case of a more general result in $[7]^2$):

Theorem 2.10 (Theorem II.24 from [29]). Given any bipartition $M \sqcup M^c$ of n qubits, and a stabilizer state $|\psi\rangle$ on n qubits, there exists a tensor product of two Clifford operators (supported on M and M^c correspondingly) that transforms $|\psi\rangle$ into Bell pairs and zero states.

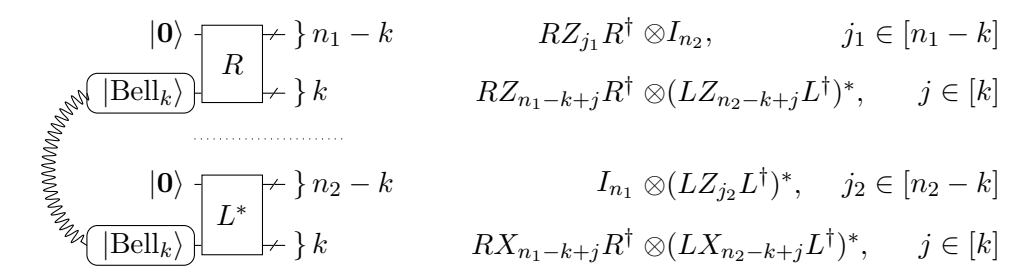


Figure 2.4: Bipartite normal form of a stabilizer state $|\psi\rangle$ on $n_1 + n_2$ qubits; a corollary of Theorem 2.10. On the left, the circuit diagram shows creation of a stabilizer state $|\psi\rangle$ starting from k Bell pairs and using Clifford unitaries R and L^* acting on, respectively, the first n_1 and last n_2 qubits. On the right, generators of the stabilizer group of $|\psi\rangle$ that follow from the circuit diagram.

An immediate corollary of the above theorem is that any stabilizer state on n_1+n_2 qubits can be prepared by a circuit as shown in Fig. 2.4. The relevant proofs in [7] and [29] are constructive and include polynomial time algorithms for constructing the circuit by solving the following:

Problem 2.11 (Bipartite normal form of a stabilizer state). Let $|\psi\rangle$ be the stabilizer state stabilized by a set of $n_1 + n_2$ commuting Pauli operators acting on $n_1 + n_2$ qubits. Find an integer k and Clifford unitaries L and R such that the circuit in Fig. 2.4 produces the state $|\psi\rangle$.

Moreover, the stabilizer group of any stabilizer states can be written as a product of three stabilizer groups

$$(S_R \otimes I_{n_2}) \cdot \left\{ R(I_{n_1-k} \otimes P)R^{\dagger} \otimes (L(I_{n_2-k} \otimes P)L^{\dagger})^* : P \in \{I, X, Y, Z\}^{\otimes k} \right\} \cdot (I_{n_1} \otimes S_L^*), \quad (10)$$

where groups S_L and S_R are defined as:

$$S_R = R\langle Z_1, \dots, Z_{n_1-k}\rangle R^{\dagger}, \quad S_L = L\langle Z_1, \dots, Z_{n_2-k}\rangle L^{\dagger}.$$

Groups S_R and S_L do not depend on the particular choice of Clifford unitaries R and L. This is because $S_R \otimes I_{n_2}$ and $I_{n_1} \otimes S_L^*$ are exactly the maximal subgroups of the stabilizer group of $|\psi\rangle$ supported on the first n_1 and the last n_2 qubits.

Another corollary of the constructive proofs in [7] and [29] is an efficient algorithm for computing a Clifford unitary, given its Choi state. The algorithm is to first compute L and R in Fig. 2.4 for the Choi state of a Clifford unitary C considered as a bipartite state between the

²Theorem 1 in [7] applies not only to pure stabilizer states, but to mixed stabilizer states proportional to projectors on stabilizer codes, but we find the result in [29] more convenient here.

first and the last n-qubits. Then return $C = RL^{\dagger}$. Correctness of the algorithm follows from the following two observations. First, for an n-qubit Clifford unitary its Choi state $(C \otimes I_n)|\text{Bell}_n\rangle$ is locally equivalent to n Bell pairs, and therefore k = n in Fig. 2.4. Second, equality $(I \otimes L^*)|\text{Bell}_n\rangle = (L^{\dagger} \otimes I)|\text{Bell}_n\rangle$ implies that the Choi states of C and RL^{\dagger} are equal and therefore $C = RL^{\dagger}$.

2.5 Linear algebra notation

Here we provide some common linear algebra notation we use. All vectors we consider are column vectors such that an n-dimensional vector can also be thought as an $n \times 1$ matrix. For matrices A, B with the same number of rows, we use (A|B) to denote a matrix with columns consisting of the columns of A followed by the columns of B. Similarly, for matrices A, B with the same number of columns, $(\frac{A}{B})$ is the matrix with rows consisting of the rows of A followed by the rows of B. In particular, for n_1 - and n_2 -dimensional vectors v_1 and v_2 , the vector $(\frac{v_1}{v_2})$ is an $(n_1 + n_2)$ -dimensional vector. We use A_n to refer to the n-th row of A, $A_{[n]}$ to refer to the matrix consisting of all rows of A starting from row n. We use [n] to denote a sequence of integers $1, \ldots, n$ and [m, n] to denote the sequence $m, m+1, \ldots, n$. More generally, for any sequences of integers J and J, J, is the J J J J J matrix with entries J J J, is refer to the matrix consisting of the first J columns of J and J, J, is refer to the matrix consisting of the first J columns of J and J, J, is refer to the matrix consisting of all columns of J starting from column J and J, J, is refer to the matrix consisting of all columns of J starting from column J.

The inner product $\langle v_1, v_2 \rangle = v_1^T v_2$ acts on column vectors. The direct sum of two vectors v_1, v_2 is $v_1 \oplus v_2 = (\frac{v_1}{v_2})$. When considering matrices with entries in $\mathbb{F}_2 = \{0, 1\}$, the matrix I_n is the $n \times n$ identity matrix and $\mathbf{0}_{n_1 \times n_2}$ is the $n_1 \times n_2$ matrix with all zero entries. For $n_1 \times n_2$ and $m_1 \times m_2$ matrices A and B, the direct sum is defined as

$$(A \oplus B)(v_1 \oplus v_2) = (Av_1) \oplus (Bv_2), \quad A \oplus B = \left(\begin{array}{c|c} A & \mathbf{0}_{n_1 \times m_2} \\ \hline \mathbf{0}_{m_1 \times n_2} & B \end{array}\right).$$

When considering matrices with entries in \mathbb{C} , I_n is the $2^n \times 2^n$ identity matrix.

We use A^{-1} for the inverse of a square matrix. We use $B^{(-1)}$ for the inverse of a rectangular matrix with full row or column rank (this is a right inverse when row rank is full, and a left inverse when column rank is full). The **row rank profile** of a rank-r matrix A is the lexicographically smallest sequence of r row indices $i_1 < i_2 < \ldots < i_{r-1}$ such that the corresponding rows of A are linearly independent. When A^T is in reduced row echelon form, the row rank profile is the sequence of columns of A^T with leading ones.

3 Algorithmic preliminaries

Here we cover some basic algorithmic concepts and definitions that underpin our main results.

3.1 Stabilizer circuit parameters

Throughout this work, unless otherwise specified, we consider the run time of algorithms given input stabilizer circuits as defined in Definition 2.3 parameterized in terms of the following quantities:

- n_{\uparrow} the maximum number of qubits used throughout the circuit,
- n_M the number of circuit outcomes,
- $N_{\rm u}$ the number of unitary operations (exp(P), $\Lambda(P, P')$),
- $N_{\rm cnd}$ the number of conditional Pauli unitary operators,
- n_r the number of random outcomes,
- n_m the number of input-dependent outcomes.

We further assume that conditional unitary and measurement operations are parameterized by Pauli operators with weight bounded by some fixed constant and that the weight of any bitstring indicating outcomes upon which Pauli operators are conditioned on is at most n_{\uparrow} .

In Section 1 we considered families of circuits with growing maximum width $n = n_{\downarrow}$ and depth D, and where all stabilizer operations appear with constant non-zero density. More specifically this assumes that n_M , $N_{\rm u}$, $N_{\rm cnd}$, n_r are all non-zero and proportional to nD, and n_m is zero for stabilizer simulation (which has no input qubits), but non-zero and proportional to n for the other cases analyzed in Section 1.

3.2 Two algorithmic cost models

We consider two cost models when analyzing the run time complexity of algorithms in this paper. The first is the standard sequential model in which which each bit-level operation has cost O(1). In the second model, bit string level operations have a cost O(1). For example, the bit-wise XOR of two length-n bit strings has cost O(n) in the sequential model and cost O(1) in the second model. More precisely, we consider bit-wise NOT, AND, OR, XOR, Hamming weight calculation and initialising the all-zero bit string 0^n to be O(1) in the second model. To distinguish the costs of these two models, we simply write 'run time' when referring to the run time in the standard sequential cost model, and 'bit-string run time' in the second model. The second model is motivated by the fact that modern computing hardware can quickly perform bit-wise operations on bit strings of length 32, 64, 128, 256 and even 512.

When considering bit string run time it is important to keep in mind how a given datastructure is organized into bit strings. For example, consider an $n \times n$ matrix with $\{0,1\}$ entries that is stored as an array of bit strings. We say that we store a matrix in a row-major order if each row corresponds to a bitstring. In this case, computing a sum of two rows of the matrix has bit string run time O(1). However, computing a sum of two columns has bit string run time O(n), because it requires modifying individual bits of n bit strings.

3.3 Data structures for Pauli and Clifford unitaries

Here we define a set of data structures to represent Pauli and Clifford unitaries, which can be used to build algorithms for stabilizer circuits. We briefly mention alternative data structures that can be used and give some justification for the choices we have made. However, our main algorithms do not require use of these specific data structures, provided the alternative data structures offer an equivalent set of procedures with the given time complexities (as described in the next subsection).

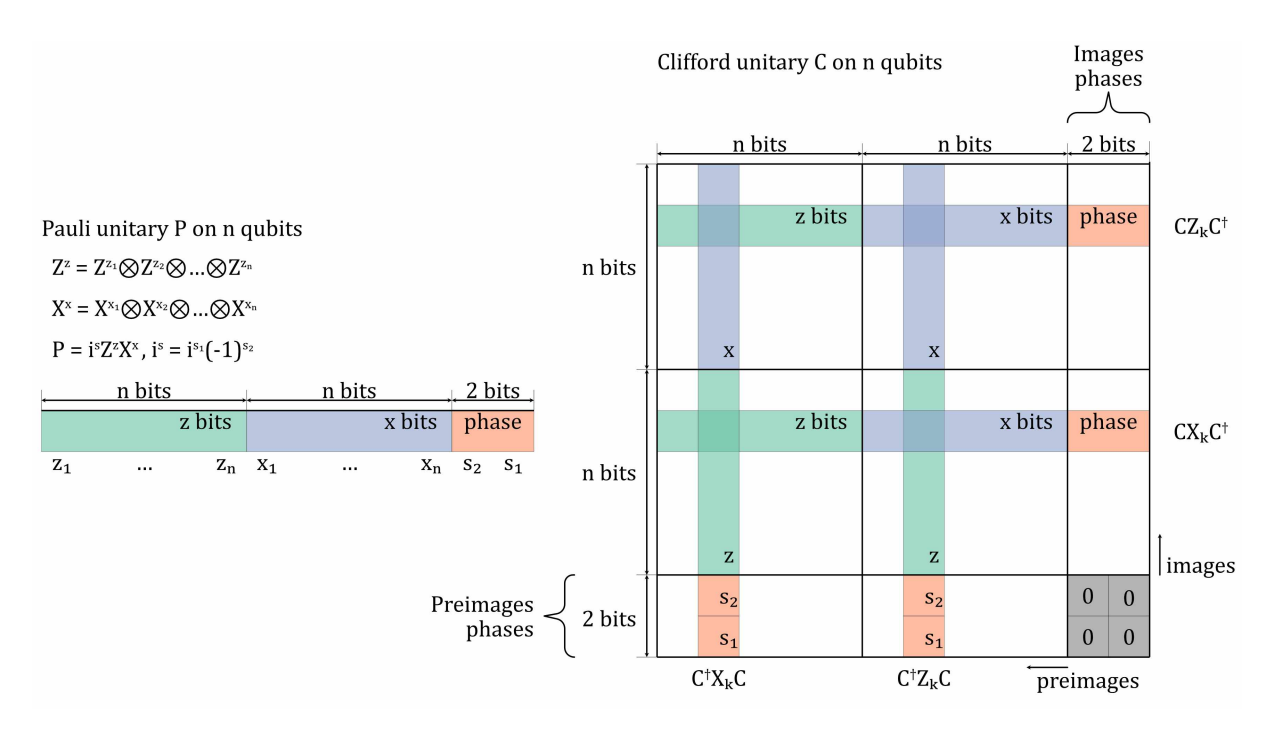


Figure 3.1: Description of Pauli unitary in terms of bit vectors as in Definition 3.1 and of a Clifford unitary using a binary matrix as in Definition 3.2.

There are two common ways of encoding a one-qubit Pauli unitary using two bits [1, 20]. The first encoding maps bits (z,x) to powers Z^zX^x , and the second encoding maps all two-bit combinations to Pauli observables (Hermitian Pauli unitaries): $(0,0) \to I$, $(0,1) \to X$, $(1,0) \to Z$, $(1,1) \to Y$. We call the first encoding the **power encoding** and the second encoding the **Hermitian encoding**.

These encodings can be readily extended to form n-qubit Pauli unitary encodings using 2n bits, and there are two standard approaches to encode those bits. The first, and most commonly used approach [1, 20], is to encode an n-qubit Pauli operator into a bit string of length 2n (or two bit strings of length n) with a batch of all z bits followed by a batch of all x bits $(z_1, \ldots, z_n, x_1, \ldots, x_n)$. We call this approach the **batch encoding**. The second approach is to encode a Pauli unitary on each qubit serially $(z_1, x_1, \ldots, z_n, x_n)$; we call this the **serial encoding**.

To fully specify an n-qubit Pauli unitary, we must include a phase, which requires two bits to encode the power of i. To encode an n-qubit Pauli observable, this cost can be reduced when a Hermitian encoding is used, because the phase can only be ± 1 . On the other hand, two bits are still needed to encode the phase for the power encoding of an n-qubit Pauli observable. Ref. [1] uses Hermitian batch encoding of n-qubit Pauli observables, while Ref. [20] uses power batch encoding. In what follows we use the batch power encoding of Pauli unitaries, see Definition 3.1.

Definition 3.1 (Pauli unitary data structure). Two length-n binary vectors x, z and one length-2 binary vector $s = (s_1, s_2)$ describe a Pauli unitary (see Fig. 3.1),

$$P = i^{s_1 + 2s_2} \cdot Z^z X^x.$$

The vectors x(P), z(P) and s(P) are, respectively, the x bits, the z bits, and the phase of P. It is convenient to also interpret s(P) as integer $s_1 + 2s_2$ and write s(P)/2 for s_1 .

Given this notation, we define supp(z(P)) and supp(x(P)) as the indices where z(P) and x(P), respectively, are non-zero.

A primary advantage of using the batch power encodings over the alternatives for our Pauli unitary data structure is that it is known to admit composition of two Clifford unitaries by way

of matrix-matrix and matrix-vector multiplications, thus allowing fast matrix multiplication algorithms [26] to be used. There are however some things which can be less efficient with this encoding. For example, checking if a Pauli unitary is Hermitian requires computing $\langle z(P), x(P) \rangle$ with run time O(n) and bit string run time O(1). This is because inner product $\langle \cdot, \cdot \rangle$ can be calculated by bit-wise AND, followed by the Hamming weight calculation. By contrast, with any Hermitian encoding this check can be done in run time O(1) (by checking the sign). However we find that in our algorithms, checking if a Pauli unitary is Hermitian is infrequent, and only used as a test. Another standard operation is to compute the commutator of two n-qubit Pauli unitaries $[P,Q] = \langle x(P), z(Q) \rangle + \langle z(P), x(Q) \rangle$, which with the batch power encoding data structure has run time O(n) and bit-string run time O(1).

We will occasionally use another data-structure for the sparse encoding of Pauli unitaries. This data structure consists of a pair, with the first part a length-n ordered list³ of integers and the second part an n-qubit Pauli observable data structure. The first part identifies the qubits on which the Pauli observable acts non-trivially.

There are two common approaches to represent n-qubit Clifford unitaries compactly. The first approach is to store the images CX_kC^{\dagger} , CZ_kC^{\dagger} of the generators of the Pauli group X_k , Z_k for k in [n] [1, 20]. The second approach is to store preimages $C^{\dagger}X_kC$, $C^{\dagger}Z_kC$ [23], which is advantageous when the Clifford unitary data structure is used for stabilizer simulation [23], as we discuss in Section 3.5. In this paper we propose a third approach, in which both images and preimages are stored simultaneously, see Definition 3.2.

Definition 3.2 (Clifford unitary data structure). $A(2n+2) \times (2n+2)$ matrix M(C) over \mathbb{F}_2 describes an n-qubit Clifford unitary C (see Fig. 3.1), where:

1. for rows $k \in [n]$ of M(C), $M(C)^T$, Z images $P_k = CZ_kC^{\dagger}$ and X preimages $Q_k = C^{\dagger}X_kC$,

$$M(C)_k = z(P_k) \oplus x(P_k) \oplus s(P_k) \tag{11}$$

$$M(C)_k^T = x(Q_k) \oplus z(Q_k) \oplus s(Q_k), \tag{12}$$

2. and rows $k \in [n+1,2n]$ of M(C), $M(C)^T$ are defined analogously for X images $P_k = CX_kC^{\dagger}$ and Z preimages $Q_k = C^{\dagger}Z_kC$.

We can see that this is a consistent definition as follows. The top-left $2n \times 2n$ sub-matrix of M(C) is a binary symplectic matrix. Using the expression for the inverse of a binary-symplectic matrix

$$\left(\begin{array}{c|c}
A_{z,x} & A_{x,x} \\
\hline
A_{z,z} & A_{x,z}
\end{array}\right)^{-1} = \left(\begin{array}{c|c}
A_{x,z}^T & A_{x,x}^T \\
\hline
A_{z,z}^T & A_{z,x}^T
\end{array}\right), \text{ where } A_{z,x}, A_{x,x}, A_{z,z}, A_{x,z} \text{ are } n \times n \text{ matrices over } \mathbb{F}_2$$
(13)

one can see that column k of M(C) encodes the preimage $C^{\dagger}X_kC$ with first n bits corresponding to the x bits, the next n bits corresponding to the z bits and the last two bits corresponding to the phase (see Fig. 3.1). Similarly, column n + k encodes preimage $C^{\dagger}Z_kC$ with the first n bits corresponding to the x bits, the next n bits corresponding to the z bits and the last two bits corresponding to the phase. Therefore, Eqs. (11) and (12) are mutually consistent.

Given an n-qubit Pauli observable supported on k qubits, Definition 3.2 admits calculation of the image CPC^{\dagger} and preimage $C^{\dagger}PC$ with run time O(kn). If C is stored in column-major (row-major) order, then calculating the preimage (image) has bit-string run time O(k).

In the algorithmic context, we say that the Pauli observable P or Clifford unitary C are given when descriptions satisfying Definition 3.1 or Definition 3.2, respectively, are provided. Similarly when we say that algorithm finds Pauli observable P or Clifford unitary C, it means that algorithm computes descriptions that satisfy Definition 3.1 or Definition 3.2.

 $^{^{3}}$ We require the list to be ordered, so that the support of the product of two sparse Pauli observables can be computed in linear time

3.4 Procedures for Pauli and Clifford unitary manipulation

Here, in Table 3.1, we list the mathematical action and run time complexities for a set of key procedures. For the purposes of bit-string run time analysis, we assume that each column of the Clifford unitary data structure Definition 3.2 is stored as three bit strings corresponding to z, x and sign bits. Similarly, Pauli unitaries are stored as three bit strings. We use an asterisk to mark basic procedures, namely those which make explicit use of our data structures for Pauli and Clifford unitaries that can be achieved using data structures Definition 3.1 and Definition 3.2. All other procedures and algorithms in this paper are built using these basic procedures in Table 3.1 without explicit reference to the underlying data structures. Therefore, if one prefers alternative data structures to those we propose here, and provides alternative basic procedures using their preferred data structures which have the same action and run time as those in Table 3.1, then they can use our proposed algorithms with their preferred data structures and will achieve the same run time guarantees by calling their versions of the procedures in Table 3.1.

In the remainder of this subsection we provide a high-level algorithmic description and an explanation of the time complexity of a few illustrative procedures. For readability here and elsewhere in this paper, we describe algorithms at a high level in terms of the mathematical action of procedures. We include explicit checks in some of our algorithms which are always 'true' in correct implementations, but may be useful for testing and debugging.

First we describe the preimage procedure, which makes explicit reference to the data structures in Definition 3.1 and Definition 3.2.

```
Procedure 3.3 (preimage*)
Input: Pauli observable P, Clifford unitary C.
Output: C^{\dagger}PC.

1: Initialize Pauli Q = \prod_{k:z(P)_k \neq 0} C^{\dagger}Z_k C \prod_{k:x(P)_k \neq 0} C^{\dagger}X_k C \cdot i^{s(P)}.

2: Check Q is Hermitian.

3: return Q.
```

In the preimage* procedure, we assume that the Pauli and Clifford unitaries P and C are specified using the data structures in Definition 3.1 and Definition 3.2 respectively. Let n be the number of qubits that P and C act on. Note that x(P) and z(P) both have at most |P| non-zero entries. The procedure first initializes a trivial n-qubit Pauli observable Q. Next, the procedure walks through $j \in \text{supp}(z(P))$, and iteratively sets $Q \leftarrow Q$ ($C^{\dagger}Z_{j}C$), where the Pauli preimage $C^{\dagger}Z_{j}C$ is read out from jth column of M(C), that is C stored using the data structure Definition 3.2. Then this process is continued for X, by walking through $j \in \text{supp}(x(P))$, and iteratively setting $Q \leftarrow Q$ ($C^{\dagger}X_{j}C$), where the Pauli preimage $C^{\dagger}X_{j}C$ is read out from j + nth column of M(C). The resulting Pauli $Q = C^{\dagger}PC$ is returned as the output of the algorithm. For both X and Z, each of the O(|P|) Pauli multiplications takes O(n) standard run time and O(1) bit-string run time, such that the overall algorithm run time is O(n|P|) or O(|P|) in the standard or bit-string cost models respectively.

Next we consider the disentangle procedure, which is expressed only in terms of asterisked procedures (which are referenced here by their mathematical action) in Table 3.1, with no explicit dependence on the underlying data structures.

```
Procedure 3.4 (disentangle)
Input: n-qubit Clifford unitary C, integer j \in [n] such that Z_jC|0^n\rangle = C|0^n\rangle.
Output: Replace C by C' \otimes_j I such that (C' \otimes_j I)|0^n\rangle = C|0^n\rangle.

> First modify Clifford C such that C|0^n\rangle is unchanged, and CZ_jC^{\dagger} = Z_j.

1: Let j' be the index of the first non-zero entry of z(C^{\dagger}Z_jC).

2: C \leftarrow \Lambda(CX_{j'}C^{\dagger}, CZ_{j'}C^{\dagger}Z_j) C SWAP_{j,j'}.

> Second modify Clifford C such that C|0^n\rangle is unchanged, and CX_jC^{\dagger} = X_j.

3: if bit j of z(C^{\dagger}X_jC) is zero then

4: C \leftarrow \Lambda(CZ_jC^{\dagger}, X_j CX_jC^{\dagger}) C.

5: else
```

Procedure	Mathematical action	Run time	Bit-string run time
$ ext{init_pauli}^*(a,b,c)$	P, where $x(P) = a$, $z(P) = b$ and $z(P) = c$	O(n)	O(1)
$\mathtt{x_bits}^*(P)$	x(P)	O(1)	O(1)
$\mathtt{z_bits}^*(P)$	z(P)	O(1)	O(1)
$\mathtt{xz_phase}^*(P)$	s(P)	O(1)	O(1)
$\mathtt{set}_{\mathtt{x}}\mathtt{bits}^{*}(P,a)$	$x(P) \leftarrow a$	O(n)	O(1)
$\mathtt{set}_\mathtt{z_bits}^*(P,a)$	$z(P) \leftarrow a$	O(n)	O(1)
$is_hermitian^*(P)$	Is $P = P^{\dagger}$	O(n)	O(1)
$\mathtt{commutator}^*(P,Q)$	$\llbracket P,Q rbracket$	O(n)	O(1)
$\mathtt{prod_pauli}^*(P,Q)$	PQ	O(n)	O(1)
$\mathtt{mult_phase}^*(P,j)$	$P \leftarrow i^j P$	O(1)	O(1)
	C , where $\forall j \in [n]$: $CX_jC^{\dagger} = P_j$, and $CZ_jC^{\dagger} = Q_j$	$O(n^{\omega})$	$O(n^2)$
	U_A , where $\forall j \in [n]$: $U_A X_j U_A^{\dagger} = X^{A_j}$, and $U_A Z_j U_A^{\dagger} = Z^{B_j}$	$O(n^2)$	$O(n^2)$
$copy_cliff^*(C)$	C, C	$O(n^2)$	O(n)
$\mathtt{num_qubits}^*(C)$	n	O(1)	O(1)
$image^*(C, P)$	CPC^{\dagger}	$O(n \cdot P))$	$O(n \cdot P)$
$\mathtt{preimage}^*(C,P)$	$C^{\dagger}PC$	$O(n \cdot P)$	O(P)
$inverse_cliff^*(C)$	C^{\dagger}	$O(n^2)$	$O(n^2)$
${\sf prod_cliff}^*(C,C')$	CC'	$O(n^{\omega})$	$O(n^2)$
$left_mult_exp^*(C, P)$	$C \leftarrow \exp(P) C$	$O(n \cdot P)$	O(P)
$ exttt{left_mult_swap}(C, i, j)$	$C \leftarrow \text{SWAP}_{i,j} C$	O(n)	O(1)
$right_mult_swap^*(C, i, j)$	$C \leftarrow C \text{ SWAP}_{i,j}$	O(n)	O(n)
$tensor_{\mathtt{prod}^*}(C,C'')$	$C\otimes C''$	$O((n+l)^2)$	$O((n+l)^2)$
$\mathtt{add_qubits}^*(C,m)$	$C \leftarrow C \otimes I_m$	$O((n+m)^2)$	$O((n+m)^2)$
${\tt remove_qubits}^*(C,m)$	$C \otimes I_m \leftarrow C$	$O(n^2)$	$O(n^2)$
$left_mult_pauli(C, P)$	$C \leftarrow PC$	$O(n \cdot P)$	O(P)
$ \begin{array}{c} \texttt{left_mult_ctrl_pauli(} \\ C,P,Q) \end{array} $	$C \leftarrow \Lambda(P,Q)C$	$O(n \cdot (P + Q))$	O(P + Q)
disentangle (C, j) where $Z_j C 0^n\rangle = C 0^n\rangle$	$C \leftarrow C' \otimes_j I_1$, where: $(C' \otimes_j I_1) 0^n\rangle = C 0^n\rangle$	$O(n^2)$	O(n)

Table 3.1: Key procedures for Pauli and Clifford unitary manipulation. Asterisks mark basic procedures which can be implemented using the data structures in Definition 3.1 and Definition 3.2. All procedures and algorithms with no asterisk (here and throughout this work) are expressed only in terms of asterisked procedures, independently of whichever underlying data structures are used. The procedure inputs are as follows: P, Q, P_j and Q_j are n-qubit Pauli observables; a and b are length-n bit strings, while c is a length-2 bit string; A and B are $n \times n$ binary matrices (with A_j being the jth row of A etc); C and C' are n-qubit Clifford unitaries, while C'' is an l-qubit Clifford unitary. By $\alpha \leftarrow \beta$, we mean that object α is replaced by object β . We define I_m to be the m-qubit identity operator, $\Lambda(P,Q)$ as the generalized controlled Pauli from Eq. (2), and SWAP $_{i,j}$ to be the operator that swaps the locations of qubits i and j; ω is the matrix-multiplication exponent [3]. The procedures' details and run time are discussed in Appendix B.

6:
$$C \leftarrow \Lambda(CZ_jC^{\dagger}, X_j \ C \ iZ_jX_j \ C^{\dagger}) \ e^{i\frac{\pi}{4}CZ_jC^{\dagger}} \ C.$$

We provide the correctness proof of Procedure 3.4 in the appendix in Proposition B.3. In what follows, we argue that its run time is $O(n^2)$ and its bit-string run time is O(n) (as in Table 3.1) and also highlight the correspondence between the mathematical action and names of procedures. In Line 1 the run time of preimage is O(n) and finding a non-zero entry is O(n). In Line 2 the run time of right_mul_swap is O(n), two uses of image has run time O(n), prod_pauli has run time O(n) and left_mul_ctrl_pauli has run time $O(n^2)$. The run time of the first part of the algorithm is dominated by left_mul_ctrl_pauli and is $O(n^2)$. Similarly, the run time of the second part of the algorithm is dominated by left_mul_ctrl_pauli, left_mul_ctrl_exp and is $O(n^2)$. A similar analysis shows that the bit-string run time is O(n).

Our choice of the Clifford unitary data structure has two important features. The first feature is the preimage $C^{\dagger}PC$ calculation of a Pauli operator P with bit-string run time O(|P|). This is ensured by storing the preimage signs and storing the matrix M(C) in column-major order. This choice is motivated by the fact that preimage is a very common procedure in the algorithms considered in this paper. The second feature is the fast calculation of the inverse of a Clifford unitary C. This is ensured by storing both images and preimages. If only images or preimages are stored, the inverse would require $O(n^{\omega})$ (and would require $O(n^3)$ if we had chosen a Hermitian rather than power encoding). Keeping standard and bit string run times low requires a careful design of procedures that update the data structure for a Clifford unitary C. This is illustrated by the pseudo-code of left_mul_exp and left_mul_ctrl_pauli procedures discussed in Appendix B.

3.5 Outcome-specific stabilizer simulation

It is well known that stabilizer circuits can be efficiently simulated, including the original Gottesman-Knill simulation algorithm [27], the improved version of this algorithm Gottesman-Aaronson [1], and further practical improvements in [23]. A precise statement of the problem that these existing stabilizer circuit algorithms solve is stated in Problem 3.5.

Problem 3.5 (Outcome-specific stabilizer circuit simulation). Consider any stabilizer circuit with no input qubits and a length- n_M outcome vector, along with any bit-string $\tilde{v} \in \{0,1\}^{n_M}$. Find the vector of non-zero conditional probabilities $\overrightarrow{p} \in \{1,1/2\}^{n_M}$, a Clifford unitary R and the unique outcome vector $v \in \{0,1\}^{n_M}$ which satisfy the following properties:

- for each \$\overline{pl}_l = 1/2\$, the corresponding element \$v_l\$ is equal to \$\vec{v}_l\$,
 \$\overline{pl}_l\$ is the probability of obtaining outcome \$v_l\$ given previous outcomes \$v_1, \ldots, v_{l-1}\$,
 \$R|0^{n(R)}\$ is the output state of the circuit given the outcome \$v\$.

The fact that the conditional probabilities are always either 1/2 or 1 is a consequence of the fact that at each point in time the state is a stabilizer state, and measuring any Pauli operator either has a definite or a uniformly random outcome. The fact that only those bits of the input bit string \tilde{v} which correspond to conditional probabilities of 1/2 correspond to observed measurement outcomes in the bit string v is then required to ensure that v occurs with non-zero probability. Note that any algorithm that solves this outcome-specific stabilizer circuit simulation problem can be used to sample faithfully from the quantum circuit, by choosing the input bit string \tilde{v} uniformly at random.

In what follows, we provide Algorithm 3.6 that solves the outcome-specific stabilizer circuit simulation problem. Our algorithm uses some key procedures listed in Table 3.1. It is also desirable to solve a stronger stabilizer circuit simulation problem which accounts for all possible measurement outcomes. At first, such a problem may seem like it could not have an efficient solution; a naive specification of the output of the simulation would involve enumeration of all possible sequences of outcomes, which can grow exponentially with the circuit size. Nonetheless, in Section 5 we leverage a general form (introduced in Section 4) to define an efficiently specified

```
Algorithm 3.6 (Outcome-specific stabilizer circuit simulation) Input:
```

- a stabilizer circuit C with no input qubits, n output qubits, and a length- n_M outcome vector.
- a length- n_M vector \tilde{v} .

Output:

- a vector $\overrightarrow{p} \in \{1, 1/2\}^{n_M}$ of conditional probabilities,
- a Clifford unitary R,
- and length- n_M outcome vector v,

that satisfy the conditions of Problem 3.5.

31: **return** vector \overrightarrow{p} , Clifford unitary R, vector v_0

```
1: Initialize an empty vector \overrightarrow{p}, a zero-qubit Clifford unitary R, and a vector v = 0^{n_M}.
```

```
2: for g in C do
```

```
▶ allocation
        if g allocates qubit j, then
 3:
 4:
             replace R \leftarrow R \otimes_i I_2.
        else if g deallocates qubit j, where Z_i R|0\rangle = R|0\rangle, then
 5:
             disentangle(R,j),
 6:
             remove qubit j from R.
 7:
         else if g allocates a random bit then
 8:
             append 1/2 to \overrightarrow{p},
 9:
             replace v_l \leftarrow \tilde{v}_l, where l = |\overrightarrow{p}|.
10:
                                                                                                          ▶ unitaries
         else if g is a unitary U then
11:
             replace R \leftarrow UR.
12:
        else if g applies a Pauli unitary P if \langle c \rangle = c_0,
13:
                    where \langle c \rangle is the parity of outcomes indicated by c \in \mathbb{F}_2^{n_M}, then
14:
             replace R \leftarrow P^{c_0+1}R followed by R \leftarrow P^{\langle c \rangle}R.
15:
                                                                                                   ▶ measurements
        else if q measures Pauli P given a hint Pauli P' such that [P, P'] = 1,
16:
                    and P'R|0^{n(R)}\rangle = \pm R|0^{n(R)}\rangle then
17:
             find b' and \alpha such that preimage R^{\dagger}P'R = \alpha Z^{b'},
18:
             replace R \leftarrow e^{(\alpha \pi/4)PP'} \hat{R},
19:
             allocate a random bit according to Line 8,
20:
             apply P' conditioned on the value of the random bit.
21:
         else if g measures Pauli P, then
22:
             find the preimage Q = R^{\dagger} P R.
23:
             if x(Q) = 0 (deterministic measurement) then
24:
                 append 1 to \overrightarrow{p},
25:
                  v_l \leftarrow s(Q)/2, where l = |\overrightarrow{p}|.
26:
             else (uniformly random measurement)
27:
                 let j be the position of first non-zero bit of x(Q),
28:
                 find image P' = RZ_iR^{\dagger} (which anticommutes with P),
29:
                 measure P with assertion that P' is a hint Pauli according to Line 16.
30:
```

outcome-complete stabilizer circuit simulation problem, and provide an algorithm to efficiently solve that stronger simulation problem.

Our presentation (Algorithm 3.6) of the well-known outcome-specific stabilizer algorithm serves two goals. First it clarifies how to use the Clifford unitary data structure as a "black box", including how the simulation complexity follows from the complexity of the procedures for Clifford and Pauli unitaries manipulation in Table 3.1. Second, using this presentation, it is easy to see the differences and similarities between this outcome-specific and the outcome-complete stabilizer simulation algorithm we provide later. The differences between outcome-specific and the outcome-complete algorithms are indicated by highlights.

We conclude with a few remarks about correctness and run time of our presentation of the outcome-specific stabilizer simulation Algorithm 3.6. First note that the preimage calculation $R^{\dagger}PR$ is commonly used throughout the algorithm. The only place where the image calculation RPR^{\dagger} is explicitly used is in Line 29. However, Line 16 where the image is used requires knowing the image only up to a sign. For this reason, in practice, one can use Clifford unitary data structure without image signs as in [23]. Another place where the image calculation is used is within procedure disentangle, but the number of image calculations associated with it can also be reduced as we discuss next.

The run time of this simulation algorithm (and also the simulation algorithm introduced in Section 5) can be significantly reduced by reducing the number of qubit allocations and deallocations. First it is beneficial to calculate the maximum number of qubits needed and allocate all of them in the beginning to reduce allocation costs. Second we can keep track of which qubits were deallocated, but keep themaround and use them next time a qubit allocation is requested. It is then sufficient to apply any deallocations at the very end of the simulation. We also discuss a more efficient way of deallocating sets of qubits together in Appendix C.

In our presentation of Algorithm 3.6 we see that a non-deterministic measurement during stabilizer simulation reduces to the application of a Pauli exponential $e^{i\pi Q/4}$, which follows from Proposition 2.2. This ensures that we can simulate these measurements treating the Clifford unitary which tracks the state as a "black box" by referring only to the basic procedures in Table 3.1, and crucially without making any reference to the Clifford unitary's underlying data structure. Note that having a 'hint' Pauli P', which anticommutes with the Pauli P being measured and which has the system's state as an eigenstate (which triggers Line 16), can reduce the run time to simulate a measurement. This improvement comes into play because the exponential $e^{(\alpha\pi/4)PP'}$ which must be applied to simulate the measurement can be applied more efficiently if PP' is sparse, and when no hint Pauli P' is provided, that which is found by the algorithm is typically dense. For example, if both P and P' have constant weight, then such a measurement can be simulated in O(n) with a hint Pauli, compared with $O(n^2)$ without a hint. For the simulation of deterministic measurements, we achieve the same O(n) run time as is achieved in [23].

The run time of the outcome-specific simulation algorithm per Clifford operation is stated and compared to the run time of the outcome-complete simulation algorithm in Table 5.1. It is informative to state the simulation run time per operation because the simulation proceeds through the circuit operation by operation. This way the reader can easily derive the run time of the simulation for specific applications, taking into account the number of occurrences of each type of operation in the circuit.

General form for stabilizer circuits 4

The goal of this section is to demonstrate that the action of any stabilizer circuit is equivalent to that of a circuit of the form shown in Fig. 4.1, with equivalence as in Definition 2.6. Having a simple general form circuit that can capture the action of any stabilizer circuit forms a useful tool that will later allow us to build efficient algorithms to check circuit equivalence, analyze the logical action of circuits on information stored in a stabilizer code and more. Note that general form stabilizer circuits are not unique, since distinct general form stabilizer circuits can have equivalent action. However, in Section 7 we present an efficient algorithm for checking the equivalence of two general forms.

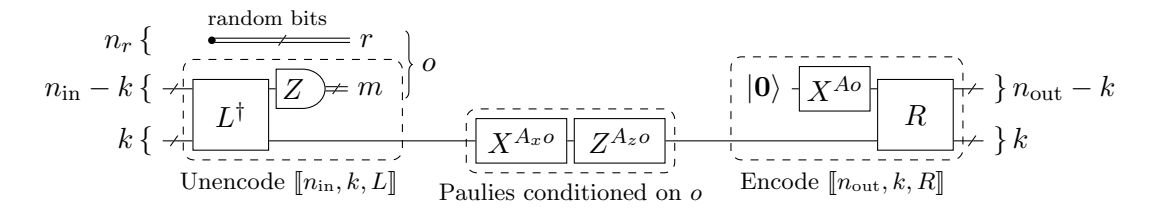


Figure 4.1: A general form stabilizer circuit with $n_{\rm in}$ input qubits and $n_{\rm out}$ output qubits and n_r classical random bits. L and R are the left and right Clifford unitaries, A, A_x , A_z are the condition matrices over \mathbb{F}_2 , r is an n_r -dimensional random bits vector over \mathbb{F}_2 , k is the number of inner qubits. A_x and A_z are $k \times n_O$ matrices, while A is an $(n_{\text{out}} - k) \times n_O$ matrix, where $n_O = (n_{\rm in} - k + n_r)$. We call the length- $(n_{\rm in} - k)$ vector m the **measurement outcome vector**, and the length- n_O vector $o = r \oplus m$ the circuit's **outcome vector**. Applying X^{v_x}, Z^{v_z} with k-bit vectors $v_x = A_x o, v_z = A_z o$ to a k-qubit register corresponds to applying X_j conditioned on $(v_x)_j = 1$ and Z_j conditioned on $(v_z)_j = 1$ for $j \in [k]$.

To describe the relation between a stabilizer circuit's outcome vector and an equivalent general from circuit's outcome vector we will need the following definition:

Definition 4.1 (Split (reduced) echelon form). A matrix M of size $m \times n$ is in (n_r, n_m) **split echelon form** if $n_r + n_m = n$, M has full column rank and the following conditions hold (Fig. 4.2):

- the left part M^T_[n_r] of M is in reduced row echelon form,
 the right part M^T_[n_r+1,n_r+n_m] of M is in row echelon form,
 for any index j of a leading column of M^T_[n_r] row M_{j,[n_r+1,n_r+n_m]} is equal to 0^{n_m}.

Given a matrix M which is in (n_r, n_m) -split echelon form, if the right part $M_{[n_r+1, n_r+n_m]}^T$ is in reduced row echelon form, we further say that M is in (n_r, n_m) -split reduced echelon form.

Theorem 4.2 (General form stabilizer circuit). Given a stabilizer circuit $\mathcal{C}(Definition\ 2.3)$, an equivalent stabilizer circuit C_{gen} can be written in the general form in Fig. 4.1. The outcome vector v of the circuit C is related to the outcome vector o of the general form circuit $C_{\rm gen}$ by an invertible affine function. That is, there there exist a vector v_0 and a matrix M such that when the relation $v = v_0 + Mo$ is satisfied, the circuits have the same action on any input state. Additionally, M is in (n_r, n_m) -split echelon form, where n_r is the number of random bits of \mathcal{C}_{gen} and n_m is the size of the measurement outcome vector of \mathcal{C}_{gen} , The entries of v_0 corresponding to the row rank profile (see Section 2.5) of the left part of M are zero.

Proof. The result follows by induction on the elementary operations contained in the stabilizer circuit. The base case is the empty stabilizer circuit, which is trivially in the general form. The induction step follows from Lemma 4.3 below.

 $^{{}^{4}}M_{[n_r]}^{T}$ refers to the first n_r rows of M^T , as opposed to the transposed of the first n_r rows of M.

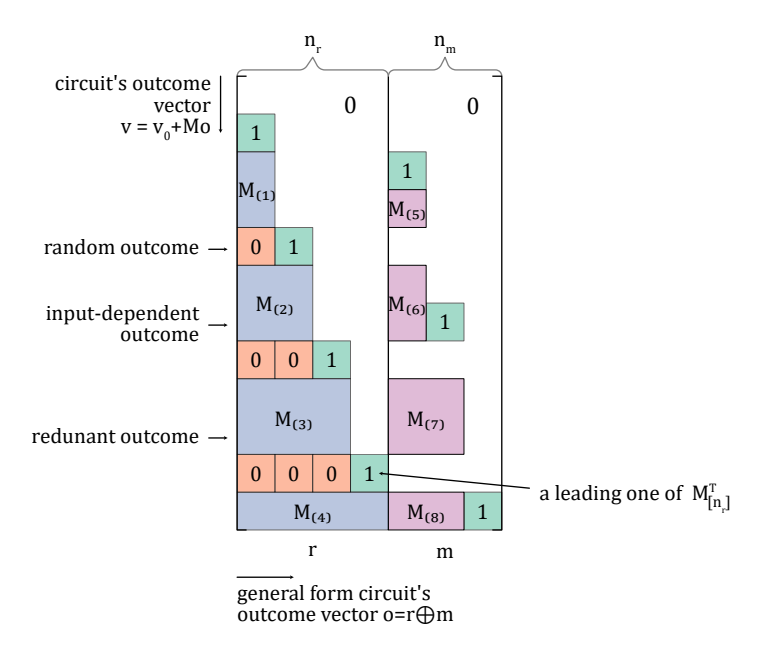


Figure 4.2: Matrix M in (n_r, n_m) -split echelon form (Definition 4.1), which relates a stabilizer circuit \mathcal{C} outcome vector v to the general form circuit \mathcal{C}_{gen} outcome vector o as described in Theorem 4.2. We label rows corresponding to different kinds of stabilizer circuit outcomes. The indices of rows in the left (right) block containing a leading one, marked in green, form the row rank profile of the left (right) part of M and correspond to random (input-dependent) outcomes. The remaining rows correspond to redundant outcomes.

The structure of the matrix M which appears in the outcome relation between a circuit and its equivalent general form circuit in Fig. 4.2 and Theorem 4.2 reflect the three kinds of stabilizer circuit outcomes which we defined in Section 2.2. (1) If the probability of an outcome being zero (conditioned on the previous circuit outcomes) is 1/2 for all input states, then the outcome is a random outcome. (2) If the probability of an outcome being zero (conditioned on the previous circuit outcomes) depends only on the input state, then it is an **input-dependent outcome**. (3) If the probability of an outcome being zero (conditioned on the previous circuit outcomes) is either zero or one for all input states, then it is a **redundant outcome**. Any row of M that contains a leading one of $M_{[n_r]}^T$, i.e., which is in the row rank profile (see Section 2.5) of the left part of M, corresponds to a random outcome. Any row of M that contains a leading one of $M_{[n_r+1,n_r+n_m],J}^T$, i.e., which is in the row rank profile of the right part of M, corresponds to an input-dependent outcome. The remaining rows correspond to redundant outcomes.

Lemma 4.3 (Induction step for Theorem 4.2). Let C be a stabilizer circuit (Definition 2.3) which is equivalent to a general form circuit. More specifically, suppose that C with outcome vector v has the same action on any input state as a general form circuit C_{gen} with outcome vector v, where $v = v_0 + Mo$ for some vector v_0 and matrix M, and where the sets of outcomes of C_{gen} and C are $\mathbb{F}_2^{n_O}$ and $v_0 + M\mathbb{F}_2^{n_O}$ respectively.

Then the circuit $\mathcal{C}' = \mathcal{C} \circ g$, consisting of \mathcal{C} followed by a stabilizer operation g (Definition 2.3), is also equivalent to a general form circuit. In particular, \mathcal{C}' with outcome vector \mathbf{v}' has the same action on any input state as a general form circuit \mathcal{C}'_{gen} with outcome vector \mathbf{v}' , where $\mathbf{v}' = \mathbf{v}'_0 + M'\mathbf{o}'$ for some vector \mathbf{v}'_0 and matrix M', and the sets of outcomes of \mathcal{C}'_{gen} , \mathcal{C}' are $\mathbb{F}_2^{n'_O}$, $\mathbf{v}'_0 + M'\mathbb{F}_2^{n'_O}$. Moreover the stabilizer group of $[n_{in}, k, L]$ is a subgroup of the stabilizer group of $[n_{in}, k', L']$. Additionally, the split echelon form property of M is inherited by M'. Specifically, M' is in (n'_r, n'_m) -split echelon form, where n'_r and n'_m are the number of random bits of \mathcal{C}'_{gen} and the size of the measurement outcome vector of \mathcal{C}_{gen} when M is in (n_r, n_m) -split echelon form, where n_r and n_m are the number of random bits of \mathcal{C}'_{gen} and the size of the measurement

outcome vector of C_{gen} . The entries of v'_0 corresponding to the row rank profile of the left part of M' are zero when entries of v_0 corresponding to the row rank profile of the left part of M are zero.

Proof. Recall that according to Definition 2.3, operation g can be one of the following:

- (A) Clifford or Pauli unitary,
- (B) Allocation of a qubit initialized to the zero state,
- (C) Deallocation of a qubit in the zero state,
- (D) Pauli unitary conditioned on the parity of a set of measurement outcomes and classical random bits,
- (E) Allocation of a classical random bit distributed as a fair coin,
- **(F)** Pauli measurement.

We will prove that the lemma holds in each of these cases. We have reordered the cases from Definition 2.3 for convenience. Our proof strategy is to use the fact that the action of the circuit $\mathcal{C}' = \mathcal{C} \circ g$ is equivalent to the circuit $\mathcal{C}_{\text{gen}} \circ g$ (where \mathcal{C}_{gen} is a general form circuit equivalent to \mathcal{C}) and to transform $\mathcal{C}_{\text{gen}} \circ g$ into a general form circuit via a series of simple action-preserving circuit transformations. In cases (A) - (D), appending g to the circuit does not modify the outcome vector and nor do the transformations that take $\mathcal{C}_{\text{gen}} \circ g$ to the general form circuit $\mathcal{C}'_{\text{gen}}$, implying that M' = M and m = m'. In cases (A) - (E), we will see that, given a general form circuit $\mathcal{C}'_{\text{gen}}$ for \mathcal{C} as described in the lemma, we can construct a general form circuit $\mathcal{C}'_{\text{gen}}$ for \mathcal{C}' such that the left Cliffords of the two general forms are equal, i.e., L = L', and therefore so too are the stabilizer groups of $[n_{\text{in}}, k, L], [n_{\text{in}}, k', L']$. In what follows, we attach the prime symbol "'" to all of the parameters of the general form circuit $\mathcal{C}'_{\text{gen}}$, and when constructing it starting from \mathcal{C}_{gen} , we explicitly describe how primed objects are obtained, omitting those which are the same for both \mathcal{C}_{gen} an $\mathcal{C}'_{\text{gen}}$.

- (A) Operation g is a Clifford or Pauli unitary U. In this case, the transformation consists of removing R and U at the end of $\mathcal{C}_{\text{gen}} \circ g$ and adding the unitary R' = UR to form $\mathcal{C}'_{\text{gen}}$.
- (B) Operation g is the allocation of a qubit initialized to the zero state. Consider the case when we allocate a qubit which is placed before the first qubit, and initialize it to the zero state. The general case reduces to this case by applying SWAP gates, which is a Clifford unitary considered in (A). In this case, the transformation simply involves removing the Clifford R at the end of $C_{\text{gen}} \circ g$ and adding the unitary $R' = I \otimes R$, and defining A' by appending a row of zeros at the beginning of the rows of A to form a general form circuit with $n_{\text{out}}' = n_{\text{out}} + 1$.
- (C) Operation g is the deallocation of a qubit in the zero state. Consider the case when we deallocate the first qubit, which is assumed to be in the zero state prior to the application of g. The general case again reduces to this case by applying SWAP gates. Our strategy is to show that we can modify R and A in C_{gen} without changing the circuit's action such that A has a zero first row and R maps states $|0\rangle \otimes |\phi\rangle$ to states $|0\rangle \otimes |\psi\rangle$. When this is the case, we can form C'_{gen} by setting A' to be A without the first row, and obtaining R' from R defined by $(R'|\psi\rangle) \otimes |0\rangle = R(|\psi\rangle \otimes |0\rangle)$. The unitary R' defined in this way has a Choi state that is a stabilizer state and is therefore a Clifford unitary according to Lemma A.13 in [11]. Moreover, the unitary R' can be efficiently computed given its Choi state as discussed in Section 2.4.

First we specify the modifications of A and R. The fact that the qubit is guaranteed to be in the zero state prior to the application of g implies that Z_1 stabilizes the output state of \mathcal{C} (and therefore also the output state of $\mathcal{C}_{\mathrm{gen}}$). Given that Z_1 stabilizes the output of $\mathcal{C}_{\mathrm{gen}}$, it must be that Z_1 is in the stabilizer group of $[n_{\mathrm{out}}, k, R]$ and as such there must be some length- $(n_{\mathrm{out}} - k)$ bit string b such that $Z_1 = R(Z^b \otimes I_k)R^{\dagger}$. Let E be an invertible $(n_{\mathrm{out}} - k)$ by $(n_{\mathrm{out}} - k)$ matrix that maps the first basis vector e_1 to b. R is modified to $R(U_{E^{-T}} \otimes I_k)$ (where E^{-T} is the inverse transpose of E and $U_{E^{-T}}$ is the unitary defined by $U_{E^{-T}}|a\rangle = |E^{-T}a\rangle$ for every length- $(n_{\mathrm{out}} - k)$ bit string a) and A is modified to $E^T A$.

Next we confirm that the action of C_{gen} on the input state is preserved by this modification of A and R. Indeed, insert $U_{E^{-T}}^{\dagger}U_{E^{-T}}$ in the original general form circuit following X^{Ao} , and insert

 $U_{E^{-T}}$ before X^{Ao} . Applying $U_{E^{-T}}$ to the all zero state leaves it unchanged, $U_{E^{-T}}^{\dagger}U_{E^{-T}} = I$, and $U_{E^{-T}}^{\dagger}X^{Ar}U_{E^{-T}} = X^{E^{T}Ar}$ (using Proposition A.2), so the circuits are equivalent.

Lastly, we confirm that the modified A and R have the claimed form. Indeed, Z_1 conjugated by $U_{E^{-T}}$ is equal to $Z^{Ee_1} = Z^b$ (using Proposition A.2), and so $RU_{E^{-T}}$ maps Z_1 to Z_1 , which implies that it maps $|0\rangle \otimes |\phi\rangle$ to states $|0\rangle \otimes |\psi\rangle$ as required. The first row of E^TA must be zero since otherwise there would be some outcome vector o for which the first qubit is not output in state $|0\rangle$. This completes the deallocation case.

(D) Operation g is a Pauli unitary conditioned on the parity of a subset of outcomes of the outcome vector v of circuit \mathcal{C} . Specifically, g is specified by a Pauli P, a bit string c with the same length as v and a bit c_0 , such that P is applied when $\langle v, c \rangle = c_0$. Expressed in terms of the outcome vector o of the general form circuit \mathcal{C}_{gen} , the parity $\langle v, c \rangle$ is $\langle Mo + v_0, c \rangle = \langle v_0, c \rangle + \langle o, M^T c \rangle$. The action of $\mathcal{C} \circ g$ is equivalent to applying $R^{\dagger}PR$ before R in \mathcal{C}_{gen} , conditioned on the parity $\langle o, M^T c \rangle$ being equal to $\langle v_0, c \rangle + c_0$. We take the case of $\langle v_0, c \rangle + c_0 = 1$ (the case of $\langle v_0, c \rangle + c_0 = 0$ is reduced to this by replacing R with PR – crucially this replacement has no dependence on the outcome vector). The conditional Pauli can be written as $(R^{\dagger}PR)^{\langle o, M^T c \rangle}$, which we will now show can be represented by modifying the matrices A, A_x, A_z . This follows from the observation that $u\langle v, w\rangle = (uv^T)w$, where u, v and w are column vectors (with v and w having the same dimension), and where uv^T is a matrix obtained by the outer product of u and v. Indeed, if we write $(R^{\dagger}PR)$ as $X^{a_x \oplus b_x} Z^{a_z \oplus b_z}$ for a_x, a_z being $n_{\text{out}} - k$ dimensional vectors over \mathbb{F}_2 and b_x, b_z being k dimensional vectors over \mathbb{F}_2 , then we have

$$(R^{\dagger}PR)^{\langle o, M^Tc\rangle} = (X^{(a_xc^TM)o} \otimes X^{(b_xc^TM)o})(Z^{(a_zc^TM)o} \otimes Z^{(b_zc^TM)o}).$$

Therefore, $A' = A + a_x c^T M$, $A'_z = A_z + b_z c^T M$, and $A'_x = A_x + b_x c^T M$. Note that Z^{a_z} can be commuted past X^{Ax} in the general form and so is applied to the all zero state and can be removed.

- (E) Operation g is the allocation of a classical random bit distributed as a fair coin. Starting with C_{gen} , we set $n'_r = n_r + 1$, and add the additional random bit to the end of r. The matrices A', A'_x, A'_z can be obtained from matrices A, A_x, A_z by inserting a zero column after column n_r . The matrix M' is obtained from M by adding a zero column after column n_r and appending row $e_{n'_r}$, where $e_{n'_r}$ is n'_r -th standard basis vector. The vector v'_0 is obtained from v_0 by appending a 0. Note that M' and v'_0 have all the required properties when M and v'_0 do.
 - (F) Operation g is a measurement of a Pauli operator P, which we separate into three cases:
- **(F1)** $\pm P$ belongs to the stabilizer group of $[n_{\text{out}}, k, R]$ (redundant outcome).
- (F2) $\pm P$ does not belong to the stabilizer group of $[n_{\text{out}}, k, R]$, but commutes with all of its elements (input-dependent outcome).
- **(F3)** $\pm P$ anti-commutes with at least one element of the stabilizer group of $[n_{\text{out}}, k, R]$ (random outcome).

Let the preimage be $Q = R^{\dagger} P R$.

In case (F1), Q must be equal to $(-1)^{b_0}Z^b\otimes I_k$ for a non-zero vector b over \mathbb{F}_2 of dimension $n_{\text{out}}-k$, where $b_0\in\{0,1\}$. In this case, the general form circuits \mathcal{C}_{gen} and $\mathcal{C}'_{\text{gen}}$ are the same, however the parameters v'_0, M' of the outcome maps differ from v_0, M . The vector v'_0 equals v_0 with b_0 appended to the end, and the matrix M' is equal to M with a row A^Tb appended to the end, because the result of measuring P is equal to $b_0 + \langle b, Ao \rangle = b_0 + \langle A^Tb, o \rangle$. Note that M' has all the required properties when M does.

In case (F2), the operator Q must be equal to $Z^b \otimes Q'$, where Q' is a non-trivial k-qubit Pauli operator and b is a vector over \mathbb{F}_2 of dimension $n_{\text{out}} - k$. The action of \mathcal{C}' is equivalent to measuring Q' after applying X^{A_xo} in \mathcal{C}_{gen} , with outcome equal to the outcome of measuring P plus $\langle Ao, b \rangle$. Let C' be any k-qubit Clifford unitary such that $Q' = C'Z_1(C')^{\dagger}$. This means that measuring Q' is equivalent to applying $(C')^{\dagger}$, measuring Z_1 , and then applying C'. This equivalence implies that the general form circuit $\mathcal{C}'_{\text{gen}}$ has R' = RC', L' = LC', and k' = k - 1.

To derive A'_x, A'_z, M', A' for the general form circuit C'_{gen} , we follow several steps. First, we note that $X^{A_xo}Z^{A_zo}$ followed by the measurement of Q' is equivalent to applying C'^{\dagger} , followed by $X^{\tilde{A}_xo}Z^{\tilde{A}_zo}$, followed by measuring Z_1 , and finally applying C', for some \tilde{A}_x, \tilde{A}_z calculated using the identity:

$$C'X^{A_xo}Z^{A_zo}C'^{\dagger} \simeq X^{\tilde{A}_xo}Z^{\tilde{A}_zo}.$$

If we move the measurement of Z_1 before $X^{\tilde{A}_xo}$, it will add $\langle \tilde{A}_xo, e_1 \rangle$ to the measurement outcome. Therefore, we can conclude that $X^{A_xr}Z^{A_zr}$ followed by the measurement of Q' is equivalent to the following sequence of operations:

- 1. C'^{\dagger} ,
- 2. destructive measurement of Z_1 with outcome o_0 ,
- 3. applying $X^{A'_x o} Z^{A'_z o}$ on the last k-1 qubits, where A'_x , A'_z are \tilde{A}_x , \tilde{A}_z with the first row removed,
- 4. allocating a new first qubit in the zero state,
- 5. applying $X^{o_0+\langle \tilde{A}_x o, e_1 \rangle}$ to the allocated qubit,
- 6. applying C'.

The outcome of measuring Q' is $o_0 + \langle \tilde{A}_x o, e_1 \rangle$, and outcome of measuring Q is $o_0 + \langle \tilde{A}_x o, e_1 \rangle + \langle Ao, b \rangle$. The new outcome vector o' is obtained by concatenating o with o_0 , $o' = o \oplus o_0$, M' is obtained by adding a zero column to M and then adding row $(\tilde{A}_x^T e_1 + A^T b) \oplus 1$, and $v'_0 = v \oplus 0$. Note that M' has all the required properties when M does. Finally, A' is obtained by adding a zero column to A and then adding row $(\tilde{A}_x^T e_1) \oplus 1$. In this case, the stabilizer group of $[n_{\rm in}, k, L]$ is a proper subgroup of the stabilizer group of $[n_{\rm in}, k', L']$.

In case (F3), let P' be a Pauli operator from the stabilizer group of $\llbracket n_{\text{out}}, k, R \rrbracket$ that anticommutes with P. In this case, the measurement outcome r_0 is a uniformly distributed random
bit. Let b'_0, b' be defined using the preimage of P' as $(-1)^{b'_0}Z^{b'}\otimes I_k=R^{\dagger}P'R$. The output
state of C (which is the same as the output state of C_{gen}) is stabilized by $(-1)^{\langle Ao,b'\rangle}P'$. Using
Proposition 2.2, we see that measuring P is equivalent to applying $(P')^{r_0+\langle Ao,b'\rangle}e^{i\frac{\pi}{4}(iP'P)}$. For
this reason, the case (F3) reduces to applying unitary $e^{i\frac{\pi}{4}(iP'P)}$ as in case (A), allocating a
classical random bit r_0 as in case (E), and applying Pauli unitary P' conditioned on the parity
of the set of measurement outcomes indicated by A^Tb' and the random bit r_0 as in case (D).
As such the form of C'_{gen} is constructed from C_{gen} using those cases. In this case, $\llbracket n_{\text{in}}, k, L \rrbracket$ and $\llbracket n_{\text{in}}, k', L' \rrbracket$ are the same.

We say that a general form circuit \mathcal{C}_{gen} with equivalent action to a stabilizer circuit \mathcal{C} is a **general form of** the circuit \mathcal{C}_{gen} . Similarly, we say that a general form circuit \mathcal{C}_{gen} with equivalent action to a given quantum instrument is a **general form of** that quantum instrument.

The proof of Lemma 4.3 can be reformulated into a polynomial time algorithm for computing the general form of a stabilizer circuit, however the step (**F2**) requires a somewhat involved computation that scales as $O(n^{\omega})$ where n is the number of qubits and $\omega = \log_2 7$ in practice [4]. Instead, in Section 6 we show an algorithm that requires at most $O(n^2)$ runtime per gate. Our algorithm takes advantage of the relation between a general form stabilizer circuit and a Choi circuit as shown in Fig. 4.3.

The circuit in Fig. 4.3, which produces the Choi state of a general form circuit C_{gen} for each outcome vector o, is derived in a few steps. First, recall that Choi states can be produced using the Choi circuit in Fig. 2.1, which involves first initializing $2n_{\text{in}}$ qubits in $|\text{Bell}_{n_{\text{in}}}\rangle$ followed by applying the general form circuit in Fig. 4.1 to the top n_{in} qubits. Second, we use the identity $(L^{\dagger} \otimes I_{n_{\text{in}}})|\text{Bell}_{n_{\text{in}}}\rangle = (I_{n_{\text{in}}} \otimes L^*)|\text{Bell}_{n_{\text{in}}}\rangle$ to remove L^{\dagger} acting on the first n_{in} qubits and add L^* acting on the last n_{in} qubits. Third we observe that destructively measuring qubits $n_{\text{in}} - k$ through n_{in} with outcome m is the same as initialising qubits $n_{\text{in}} + 1, \ldots, 2n_{\text{in}} - k$ in the zero state before applying X^m to them. Finally, we remove Z^{Ao} acting on qubits $n_{\text{in}} - k$ through $n_{\text{in}} + k$

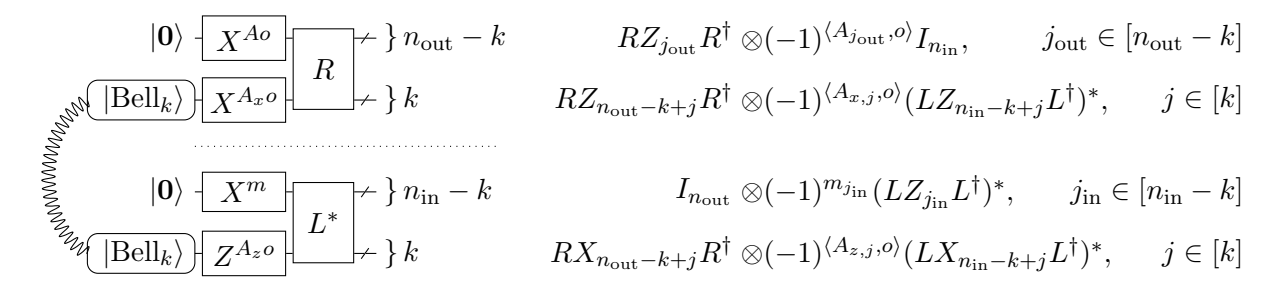


Figure 4.3: The circuit and the stabilizer group generators of the Choi state of the general form of a stabilizer instrument with $n_{\rm in}$ input qubits, $n_{\rm out}$ output qubits and n_r classical random bits. Clifford unitaries L and R act on $n_{\rm in}$ and $n_{\rm out}$ qubits, A, A_x , A_z are matrices over \mathbb{F}_2 , r is an n_r dimensional random vector over \mathbb{F}_2 . The general form outcome vector $o = r \oplus m$ has dimension $n_O = (n_{\rm in} - k + n_r)$, matrix A is $(n_{\rm out} - k) \times n_O$ matrix, A_x , A_z are $k \times n_O$ matrices.

We conclude with a couple observations that may aid the conceptual understanding of the general form and the next sections of the paper. The first observation concerns learning some parameters of a general form of a given circuit \mathcal{C} . Note that for all measurement outcomes, the Choi states in Fig. 4.3 are the same up to Pauli corrections, or, in other words, up to the signs of the Choi states' stabilizer group generators. This leads to a simple way of finding k and also learning L and R up to Pauli corrections as follows. First, compute the circuit's Choi state $|\Psi(o)\rangle$ using Algorithm 3.6 for any outcome vector o. Second, apply Theorem 2.10 and Fig. 2.4 to identify the k, L(o) and R(o) of that Choi state $|\Psi(o)\rangle$. One can see that when o is the zero vector, the variables L(o) and R(o) coincide with L and R in Fig. 4.3, which implies that L(o) and R(o) coincide with L and R up to Pauli corrections for any o. In Section 6 we extend this approach to form an algorithm to efficiently fully compute a general form of a stabilizer circuit.

The second observation is about interpreting the general form circuit from the perspective of quantum error correction. As already highlighted in Fig. 4.1 the general form circuit consists of three steps. The first step measures the generators of a stabilizer code $[n_{\rm in}, k, L]$, and then unencodes the code that was projected onto into the bottom k qubits. The second step applies Pauli operators to the bottom k qubits conditioned on both the syndrome of $[n_{\rm in}, k, L]$ measured in the first step and random bits r. The third step encodes the state of the k bottom qubits into a new stabilize code $[n_{\rm out}, k, R]$, with syndrome conditioned on both the syndrome of $[n_{\rm in}, k, L]$ and the random bits r.

In summary, the general form provides a convenient description of the action of a circuit: the input observables that it measures, the output observables that it stabilizes, and a mapping of the remaining observables. The input observables that the circuit measures are captured by the stabilizer group of $[n_{\text{in}}, k, L]$. The output observables that the circuit stabilizes are captured by the stabilizer group of $[n_{\text{out}}, k, R]$ up to a sign. The mapping of the remaining observable is captured by the left and right Clifford unitaries L and R up to signs as:

$$LZ_{n_{\rm in}-k+j}L^{\dagger} \to \pm RZ_{n_{\rm out}-k+j}R^{\dagger}, \quad LX_{n_{\rm in}-k+j}L^{\dagger} \to \pm RX_{n_{\rm out}-k+j}R^{\dagger}, \quad j \in [k].$$

The condition matrices A, A_x, A_z and M capture the dependence of the signs of the observables of the output state on the circuit outcomes.

5 Outcome-complete stabilizer circuit simulation

In Section 3.5 we provided an algorithm, similar to those already known in the literature [1], to solve the stabilizer circuit simulation problem given a specific outcome vector. Here we consider a stronger stabilizer circuit simulation problem which accounts for all possible outcome vectors. To efficiently encode the output of this outcome-complete stabilizer simulation problem Problem 5.1 (which naively would involve enumeration of an exponential number of possible outcome vectors) we leverage the general form in Section 4.

Problem 5.1 (Outcome-complete stabilizer circuit simulation). Consider any stabilizer circuit with no input qubits, n output qubits, and a length- n_M outcome vector. Find the vector of nonzero conditional probabilities $\overrightarrow{p} \in \{1, 1/2\}^{n_M}$, a Clifford unitary R, matrices A and M and a vector v_0 with entries in \mathbb{F}_2 that satisfy the following properties:

- each possible outcome vector v is an element of the set $\{Mr : r \in \{0,1\}^{n_r}\}$, where $n_r = |\{\overrightarrow{p}_k = 1/2 : k \in [n_M]\}|$,
- for any outcome vector, \overrightarrow{p}_j is the probability of obtaining outcome v_j given previous outcomes v_1, \ldots, v_{j-1} ,
- $R|Ar\rangle$ is the output state of the circuit given the outcome vector $v = v_0 + Mr$.

This outcome-complete Problem 5.1 differs from the outcome-specific Problem 3.5 in that the random outcomes of the circuit are no longer selected ahead of time. Instead, those outcomes are represented by a bit-vector r of arbitrary value. Note that when a circuit has no input qubits $(n_{\rm in} = 0)$, its general form (Fig. 4.1) simplifies to include only random bits r, state preparation based on those bits $X^{Ar}|0^n\rangle = |Ar\rangle$, and a subsequent Clifford unitary R, which sets the form of the output of Problem 5.1. Before we consider algorithms to solve Problem 5.1, we discuss various aspects of the problem structure and explain how a solution to Problem 5.1 for a given circuit can be used to solve any problem instance of Problem 3.5 for the same circuit.

A number of degrees of freedom exist for solutions to Problem 5.1 arising from the fact that the general form itself is not unique for a given circuit. First we describe a degree of freedom is for the matrix M. Note that given an invertible $n_r \times n_r$ matrix B, we can write set $\{r: r \in \{0,1\}^{n_r}\}$ as $\{Br': r' \in \{0,1\}^{n_r}\}$. Therefore for any such B, matrices M' = MB, A' = AB and B' = B satisfy the conditions in Problem 5.1 when matrices $B' = B^T M^T$ is in reduced row echelon form. This allows us, without loss of generality, to focus on solutions to Problem 3.5 for which the transpose of the matrix $B' = B^T M^T$ is in reduced row echelon form, which simplifies a number of linear-algebraic computations involving $B' = B^T M^T$ in reduced row echelon form, is to recall that Theorem 4.2 implies that $B' = B^T M^T$ in reduced row echelon form, is to recall that Theorem 4.2 implies that $B' = B^T M^T$ in reduced row echelon form.

It is informative to consider the structure of the matrix M in the solution to Problem 5.1, where M^T is in row-echelon form, in more detail (see Fig. 5.1). The number of rows and columns of M is n_M and n_r respectively. Since M has full column rank (as shown in Lemma 4.3), for each $j \in [n_r]$ there is a row in M with the form $0^{j-1}10^{n_r-j}$. These leading-zero rows appear in order of increasing j, and the sequence (l_1, \ldots, l_{n_r}) of row indices is the row rank profile of M.

Next we see that the vector \overrightarrow{p} in the solution to Problem 5.1 is redundant and can be constructed using the matrix M. Specifically the entry \overrightarrow{p}_l is equal to 1/2 for each l in the row rank profile of M, and is equal to 1 for each l not in the row rank profile of M. To see this, note that $r \in \{0,1\}^{n_r}$ is a uniformly random vector and consider the probability \overrightarrow{p}_l of obtaining the outcome v_l given previous outcomes v_1, \ldots, v_{l-1} , given the equation $v = v_0 + Mr$. We see that $\overrightarrow{p}_l = 1/2$ when l in the row rank profile of M since the lth row of M then has the form $0^{j-1}10^{n_r-j}$, and therefore the entry v_l is set by r_j (which is uniformly random), since $v_l = (v_0)_l + r_j$ (see Fig. 5.1) and r_j did not appear in v_1, \ldots, v_{l-1} . When l not in the row rank profile of M on the other hand, the lth row of M is not equal to $0^{j-1}10^{n_r-j}$, and the entry v_l equals $(v_0)_l$ plus a linear function of entries of r that have already appeared in

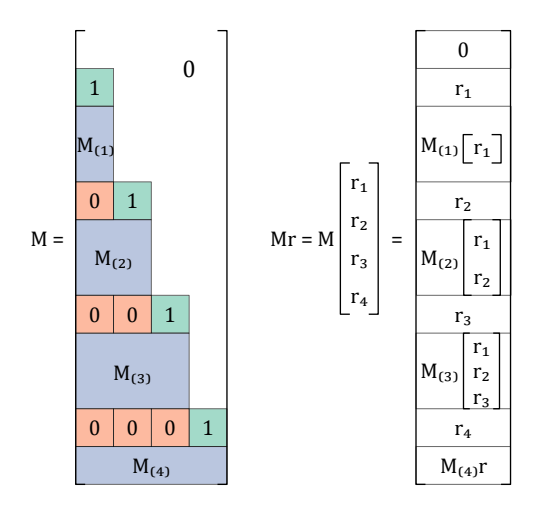


Figure 5.1: An illustration of an $n_M \times n_r$ matrix M that specifies the output of an instance of the outcome-complete Problem 5.1, where M^T is in reduced row-echelon form. For any such matrix M, for each $j \in [n_r]$ the l_j th row of M is $0^{j-1}10^{n_r-j}$, where l_j is the jth entry in the row rank profile of M. This structure ensures that when M acts upon any length- n_M bit string r, the jth entry of r appears as the l_j th entry of (Mr).

 v_1, \ldots, v_{l-1} (see Fig. 5.1), and therefore since \overrightarrow{p}_l is the *conditional* probability of v_l given v_1, \ldots, v_{l-1} , we see that it must be $\overrightarrow{p}_l = 1$.

Another freedom in the solution to Problem 5.1 allows us to assume without loss of generality that the vector $(v_0)_l = 0$ for l in the row rank profile of M. We can make this assumption because one can always replace r by $r' = r + r_{\text{shift}}$ and v_0 by $v'_0 = v_0 + Mr_{\text{shift}}$ in $v = Mr + v_0$, giving $v = Mr' + v'_0$ for any r_{shift} . Choosing $(r_{\text{shift}})_j = (v_0)_{l_j}$, where l_j is the jth entry in row rank profile of M, we see that $(v'_0)_l = 0$ for all l in the row rank profile of M.

We conclude with an explanation of how to solve the outcome-specific simulation Problem 3.5 using a solution to outcome-complete simulation Problem 5.1. As before, we assume that M^T is in reduced row echelon form. We first select the r that corresponds to the specific outcome for Problem 3.5 as follows. For each l such that the lth row of M is $0^{j-1}10^{n_r-j}$, set $r_j = \tilde{v}_l + (v_0)_l$. The solution to outcome specific simulation problem then has conditional probabilities \overrightarrow{p} , Clifford unitary RX^{Ar} and outcome vector $v = Mr + v_0$. This reduction from the outcome-complete simulation Problem 5.1 to the outcome-specific simulation Problem 3.5 is instructive for understanding the reduction in the opposite direction discussed in Section 5.1.

5.1 Solution with outcome-specific algorithm as a subroutine

One approach to solve the outcome-complete Problem 5.1 is Algorithm 5.2 which calls the outcome-specific Algorithm 3.6 $n_r + 1$ times.

Algorithm 5.2 constructs a solution to Problem 5.1 defined by M, v_0 , R and A, where M^T is in reduced row echelon form, and $(v_0)_l = 0$ for all l in the row rank profile of M. Such a solution always exists, as discussed above. The algorithm begins by calling the outcomespecific Algorithm 3.6 with $\tilde{v} = 0^{n_M}$, obtaining a Clifford $R^{(0)}$, an outcome vector $v^{(0)}$ and a conditional probability vector $\overrightarrow{p}^{(0)}$. From this, one can obtain some information about the outcome-complete solution, for example, we can straightforwardly identify $\overrightarrow{p} = \overrightarrow{p}^{(0)}$ since the conditional probability vector is independent of \tilde{v} . The vector \overrightarrow{p} allows us to identify the row rank profile of M, formed by sorting the set $\{l \mid \overrightarrow{p}_l = 1/2, l \in [n_M]\}$ into ascending order, and n_r is the size of the row rank profile of M.

Next, note that when we execute outcome-specific simulation algorithm for circuit \mathcal{C} with input vector \tilde{v} , the outcome vector v satisfies equality $v_{l_j} = (\tilde{v})_{l_j}$ for $j \in [n_r]$. This is because $p_l = 1/2$ if and only if $l = l_j$ for some $j \in [n_r]$. For input vector \tilde{v} , the outcome-specific simulation

Algorithm 5.2 (Outcome-complete via outcome-specific stabilizer simulation) Input: A stabilizer circuit \mathcal{C} with no input qubits, n output qubits, and n_M outcomes. Output:

- a vector $\overrightarrow{p} \in \{1, 1/2\}^{n_M}$ of conditional probabilities,
- a Clifford unitary R,
- matrices A, M and vector v_0 with entries in \mathbb{F}_2 ,

that satisfy conditions of Problem 5.1, additionally M^T is in reduced row echelon form and entries of v_0 corresponding to the row rank profile of M are zero.

- 1: Let $\overrightarrow{p}^{(0)}$, $R^{(0)}$, $v^{(0)}$ be results of outcome-specific stabilizer simulation of \mathcal{C} with $\tilde{v} = 0^{n_M}$
- 2: Set $R \leftarrow R^{(0)}, v_0 \leftarrow v^{(0)}, \overrightarrow{p} \leftarrow \overrightarrow{p}^{(0)}, j \leftarrow 1$
- 3: **for** $l \in [n_M]$ such that $\overrightarrow{p}_l = 1/2$ **do**

 $\triangleright n_r$ loop iterations

- 4: Let $\overrightarrow{p}^{(j)}$, $R^{(j)}$, $v^{(j)}$ be results of outcome-specific stabilizer simulation of \mathcal{C} with $\tilde{v} = e_l$
- 5: Set column j of M to $v^{(j)} + v_0$
- 6: Find bit string a from equality $|a\rangle = R^{\dagger}R^{(j)}|0^{n}\rangle$ and set column j of A to a
- 7: $j \leftarrow j+1$ \triangleright Ensures $M_l = 0^{j-1}10^{n_r-j}$
- 8: **return** vector \overrightarrow{p} , Clifford unitary R, matrices A, M and vector v_0

algorithm returns unitary $R^{(\tilde{v})}$ and vector $v^{(\tilde{v})}$ such that the output state upon outcome $v^{(\tilde{v})}$ is $R^{(\tilde{v})}|0^n\rangle=R|Ar^{(\tilde{v})}\rangle$, $r^{(\tilde{v})}$ must satisfy equation $v^{(\tilde{v})}=Mr^{(\tilde{v})}+v_0$ and $v^{(\tilde{v})}_{l_j}=(\tilde{v})_{l_j}$. We have $\tilde{v}_{l_j}=v^{(\tilde{v})}_{l_j}=(v_0)_{l_j}+Mr^{(\tilde{v})}_{l_j}=r^{(\tilde{v})}_j$ by definition of l_j , because M^T is in reduced row-echelon form and $(v_0)_{l_j}=0$.

Setting $\tilde{v}=0$ implies that we compute action corresponding to r=0, $R^{(0)}|0^n\rangle=R|0^n\rangle$. Setting $\tilde{v}=e_{l_j}$ gives us $R^{(e_{l_j})}|0^n\rangle=R|Ae_j\rangle$, $v^{(e_{l_j})}=Me_j+v_0$ which allows us to compute columns j of A and M. In total then we have used n_r calls of the outcome-specific algorithm.

5.2 Solution with explicit outcome-complete algorithm

Here we offer an alternative approach to solve the outcome-complete Problem 5.1 in the form of Algorithm 5.3, which is more efficient than the iterative approach.

The outcome-complete Algorithm 5.3 is structured similarly to the outcome-specific Algorithm 3.6. Each operation in the circuit is handled sequentially and the quantum state of the system is tracked as the algorithm proceeds. Most information about the state is encoded using a Clifford R, which is updated to reflect the corresponding action. In addition, the state depends on the random outcomes in the circuit – the effect of all possible outcomes are encoded by the the matrices A and M, which are updated incrementally as the algorithm proceeds. For qubit and bit allocation, the additional steps serve to properly adjust the dimensions of A and M. For random bit allocation in the outcome-specific simulation retrieves the value from \tilde{v} , while outcome-complete simulation adjusts M so that last entry of Mr is equal to the last entry of r for all r.

For qubit deallocation, additional steps make sure that matrix A is consistent with the modification of R by the disentangle procedure. In addition, in outcome complete-simulation it is required that the deallocated qubit is in the zero state prior to deallocation for all possible outcomes. Unconditional unitary operations are handled identically in both simulation algorithms. The most significant difference between the outcome-specific Algorithm 3.6 and the outcome-complete Algorithm 5.3 is in the handling of a conditional Pauli unitary, Lines 14 and 19, respectively. Note that conditional Paulis are also used to handle measurements with random outcomes.

In the outcome-specific case, values of outcomes on which the Pauli P is conditioned are known and phases of the Clifford R can be adjusted by direct application of P. In the outcome-complete case, P is first commuted through R by calculating the preimage $R^{\dagger}PR$. The z-part of this preimage commutes with input $|0^n\rangle$. The x-part of this preimage identifies inputs that

Algorithm 5.3 (Outcome-complete stabilizer circuit simulation)

Input: A stabilizer circuit \mathcal{C} with no input qubits, n output qubits, and n_M outcomes. Output:

- a vector $\overrightarrow{p} \in \{1, 1/2\}^{n_M}$ of conditional probabilities,
- a Clifford unitary R
- matrices A, M and vector v_0 with entries in \mathbb{F}_2

that satisfy conditions of Problem 5.1, additionally M^T is in reduced row echelon form and the entries of v_0 corresponding to the row rank profile of M are zero.

- 1: Initialize an empty vector \overrightarrow{p} , zero-qubit Clifford unitary R, dimension-zero matrices A, M, vector v_0 .
- 2: for g in C do

```
▶ allocation
 3:
        if g allocates qubit j, then
            replace R \leftarrow R \otimes_i I_2,
 4:
             insert a zero row into A after row j-1.
 5:
        else if g deallocates qubit j, where Z_j R |Ar\rangle = R |Ar\rangle for all r, then
 6:
             let j' be the position of the first non-zero bit of z(R^{\dagger}Z_{i}R)
 7:
             swap rows j, j' of A and remove row j from A
 8:
            disentangle(R, j)
 9:
            remove qubit j from R,
10:
        else if g allocates a random bit then
11:
            append 1/2 to \overrightarrow{p},
12:
             add a zero column to A,
13:
14:
             append zero to the end of v_0,
             add a zero column and row to M and set the last bit in the row to 1.
15:
                                                                                                    ▶ unitaries
        else if g is a unitary U then
16:
            replace R \leftarrow UR.
17:
18:
        else if g applies a Pauli unitary P if \langle c \rangle = c_0,
                   where \langle c \rangle is the parity of outcomes indicated by c \in \mathbb{F}_2^{n_M}, then
19:
            replace R \leftarrow P^{c_0+1}R followed by R \leftarrow P^{\langle v_0,c\rangle}R followed by a \leftarrow M^Tc
20:
             find preimage \tilde{P} = R^{\dagger}PR
                                                     \triangleright apply P conditioned on bits of r indicated by a
21:
             for all j such that x(\tilde{P})_i = 1, replace row A_i \leftarrow A_i + a.
22:
                                                                                              ▶ measurements
        else if g measures Pauli P given a hint Pauli P' such that [P, P'] = 1
23:
                  and P'R|0^{n(R)}\rangle = \pm R|0^{n(R)}\rangle then
24:
            find b' and \alpha such that preimage R^{\dagger}P'R = \alpha Z^{b'},
25:
            replace R \leftarrow e^{(\alpha^* \pi/4)PP'}R followed by a \leftarrow A^Tb' \oplus 1
26:
            allocate a random bit according to Line 11,
27:
             apply P' conditioned on bits of r indicated by a, according to Line 21.
28:
        else if q measures Pauli P, then
29:
            find preimage Q = R^{\dagger} P R.
30:
            if x(Q) = 0 (deterministic measurement) then
31:
                append 1 to \overrightarrow{p},
32:
                 add row A^T z(Q) to M and append s(Q)/2 to the end of v_0.
33:
            else (uniformly random measurement)
34:
35:
                let j be the position of first non-zero bit of x(Q),
                find image P' = RZ_iR^{\dagger} (which anticommutes with P).
36:
                measure P with assertion P' according to Line 24.
37:
```

38: **return** vector \overrightarrow{p} , Clifford unitary R, matrices A, M and vector v_0

can be flipped in order to induce the correct phases on the output.

Both algorithms differentiate between random and deterministic measurements in the same way. For deterministic measurement, the outcome-complete algorithm determines its dependence on the values of random bits, while outcome-specific algorithm simply calculates the deterministic outcome value. The random measurement is reduced to the measurement with a hint in both algorithms. In outcome-specific case the conditional Pauli operator only depends on the random bit corresponding to the random outcome, while in the outcome-complete case the conditional Pauli can depend on multiple random bits. This is because the phase of the hint Pauli can depend on multiple random bits. See Proposition 2.2 for more details on conditional Pauli use in the random measurement. The full set of differences between Algorithms 3.6 and 5.3 is indicated by highlights.

We omit a detailed discussion of the correctness of Algorithm 5.3 because the algorithm mirrors the proof of Lemma 4.3 for the special case where the number of input qubits is zero. There are two subtle details in the algorithm design that deserve a highlight. First, in Line 28 we apply Pauli P' conditioned on bits r indicated by a. This is different from applying P conditioned on the outcome vector bits indicated by c in Line 19, which is reduced to applying P conditioned on bits r indicated by a in Line 21. Second, we perform swap rows of A during deallocation in Line 6. The goal here is to make modification of A consistent with the modification of R by the procedure disentangle. Correctness of this step relies on the implementation details of the procedure disentangle and the step might need to be modified if a different implementation of procedure disentangle is used. The correctness of this step follows from propagating X^{Ar} (representing current simulation state $RX^{Ar}|0^n\rangle$) through Clifford unitaries applied within procedure disentangle using Proposition A.4. Finally we note that M^T constructed by Algorithm 5.3 is in reduced row-echelon normal form, which ensures that it has full column rank. This simplifies further linear-algebraic operations with M, such as computing left inverse of M.

5.3 Comparison of solutions

In Table 5.1 we summarize the run time complexities of the outcome-specific Algorithm 3.6 and the outcome-complete Algorithm 5.3.

In order to take advantage of constant-time bit string operations, we assume that each row of matrices A and M is represented by a bit string. In other words, matrices A and M are contiguous row-major arrays. To compute matrix-vector products M^Ta and A^Tb it is sufficient to compute the sum of rows of M and A indicated by a and b. This choice justifies the bit-string run time of conditional Paulis and measurements.

This choice of representation has tradeoffs. In particular, allocation and deallocation operations are limited by re-writing the corresponding arrays with new dimensions. A linked-list implementation would yield lower run time complexities of those operations, but increase the bit-string run time complexities of measurement operations.

Workarounds for allocation and deallocation costs are available. For example, maximum array sizes can be determined by pre-processing the circuit and re-using qubits when possible. As a practical matter, this can reduce cost by allocating memory as a single step up-front. It also reduces the run time complexity by eliminating the need to re-dimension matrices. If pre-processing is undesirable, one can use a qubit and random bit allocation strategy similar to those used for contiguous dynamically sized arrays, such as std::vector in C++. Consequently, we exclude random bit allocation from measurement operation run times in Table 5.1.

The run time per unitary operation is faster than the run time per measurement in Algorithm 5.3. One potential way to make these run times more balanced is to represent the state during outcome complete simulation as $X^{A_xr}Z^{A_zr}R|0^n\rangle$ as opposed to $RX^{Ar}|0^n\rangle=R|Ar\rangle$. We leave the investigation of this option for future work.

For our run time analysis we rely on both the image RPR^{\dagger} and preimage $R^{\dagger}PR$ calculation being possible in $O(|P|n_{\uparrow})$. The only line where we calculate the image is Line 36, where it is sufficient to calculate image up-to a phase because it is used to derive a hint Pauli P'. Omitting

	Outcome-complete (Algorithm 5.3)			Outcome-specific (Algorithm 3.6)		
Stabilizer operation	Line	Run time	bit string run time	Line	Run time	bit string run time
Qubit allocation	3	$O(n_{\updownarrow}^2 + n_r n_{\updownarrow})$	$O(n_{\updownarrow})$	3	$O(n_{\updownarrow}^2)$	$O(n_{\updownarrow})$
Qubit deallocation	6	$O(n_{\updownarrow}^2 + n_r n_{\updownarrow})$	$O(n_{\updownarrow})$	5	$O(n_{\updownarrow}^2)$	$O(n_{\updownarrow})$
Random bit allocation	11	$O(n_M n_{\updownarrow} + n_r n_{\updownarrow})$	$O(n_{\updownarrow})$	8	O(1)	O(1)
Unitary P , $\exp(P)$ Unitary $\Lambda(P,Q)$	16	$\frac{O(n_{\updownarrow} P)}{O(n_{\updownarrow}(P + Q))}$	$\frac{O(P)}{O(P + Q)}$	11	$\frac{O(n_{\updownarrow} P)}{O(n_{\updownarrow}(P + Q))}$	$\frac{O(P)}{O(P + Q)}$
Pauli P conditional on outcomes indicated by c	19	$O(n_{\updownarrow} P + n_r c + \frac{1}{n_r n_{\updownarrow}})$	$O(c + n_{\updownarrow})$	14	$O(n_{\updownarrow} P + c)$	O(P + c)
Measure Pauli P with a hint Pauli P'	24	$O(n_{\updownarrow}(P + P') + n_r n_{\updownarrow})$	$O(n_{\updownarrow})$	16	$O(n_{\updownarrow}(P + P'))$	O(P + P')
Measure Pauli P (deterministic)	31	$O(n_{\updownarrow} P +n_rn_{\updownarrow})$	$O(n_{\updownarrow})$	24	$O(n_{\updownarrow} P)$	O(P)
Measure Pauli P (random)	34	$O(n_{\downarrow}^2 + n_r n_{\uparrow})$	$O(n_{\updownarrow})$	27	$O(n_{\downarrow}^2)$	$O(n_{\updownarrow})$

Table 5.1: Complexity of outcome-complete (Algorithm 5.3) and outcome-specific (Algorithm 3.6) stabilizer simulation for each type of stabilizer operation (Definition 2.3). The integers n_{\downarrow} , n_r and n_M are the maximum number of qubits, the number of random outcomes, and the total number of outcomes in the circuit respectively. We neglect the run time required to increase the sizes of matrices A and M, or of vector v_0 in the run time of measurement operations.

the phase calculation can further speed-up the implementation of outcome-complete simulation by a constant factor.

Lastly, we compare the run time (in terms of the circuit parameters defined in Section 3.1) of the outcome-complete Algorithm 5.3 with that of Algorithm 5.2, which is built from $n_r + 1$ calls of the outcome-specific Algorithm 3.6. Comparing Eqs. (14) and (16) below, we find that outcome-complete simulation via Algorithm 5.3 saves a factor of $n_r + 1$ over Algorithm 5.2 for contributions from unitaries, measurements with random outcomes and qubit deallocations.

The run time of the outcome-complete simulation Algorithm 5.3 is

$$O(n_{1} \cdot (N_{u} + (N_{cnd} + n_{M})(n_{r} + 1) + n_{1}(n_{1} + n_{r}))). \tag{14}$$

This formula is a sum of contributions from Table 5.1 including: $O(n_{\updownarrow} \cdot N_{\rm u})$ for unitaries, $O(n_{\updownarrow} \cdot N_{\rm cnd} \cdot (n_r + 1))$ for conditional Paulis, and $O(n_M(n_{\updownarrow}n_r + n_{\updownarrow}) + n_r \cdot n_{\updownarrow}^2)$ for measurements. For this analysis we assume that matrices M, A and R, are pre-allocated with run time costs $O(n_M \cdot n_r)$, $O(n_{\updownarrow} \cdot n_r)$ and $O(n_M^2)$, which are less than the other stabilizer operation costs. Additionally we use a qubit deallocation strategy described in Appendix C that contributes run time $O(n_{\updownarrow}^2 \cdot (n_{\updownarrow} + n_r))$.

An analogous analysis of the outcome-specific simulation Algorithm 3.6 yields a run time of

$$O\left(n_{\updownarrow}\cdot\left(N_{\mathsf{u}}+N_{\mathsf{cnd}}+n_{M}+n_{\updownarrow}(n_{\updownarrow}+n_{r})\right)\right). \tag{15}$$

Using $n_r + 1$ calls of outcome-specific Algorithm 3.6, the run time of Algorithm 5.2 is then

$$O(n_{\uparrow} \cdot (N_{\mathsf{u}}(n_r+1) + (N_{\mathsf{cnd}} + n_M)(n_r+1) + n_{\uparrow}(n_{\uparrow} + n_r)(n_r+1))). \tag{16}$$

Algorithm 5.2 includes n_r Clifford unitary multiplications, each with run time $O(n_{\downarrow}^3)$. But that contribution is less than the cost of $n_r + 1$ outcome-specific simulations.

6 Computing a general form of a stabilizer circuit

In Theorem 4.2 in Section 4 we showed that every stabilizer circuit, no matter how long and complex, has equivalent action to some circuit of the simple class of **general form circuits** shown in Fig. 4.1. In this section we present Algorithm 6.2, which efficiently finds an explicit general form circuit with equivalent action for any input stabilizer circuit. This algorithm is built upon the outcome-complete stabilizer simulation Algorithm 5.3 presented in the previous section.

Our general form Algorithm 6.2 produces a general form circuit \mathcal{C}_{gen} with equivalent action to the input stabilizer \mathcal{C} in two stages. First, the algorithm computes a general form circuit $\mathcal{C}'_{\text{gen}}$ for the Choi circuit \mathcal{C}' of \mathcal{C} (Fig. 2.1). Second, the algorithm computes the general form circuit \mathcal{C}_{gen} from the Choi circuit's general form $\mathcal{C}'_{\text{gen}}$. The first stage performs an outcome-complete simulation of the Choi circuit \mathcal{C}' , which can be done since the Choi circuit has no input qubits. The description of the circuit can be made more compact by using an outcome compression procedure, which also ensures that the run time of the second stage depends only on the number of input and output qubits in \mathcal{C} , and not on its length. The second stage relies on a subroutine to compute the bipartite normal form of the family of stabilizer states corresponding to the Choi circuit general form.

In the remainder of this section, we first specify the bipartite normal form Problem 6.1 for a family of stabilizer states. This is a generalization of the bipartite normal form Problem 2.11 for a single stabilizer state, and its structure is crucial to understand our general form Algorithm 6.2. We then present Algorithm 6.2, discuss its correctness and analyze its run time. Lastly, in Section 6.1 we provide the procedure which solves Problem 6.1, and in Section 6.2 we provide the compression map subroutine which can be optionally used following Algorithm 6.2 to make the output more compact.

Problem 6.1 (Bipartite normal form of a family of stabilizer states). Consider an n-qubit Clifford C that defines a family of stabilizer states $\{C|a\}_{a\in\{0,1\}^n}$ and an integer $n_1 < n$ that defines a bipartition into the first n_1 qubits and the remaining $n_2 = n - n_1$ qubits. Find an $n \times n$ matrix F over \mathbb{F}_2 , an integer k and Clifford unitaries L, R such that the circuit identity in Fig. 6.1 holds for all $a \in \{0,1\}^n$.

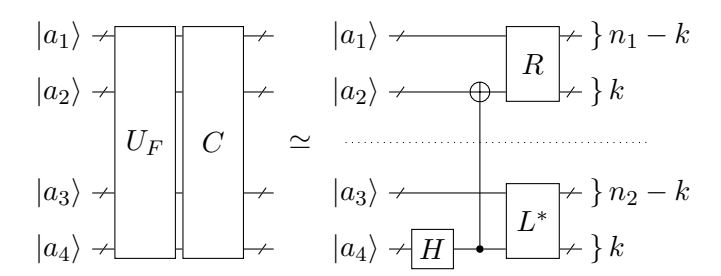


Figure 6.1: For any Clifford unitary C there exist an $n \times n$ invertible matrix F such that the states produced by applying C to computational basis states $|Fa\rangle$ can instead be produced (up to a global phase) by applying the sequence of smaller unitaries to $|a\rangle$ as shown. Note that the Hadamards followed by CNOTs produce k Bell states (up to Paulis) across the bipartition $[n_1], [n_1 + 1, n_1 + n_2]$ of the $n_1 + n_2$ qubits, and the Clifford unitaries R, L^* which follow act on qubits $[n_1], [n_1 + 1, n_1 + n_2]$. Also note that this figure coincides with Fig. 2.4 when $a = 0^n$.

Given a procedure that solves Problem 6.1, the following Algorithm 6.2 finds the general form of a stabilizer circuit C.

Algorithm 6.2 (Stabilizer circuit general form)

Input: A Clifford circuit C with n_{in} input qubits, n_{out} output qubits, n_M outcomes. Output:

- A general form C_{gen} of C (i.e. of the form shown in Fig. 4.1) with left Clifford unitary L, right Clifford unitary R, and condition matrices A, A_x, A_z, n_r random bits, n_m measurement outcomes,
- A matrix M and vector v_0 over \mathbb{F}_2 defining the outcome relation, that is action of \mathcal{C}_{gen} upon outcome o is equivalent to the action of C upon outcome $v = v_0 + Mo$. Additionally M is in (n_r, n_m) -split reduced echelon form, and entries of v_0 corresponding to the row rank profiles of the left and right parts of M are zero.

 \triangleright Find general form C'_{gen} of the Choi circuit of C

- 1: Let \mathcal{C}' be the Choi circuit of \mathcal{C} (see Section 2.2).
- 2: Find the Clifford unitary C, matrices A', M' and the vector v_0 over \mathbb{F}_2 corresponding to outcome-complete simulation of \mathcal{C}' (Algorithm 5.3), defining its general form $\mathcal{C}'_{\text{gen}}$.
 - \triangleright Find a general form \mathcal{C}_{gen} of \mathcal{C} from \mathcal{C}'_{gen}
- 3: Find the integer k, the basis-change matrix F that brings $C|A'r'\rangle$ (for all r') into bipartite normal form with unitaries L, R over the qubit bipartition $[n_{\text{out}}]$, $[n_{\text{out}}+1, n_{\text{out}}+n_{\text{in}}]$ (Fig. 6.1, Problem 6.1, Procedure 6.5).
- 4: Let $\tilde{C} = CU_F$, set $k_1 = n_{\text{out}} k$, $k_2 = n_{\text{in}} k$, n'_r to the number of columns of A'
- 5: Find an $n'_r \times n'_r$ invertible matrix B and a $k_2 \times k_2$ matrix A_μ such that \triangleright Procedure B.1

$$(F^{-1}A')_{[n_{\text{out}}+1,n_{\text{out}}+k_2]}B = (\mathbf{0}_{k_2 \times (n'_r-k_2)}|A_\mu),$$

and such that B is in $(n'_r - k_2, k_2)$ -split reduced echelon form.

- 6: $L \leftarrow L(U_{A_{\mu}} \otimes I_k)$
- 7: Assign matrices A, A_x, A_z, M as follows:

 - $A = (F^{-1}A'B)_{[k_1]}$. $A_x = (F^{-1}A'B)_{[k_1+1,n_{\text{out}}]}$. $A_z = (F^{-1}A'B)_{[n_{\text{out}}+k_2+1,n_{\text{out}}+n_{\text{in}}]}$.
 - \bullet M = M'B.
- 8: **return** L, R, A, A_x, A_z defining \mathcal{C}_{gen} , and M, v_0 defining outcome map

To verify the correctness of Algorithm 6.2, it can be interpreted as a sequence of transformations. In the first stage of the algorithm (consisting of Lines 1 and 2) we construct the Choi circuit \mathcal{C}' of the input circuit and then find a general form $\mathcal{C}'_{\mathrm{gen}}$ of \mathcal{C}' . In more detail, Line 2 replaces the Choi circuit \mathcal{C}' of \mathcal{C} with an equivalent general form circuit $\mathcal{C}'_{\mathrm{gen}}$ that allocates qubits $|0^{n_{\text{out}}+n_{\text{in}}}\rangle$, allocates random bits r, applies Pauli unitaries $X^{A'r}$ conditioned on r, and then applies a Clifford unitary C, by applying the outcome-complete stabilizer simulation Algorithm 5.3.

Now we enter the second stage of the algorithm (consisting of Line 3 to Line 7), in which the circuit C'_{gen} is further transformed into the Choi circuit $(C_{gen})'$ of the general form (Fig. 4.3), from which the parameters of the desired general form \mathcal{C}_{gen} of \mathcal{C} can be read off. To do so we begin by inserting $I = U_F U_{F^{-1}}$ between $X^{A'r}$ and C, after which U_F is absorbed into C (Line 4) and F^{-1} is absorbed into A' via $U_{F^{-1}}X^{A'r}|0^{n_{\text{out}}+n_{\text{in}}}\rangle = |F^{-1}A'r\rangle$ (Line 5). The basis change Flets us replace the Clifford unitary C with a circuit that creates k Bell pairs from $|0^{2k}\rangle$ followed by $D \otimes B^*$, as in Fig. 6.1. By the end of Line 4, the transformation to $(\mathcal{C}_{gen})'$ is nearly complete, except that unitary $X^{F^{-1}A'r}$ is parameterized by r, the random outcomes of \mathcal{C}' , and not by o, the outcomes of the general form \mathcal{C}_{gen} . Line 5 finds a relation between the two, r = Bo, which is then used to make the necessary adjustments on Line 7. The relation matrix B is obtained by using Procedure B.1 to ensure that M = M'B is in $(n'_r - k_2, k_2)$ -split reduced echelon form. It follows from Proposition A.10 that M is in $(n'_r - k_2, k_2)$ -split reduced echelon form since $(M')^T$ is in $(n'_r,0)$ -split echelon form and B is in (n'_r-k_2,k_2) -split reduced echelon form. We can successfully find B in Line 5 according to Proposition A.9. The proposition applies because according to Lemma A.8 the set of stabilizer states $\{\tilde{C}|F^{-1}A'r'\rangle\}_{r\in\mathbb{F}_2^{n'r}}$ has a certain property, called phase-completeness, defined in Appendix A (Definition A.7). In Line 6 we use the identity

 $U_{A_{\mu}}X^{m}U_{A_{\mu}}^{\dagger}=X^{A_{\mu}m}$ (Proposition A.2), note that $U_{A_{\mu}}^{\dagger}|0^{k_{2}}\rangle=|0^{k_{2}}\rangle$, and absorb $U_{A_{\mu}}$ into L. The last circuit transformation step to get to $(\mathcal{C}_{\text{gen}})'$ is to propagate $X^{A_{x}o}, X^{A_{z}o}$ through the unitary that creates k Bell pairs in Fig. 6.1. Then we have $a_{1}=Ao, a_{2}=A_{x}o, a_{3}=(0|I_{n_{\text{in}}-k})o, a_{4}=A_{z}o$. The entries of v_{0} corresponding to the row rank profile of M' are exactly the entries of v_{0} corresponding to the row rank profiles of the left and the right parts of M', and are therefore zero.

We conclude with a run time analysis. In terms of the circuit parameters defined in Section 3.1, the run time of the general form Algorithm 6.2 is

$$O(n_{\uparrow} \cdot (N_{u} + (N_{cnd} + n_{M})(n_{r} + n_{m} + 1) + n_{\uparrow}(n_{\uparrow} + n_{r}))). \tag{17}$$

This expression is equal to Eq. (14) (the run time of the outcome-complete simulation Algorithm 5.3), but with n_r replaced by $n_m + n_r$. This is because the run time of the general form Algorithm 6.2 is dominated by the outcome-complete simulation of the Choi circuit \mathcal{C}' of the input circuit in Line 2. The Choi circuit \mathcal{C}' has most of the same parameters as the input circuit \mathcal{C} except the number of random outcomes $n'_r = n_r + n_m$, the number of unitary operations $N'_{\tt u} \leq N_{\tt u} + 2n_{\tt t}$ and the maximum number of qubits used throughout the circuit $n'_{\tt t} \leq 2n_{\tt t}$.

Let us now discuss the run time for the rest of the steps of Algorithm 6.2 and establish that they are all less than the run time of the outcome-complete simulation Line 2 (and can therefore be neglected). The bipartite normal form computation in Line 3 has run time $O((n_{\rm in} + n_{\rm out})^3)$ which is $O(n_{\downarrow}^3)$ (Eq. (19)). The run time of finding the Clifford \tilde{C} in Line 4 and of updating the Clifford L in Line 6 is $O(n_{\downarrow}^3)$. The run time of computing the outcome relabelling matrix L in Line 5 is $O(n_m(n_r + n_m))$ (Eq. (46)). The run time of updating matrices L and L in Line 7 is L is L in L in Eq. (49), and the run time of updating the matrix L is L in Eq. (50). The run time of optionally finding a more compact representation of the general form circuit using Procedure 6.6 is L is L (10). The bound L in Eq. (20). The bound L in the implies that run time of the general form algorithm is dominated by the outcome-complete simulation of the Choi circuit L.

6.1 Bipartite normal form of a family of stabilizer states

Here we introduce the bipartite normal form Procedure 6.5, which forms a key subroutine of our stabilizer circuit general form Algorithm 6.2. This procedure solves the bipartite normal form Problem 6.1 for a family of stabilizer states, which was stated at the beginning of Section 6 and which generalizes the previously studied bipartite normal form Problem 2.11 for a single stabilizer state stated in Section 2.4.

To solve Problem 6.1, the bipartite normal form Procedure 6.5 must find a basis-change matrix F that ensures the following properties of the matrix $\tilde{C} = CU_F$:

- (A) images $\tilde{C}Z_1\tilde{C}^{\dagger}$, ..., $\tilde{C}Z_{n_1-k}\tilde{C}^{\dagger}$ are supported on $[n_1]$,
- (B) images $\tilde{C}Z_{n_1+1}\tilde{C}^{\dagger}$, ..., $\tilde{C}Z_{n-k}\tilde{C}^{\dagger}$ are supported on the complement $[n_1+1,n]$,
- (C) images $\tilde{C}Z_{n_1-k+j}\tilde{C}^{\dagger}$, $\tilde{C}Z_{n-k+j}\tilde{C}^{\dagger}$ for $j\in[k]$ form a symplectic basis when restricted to $[n_1]$, and also form a symplectic basis when restricted to $[n_1+1,n]$.

To construct such a basis-change matrix F, Procedure 6.5 uses two subroutines. The first subroutine, Procedure 6.3, helps us find blocks of F that ensure properties (A) and (B) hold, while the second subroutine, Procedure 6.4, helps fill in the remaining parts of F to ensure property (C) holds. As an abstract algorithm, Procedure 6.3 computes the subgroup of a stabilizer group $G = \langle P_1, \ldots, P_m \rangle$ for which the support of every element is contained in some subset of qubits K. We will see later how this helps to ensure (A) and (B) hold within Procedure 6.5.

Procedure 6.3 (support-restricted subgroup) Input:

• A sequence of *n*-qubit commuting Pauli unitaries P_1, \ldots, P_m ,

• a set $K \subset [n]$.

Output: An $m' \times m$ full-row-rank matrix F over \mathbb{F}_2 such that

$$\langle P_1^{F_{j,1}} \dots P_m^{F_{j,m}} : j \in [m'] \rangle = \{P : P \in \langle P_1, \dots, P_m \rangle, \operatorname{supp}(P) \subseteq K\}.$$

- 1: Define $K^c = \{j_1, \dots, j_{|K^c|}\}$, the complement of K.
- 2: Initialize an $m \times 2|K^c|$ matrix A over \mathbb{F}_2 with rows

$$A_i = (z(P_i)_{j_1}, \dots, z(P_i)_{j_{|K^c|}}, x(P_i)_{j_1}, \dots, x(P_i)_{j_{|K^c|}}), \text{ for } i \in [m].$$

3: Find F such that rows of F form a basis of kernel of A^T and **return** F.

Procedure 6.3 works by noting that the desired products of P_1, \ldots, P_m are those that have trivial support on the **complement** of K. The matrix A, constructed on Line 2, identifies the support of G on the complement. Then, the kernel of A^T corresponds to indicator vectors v for which the product $A^T v = 0$ has trivial support on K^c . That is, the support of $P_1^{v_1} \dots P_m^{v_m}$ is a subset of K. Using a row reduced echelon form to compute the kernel basis (Eq. (52)), the runtime complexity of Procedure 6.3 is $O(nm^{\omega-1})$. We call F an **indicator matrix**, and rows of F indicator vectors, because they indicate how to construct new Pauli unitaries $P_1^{F_{j,1}}\dots P_m^{F_{j,m}}$ out of Pauli unitaries P_1, \ldots, P_m .

Next we provide Procedure 6.4, which finds a symplectic basis of a Pauli group. We will see later how this helps to ensure property (C) holds within Procedure 6.5.

Procedure 6.4 (symplectic basis)

Input: Pauli unitaries P_1, \ldots, P_{2m} such that $B_{i,j} = \llbracket P_i, P_j \rrbracket$ is an invertible matrix. **Output:** A $2m \times 2m$ matrix F over \mathbb{F}_2 such that generators $\{P_1^{F_{j,1}} \ldots P_{2m}^{F_{j,2m}} : j \in [2m]\}$ form a symplectic basis (Definition 2.1).

```
1: Initialize F = I_{2m}, and Pauli unitaries Q_j = P_j for j \in [2m].
```

- 2: **for** $k \in [m]$ **do**
- Find the minimum j > 2k 1 such that $[Q_{2k-1}, Q_j] = 1$.
- Swap rows F_{2k} and F_i , Q_{2k} and Q_i 4:
- for $i \in [2k+1, 2m]$ do 5:
- let $a = [Q_{2k-1}, Q_i]$ and $b = [Q_{2k}, Q_i]$, 6:
- replace row $F_i \leftarrow F_i + a \cdot F_{2k-1} + b \cdot F_{2k}$, 7:
- replace $Q_i \leftarrow Q_i Q_{2k-1}^a Q_{2k}^b$.
- 9: **return** $2m \times 2m$ matrix F

Procedure 6.4 works by sequentially selecting each anticommuting pair (Line 3), which always succeeds because we require that matrix B is invertible. Once a pair is selected, the remaining generators are adjusted in order to commute with both elements of the pair (Line 8). The complexity of Line 8 (which is O(n) for run time and O(1) for bit-string run time) limits the overall complexity, which is $O(nm^2)$ for run time and $O(m^2)$ for bit-string run time. If the $2m \times 2m$ matrix $B_{i,j} = [P_i, P_j]$ is known ahead of time then Lines 3, 6 and 8 can be replaced with cheaper operations on B, reducing the run time to $O(m^3)$. Finally, note that it is easy to modify the algorithm to simultaneously compute F and F^{-1} . This is because adding row 2k-1 to row i of F in Line 7 is the same as $F \leftarrow (I+e_ie_i^T)F$, and so F^{-1} can be updated as $F^{-1} \leftarrow F^{-1}(I + e_i e_i^T)^{-1}.$

With Procedure 6.3 and Procedure 6.4 in hand we are in position to solve Problem 6.1. Procedure 6.5 outputs a basis-change matrix F for a Clifford C such that the Z images of the Clifford CU_F are partitioned into three subsets with specific properties (see Fig. 6.2b).

Procedure 6.5 (Bipartite normal form of a family of stabilizer states)

Input: An n-qubit Clifford C, integer n_1 .

Output: An $n \times n$ matrix F over \mathbb{F}_2 , integer k and Clifford unitaries L, R that satisfy conditions

1: Find a $k_1 \times n$ indicator matrix F_1 for $\langle CZ_1C^{\dagger}, \ldots, CZ_nC^{\dagger} \rangle$ restricted to $[n_1]$ (Procedure 6.3).

- 2: Find a $k_2 \times n$ indicator matrix F_2 for $\langle CZ_1C^{\dagger}, \ldots, CZ_nC^{\dagger} \rangle$ restricted to $[n_1+1, n]$ (Procedure 6.3).
- 3: Set $k = n_1 k_1$, set $n_2 = n n_1$.
- 4: Let $F_{12} = \left(\frac{F_1}{F_2}\right)$, the concatenation of rows from F_1 and F_2 .
- 5: Complete F_{12} into a full-rank $n \times n$ invertible matrix \hat{F} .
- 6: Let $\hat{C} = CU_{\hat{F}^{-1}}$, find a matrix \tilde{F} for transforming $\hat{C}Z_{k_1+k_2+1}\hat{C}^{\dagger}$, ..., $\hat{C}Z_n\hat{C}^{\dagger}$ restricted to first n_1 qubits into a symplectic basis (Procedure 6.4).
- 7: Let $A = (I_{k_1 + k_2} \oplus \tilde{F})\hat{F}$, set⁵

$$F = \left(\frac{\frac{A_{[k_1]}}{A_{[n-2k+1:2:n]}}}{\frac{A_{[k_1+1,k_1+k_2]}}{A_{[n-k+2:2:n]}}}\right)^{-1}.$$

- 8: Set $\tilde{C} = CU_F$.
- 9: Construct R acting on n_1 qubits as follows (see Fig. 6.2b):
 - 1. Set images RZ_jR^{\dagger} so that $RZ_jR^{\dagger}\otimes I_{n_2}=\tilde{C}Z_j\tilde{C}^{\dagger}$, for $j\in[k_1]$. 2. Set images $RZ_{k_1+j}R^{\dagger}$ to $\tilde{C}Z_{k_1+j}\tilde{C}^{\dagger}$ restricted to K, for $j\in[k]$.

 - 3. Set images $RX_{k_1+j}R^{\dagger}$ to $\tilde{C}Z_{n_2+k_1+j}\tilde{C}^{\dagger}$ restricted to K, for $j\in[k]$.
 - 4. Complete R to a full Clifford by setting (arbitrarily) images RX_jR^{\dagger} for $j \in [k_1]$.
- 10: Construct L acting on n_2 as follows (see Fig. 6.2b):
 - 1. Set images $L^*Z_j(L^*)^{\dagger}$ so that $I_{n_1} \otimes L^*Z_j(L^*)^{\dagger} = \tilde{C}Z_{n_1+j}\tilde{C}^{\dagger}$, for $j \in [k_2]$.
 - 2. Set images $L^*Z_{k_2+i}(L^*)^{\dagger}$ so that

$$RZ_{k_1+j}R^{\dagger} \otimes L^*Z_{k_2+j}(L^*)^{\dagger} = \tilde{C}Z_{k_1+j}\tilde{C}^{\dagger}, j \in [k].$$

3. Set images $L^*X_{k_2+i}(L^*)^{\dagger}$ so that

$$RX_{k_1+j}R^{\dagger} \otimes L^*X_{k_2+j}(L^*)^{\dagger} = \tilde{C}Z_{n_1+k_2+j}\tilde{C}^{\dagger}, j \in [k].$$

- 4. Complete L to a full Clifford by setting (arbitrarily) images $L^*X_j(L^*)^{\dagger}$ for $j \in [k_2]$.
- 11: **return** matrix F, integer k, Clifford unitaries L, R

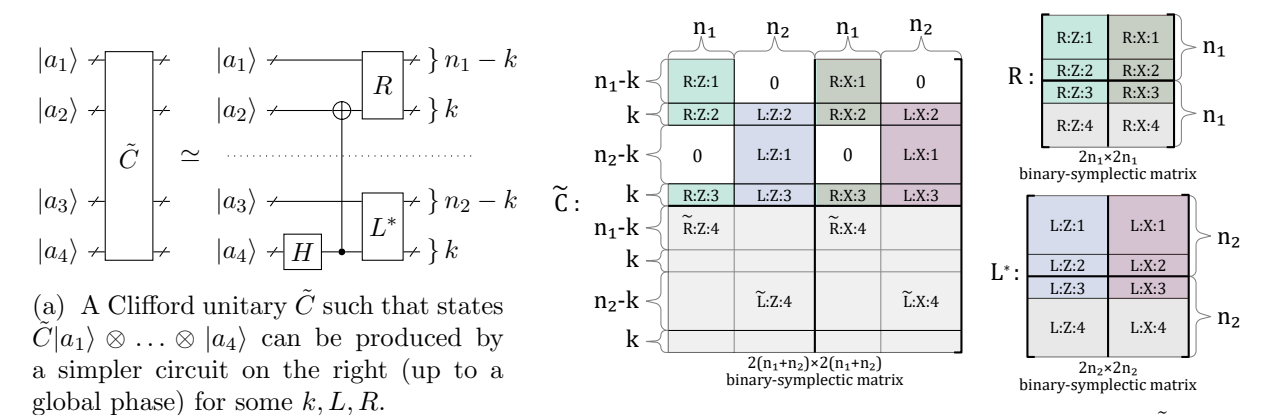
Next we briefly discuss the correctness of Procedure 6.5. The matrix \tilde{C} in Line 8 satisfies properties in Problem 6.1 since, by Proposition A.2,

$$(CU_F)Z_j(U_F^{\dagger}C^{\dagger}) = CZ^{(F^{-1})^T}e_jC^{\dagger} = CZ^{F_j^{-1}}C^{\dagger} = \prod_{i=1}^n (CZ_iC^{\dagger})^{(F^{-1})_{j,i}}.$$

It is then sufficient to check that rows of F^{-1} assigned in Line 7 are ordered as required by Problem 6.1 and also satisfy the required properties. Note that F^{-1} is matrix A with permuted rows. We constructed matrix A such that first k_1 rows indicate products of $CZ_1C^{\dagger}, \ldots, CZ_nC^{\dagger}$ supported on first n_1 qubits (Line 1), next k_2 rows indicate the products supported on the last n_2 qubits (Line 2), and the rest of rows indicate the products that form a symplectic basis when restricted to first n_1 qubits (Line 6). Fig. 6.2b shows how binary-symplectic parts of L, R can be constructed from C. We need to make sure that image and preimage phases of L,R are assigned so the that circuit in Fig. 6.1 is correct. One way to ensure this is shown in steps 2 and 3 within Line 10.

For step 4 in Lines 9 and 10 we note that images RX_jR^{\dagger} for $j \in [k_1], L^*X_j(L^*)^{\dagger}$ for $j \in [k_2]$ can be set arbitrarily. We can use blocks of binary-symplectic matrix of C to make these steps more efficient. In Fig. 6.2b we can set blocks R:Z:4, R:X:4 of R to blocks R:Z:4, R:X:4 of C.

⁵We use notation $A_{[k:2:l]}$ for rows $k, k+2, \ldots$ of matrix A



(b) Blocks of binary-symplectic representations of \tilde{C} , L, R

Figure 6.2: Given any Clifford unitary \tilde{C} , such that the circuit identity (a) holds for all computational basis states $|a_1\rangle, \ldots, |a_4\rangle$, Clifford unitaries L^* , R can be constructed using blocks of \tilde{C} as shown in (b). Blocks \tilde{R} :Z:4, \tilde{R} :X:4, \tilde{L} :X:4, \tilde{L} :X:4 do not appear in blocks of D, B^* , however can be used to compute blocks R:Z:4, R:X:4, L:X:4, L:Z:4 that appear in R, L^* more efficiently (see discussion around Eq. (18)).

This ensures that images RX_jR^{\dagger} for $j \in [k_1]$ have correct commutation relations with images of RZ_jR^{\dagger} for $j \in [k_1]$:

$$[\![RX_jR^{\dagger}, RZ_{j'}R^{\dagger}]\!] = \delta_{j,j'}, \ j,j' \in [k_1].$$
 (18)

It remains then to adjust images RX_jR^{\dagger} for $j \in [k_1]$ so that they have correct commutation relations with RX_jR^{\dagger} , RZ_jR^{\dagger} for $j \in [n_1 - k + 1, n_1]$ which has run time $O(kn^2)$. Similarly we can set $L^*X_j(L^*)^{\dagger}$ for $j \in [k_2]$ more efficiently.

We discuss run time of Procedure 6.5 in terms of parameters n and k. The second parameter k is computed by the procedure, however it is frequently known ahead of time in practice. The matrix multiplications, matrix inversions, full-rank completions and kernel basis calculations are all $O(n^{\omega})$ (Eq. (52),Eq. (54)). Finding a symplectic basis in Line 6 is $O(nk^2)$ and constructing unitaries L, R is $O(kn^2)$. We conclude that run time of Procedure 6.5 is

$$O(n^{\omega} + kn^2). \tag{19}$$

6.2 Outcome compression

The general form circuit in Fig. 4.3 is not unique, in part, because there are degrees of freedom in the use of the random vector r. For example, two general form circuits may be equal up to remapping of random vectors. More precisely, given any invertible square matrix F, we can produce a new general form circuit equivalent to a given general form circuit by substituting r = Fr' and changing matrices A, A_x, A_z to $A(F \oplus I_{n_{\text{in}}-k}), A_x(F \oplus I_{n_{\text{in}}-k}), A_z(F \oplus I_{n_{\text{in}}-k})$. Additionally, a general form circuit may contain redundancy in r. That is, for two different values r_1, r_2 of r the actions of the two corresponding circuits may be identical. This happens when $(r_1 - r_2) \oplus 0^{n_{\text{in}}-k}$ belongs to the kernel of each of A, A_x, A_z . To summarize these degrees of freedom, one can replace the first n_r columns of A, A_x, A_z with another n'_r columns, as long as the linear span is the same. We can eliminate these degrees of freedom by "compressing" r with the following algorithm. This algorithm corresponds to constructing an outcome compression map for the quantum instrument corresponding to the general form circuit in Definition 2.5. This is also useful for computing an outcome compression map for the action of arbitrary stabilizer circuits.

Procedure 6.6 (compression map)

Input: A general form circuit C_{gen} in Fig. 4.3, with n_r random bits, n_{in} input qubits, n_{out} output qubits, k inner qubits, condition matrices A, A_x, A_z

Output:

- Integer n'_r , condition matrices A', A'_x , A'_z that define a general form circuit $\mathcal{C}'_{\text{gen}}$, equivalent to \mathcal{C}_{gen} , with $n'_r \leq n_r$ random bits, same left Clifford unitary, same right Clifford unitary.
- Compression matrix $F_{o \to o'}$ over \mathbb{F}_2 , embedding matrix $F_{o' \to o}$ over \mathbb{F}_2 .

such that general form circuits C_{gen} and C'_{gen} have the same action for outcome vectors o and $o' = F_{o \to o'}o$. Furthermore, first n'_r rows of $((A')^T | (A'_x)^T | (A'_z)^T)$ are in reduced row echelon form and have full rank, $F_{o \to o'}F_{o' \to o} = I$.

1: Let \tilde{A} be the first n_r columns of

$$\left(\frac{A}{A_x}\right)$$
.

- 2: Find matrices F, F^{-1} such that $\hat{A}^T = F^T \tilde{A}^T$ is in reduced row echelon form.
- 3: Set n'_r to be the number of non-zero columns of \hat{A} .
- 4: Set matrices

$$F_{o \to o'} \leftarrow \left(\left(I_{n'_r} | 0_{n'_r \times (n_r - n'_r)} \right) F^{-1} \right) \oplus I_{n_{\text{in}} - k},$$

$$F_{o' \to o} \leftarrow \left(F \left(\frac{I_{n'_r}}{0_{(n_r - n'_r) \times n'_r}} \right) \right) \oplus I_{n_{\text{in}} - k},$$

$$A' \leftarrow AF_{o' \to o}, \quad A'_x \leftarrow A_x F_{o' \to o}, \quad A'_z \leftarrow A_z F_{o' \to o}.$$

5: **return** n'_r , condition matrices A', A'_x, A'_z , compression and embedding matrices $F_{o \to o'}, F_{o' \to o}$

The goal of Procedure 6.6 is to first identify all random bit vectors that result in the same linear map being applied by the general form circuit (Line 2). All vectors from the kernel of $\tilde{A} = \hat{A}F^{-1}$ lead to the same map being applied. It is easy to identify the kernel of \hat{A} , those are exactly its zero columns, that is columns from $n'_r + 1$ to n_r (Line 3). The basis of kernel of \tilde{A} is then $Fe_{n'_r+1}, \ldots, Fe_{n_r}$.

Vectors from within each coset in $\mathbb{F}_2^{n_r}/\ker(A)$ also lead to the same map being applied. Vectors from the distinct cosets result in the distinct maps applied by the general form circuit. The basis $b_1 = Fe_1, \ldots, b_{n'_r} = Fe_{n'_r}$ corresponds to a basis $b_1 + \ker(\tilde{A}), \ldots, b_{n'_r} + \ker(\tilde{A})$ of the coset vector space $\mathbb{F}_2^{n_r}/\ker(\tilde{A})$. Matrix F defined in Line 2 maps standard basis vectors $e_1, \ldots, e_{n'_r}$ to the coset-basis vectors $b_1, \ldots, b_{n'_r}$, and the rest $e_{n'_r+1}, \ldots, e_{n_r}$ to the kernel basis. For this reason, columns $n'_r + 1, \ldots, n_r$ of the products $A(F \oplus I_{n_{\text{in}}-k}), A_x(F \oplus I_{n_{\text{in}}-k}), A_z(F \oplus I_{n_{\text{in}}-k})$ are zero and so we can remove those columns and shrink the random bit vector of the general form to n'_r . This is exactly the effect of matrix $F_{o \to o'}$. Distinct values of r' correspond to distinct cosets of r and so the outcome space of an the quantum instrument corresponding to general from circuit is compressed as in Definition 2.5. Finally we notice that the first n'_r rows of $((A')^T|(A'_x)^T|(A'_z)^T)$ are equal to first n'_r rows of \hat{A} , which ensures required properties of the rows.

An important edge case of the compression map Procedure 6.6 is when $n'_r = 0$ and $n_{\rm in} = k$, that is, when the general form circuit's action is independent on the random bits and no observables of the input are measured. In this case matrix $F_{o \to o'}$ is of size $n_r \times 0$ and matrices A', A'_x, A'_z are of size $(n_{\rm out} - k) \times 0, k \times 0, k \times 0$. We use the convention that an $n_r \times 0$ matrix takes n_r -dimensional vectors as input and returns nothing as the output, similarly $k \times 0$ takes nothing as an input and returns a zero vector of dimension k. When zero-dimensional matrices are used in direct sum operation they pad the other matrix with rows or columns full of zeros. For example, if F is $n_r \times 0$ matrix, then $F \oplus I_k = (0_{k \times n_r} | I_k)$.

Additionally, a circuit's general form Algorithm 6.2 together with randomness compression Procedure 6.6 can be used to find an outcome compression map for the quantum instrument corresponding to any stabilizer circuit C. This is achieved in three steps. First find the stabilizer circuit's general form circuit C_{gen} with $o \mapsto Mo + v_0$. Second apply the compression

map algorithm and find compression matrix $F_{o\to o'}$. Third, find $M^{(-1)}$, the left inverse of M, that is a rectangular matrix such that $M^{(-1)}M=I$. This is always possible because M has full column rank. An outcome compression map for stabilizer circuit \mathcal{C} with outcome vector v is then $v\mapsto F_{o\to o'}M^{(-1)}(v-v_0)$. The outcome compression map computes outcome o' of the compressed general form corresponding to the circuit outcome v. Computing the compression map is useful when checking equivalence of the action of two stabilizer circuits discussed in the next section.

The run time of Procedure 6.6 is

$$O(n_r n_{\text{out}} \min(n_r, n_{\text{out}})^{\omega - 2}). \tag{20}$$

This is because the run time of the row reduced echelon form calculation is exactly Eq. (20), as discussed in Appendix B, Eq. (48). The matrix F^T is sparse with a dense sub-matrix of size $n_r \times O(n_{\text{out}})$, so there is no $O(n_r^2)$ contribution to the run time when $n_r > O(n_{\text{out}})$.

Stabilizer circuit verification 7

Given two stabilizer circuits, it is useful to know if they have equivalent action or not. For example, we might want to verify that a circuit that meets certain hardware-related connectivity requirements performs the same action as a (simpler) reference circuit. This motivates the following problem.

Problem 7.1 (Stabilizer circuit comparison). Given two stabilizer circuits C_1 and C_2 with outcome vectors v_1 and v_2 , find if they have equivalent action, i.e, if their corresponding quantum instruments are equivalent according to Definition 2.6. If their actions are equivalent, find matrices M_1 and M_2 and vectors u_1 and u_2 such that: (i) the action of C_1 given outcome v_1 is the same as the action of C_2 given outcome v_2 if and only if $M_1(v_1 + u_1) = M_2(v_2 + u_2)$, and (ii) the action of C_j given outcome v_j is the same as the action of C_j given outcome v'_j if and only if $M_i(v_i - v'_i) = 0$.

First let us understand this problem statement in the context of the quantum instrument equivalence Definition 2.6. For two quantum instruments to be equivalent, there must be a bijection f between outcomes of the outcome-compressed versions of the two instruments such that their action on any quantum state is the same for outcomes related by the bijection. In Problem 7.1, we are tasked with finding the maps $v_1 \mapsto M_1(v_1 + u_1)$ and $v_2 \mapsto M_2(v_2 + u_2)$ such that when the output of these maps match, the circuits \mathcal{C}_1 and \mathcal{C}_2 have identical action on any input. These maps are in effect implementing the outcome compression for both circuits, but also an outcome relabeling that implements the bijection f.

Next, it can useful to consider a special set of scenarios in which not only are two input circuits equivalent, but where we can find an explicit map from the outcomes of one circuit to the other. This is the case for example if the reference circuit C_2 has no redundancy in its measurement outcomes, then $\ker(M_2)$ is trivial making it possible to construct a map from the outcomes of \mathcal{C}_1 to the outcomes of \mathcal{C}_2 . In this case there exists a left inverse $M_2^{(-1)}$ of M_2 and we can write $v_2 = v_0 + Mv_1$ for $v_0 = u_2 + M_2^{(-1)}u_1$ and $M = M_2^{(-1)}M_1$. A naive strategy aiming to solve Problem 7.1 would be to construct general form circuits

for \mathcal{C}_1 and \mathcal{C}_2 and to check equality of the objects comprising the general forms, namely their left and the right Clifford unitaries and the condition matrices. However, this strategy would fail because general form circuits are not unique and therefore even if two circuits have identical action, the general form circuits we find for each may be different. For this reason we develop an algorithm in Section 7.2 to compare two general form circuits, thereby solving a special case of Problem 7.1 when C_1 and C_2 are general form circuits. The solution to the general case of Problem 7.1 reduces to this special case as shown below.

Algorithm 7.2 (Stabilizer circuit comparison) Input:

• Stabilizer circuits C_1 , C_2 with the same number of input and output qubits.

Output: One of the following:

- False (the stabilizer circuits are not equivalent).
- True (the stabilizer circuits are equivalent), matrices M_1, M_2 and vectors u_1, u_2 such that conditions in **Problem 7.1** are satisfied.
- 1: Find a general form circuit $C_{\text{gen},j}$ for C_j and outcome map $o_j \mapsto \tilde{u}_j + \tilde{M}_j o_j$ from the outcomes of $C_{\text{gen},j}$ to the outcomes of C_j , for $j \in [2]$. \triangleright Algorithm 6.2
- 2: Solve the stabilizer circuit comparison Problem 7.1 for $C_{\text{gen},1}$ and $C_{\text{gen},2}$. \triangleright Algorithm 7.5
- 3: if $\mathcal{C}_{\text{gen},1}$ and $\mathcal{C}_{\text{gen},2}$ are equivalent, with matrices M_1, M_2 and vectors \hat{u}_1, \hat{u}_2
- defining the equivalent outcomes, **then** $M_j \leftarrow \hat{M}_j \tilde{M}_j^{(-1)}, \ u_j \leftarrow \hat{u}_j + \tilde{M}_j^{(-1)} \tilde{u}_j \text{ for } j \in [2] \qquad \qquad \triangleright \tilde{M}_j^{(-1)} \text{ is a left-inverse of } \tilde{M}_j$ **return** True, M_1, M_2, u_1, u_2 5:

7: else

8: return False

We briefly discuss the correctness of Algorithm 7.2. By definition, each input circuit is equivalent to its general form circuit, and therefore if one observes that the two general form circuits are inequivalent, this implies the two input circuits are also inequivalent. When the input circuits are equivalent, we need to establish that the matrices M_1, M_2 and vectors u_1, u_2 have the required properties. This immediately follows from the fact that there is an affine one-to-one correspondence between a circuit's outcomes and its general form outcomes.

To analyze the run time of Algorithm 7.2 we assume that the stabilizer circuits C_1 and C_2 use bounded-weight Pauli operators and have the same properties as in our analysis of the general form Algorithm 6.2 run time in Eq. (17). Let the parameters of the input circuit C_j be as in Section 3.1 but with superscript (j). The run time of Algorithm 7.2 is

$$O\left(\sum_{j\in\{1,2\}} n_{\downarrow}^{(j)} \cdot \left(N_{\mathrm{u}}^{(j)} + (N_{\mathrm{cnd}}^{(j)} + n_{M}^{(j)})(n_{r}^{(j)} + n_{m}^{(j)} + 1) + n_{\downarrow}^{(j)}(n_{\downarrow}^{(j)} + n_{r}^{(j)})\right)\right). \tag{21}$$

The run time of Algorithm 7.2 is dominated by the cost of finding general forms for the input circuits rather than the cost of comparing those general forms. The run time of Line 5 is also negligible because the left inverse of matrices \tilde{M}_j is one-sparse.

When we find that two circuits are inequivalent, sometimes it is possible to find a "correction" unitary that can be appended to one of the circuits to achieve equivalence. We have designed Algorithm 7.2 in such a way that the correction unitary can be easily found when it exists (Table 7.1). We either find a Clifford correction unitary or a Pauli correction unitary conditioned on the circuit's general form outcomes. The map $o_1 = \tilde{M}_1^{(-1)}(v_1 + \tilde{u}_1)$ from the circuit's outcomes to its general form outcomes allows us to easily convert Pauli correction unitaries $X^{\langle c_x, o_1 \rangle} Z^{\langle c_z o_1 \rangle}$ conditioned on the general form's outcomes o_1 to the Pauli correction unitaries conditioned on the circuit's outcomes v_1 :

$$X_j^{\langle c_x, o_1 \rangle} Z_j^{\langle c_z, o_1 \rangle} = X_j^{\langle (\tilde{M}_1^{(-1)})^T c_x, v_1 + \tilde{u}_1 \rangle} Z_j^{\langle (\tilde{M}_1^{(-1)})^T c_z, v_1 + \tilde{u}_1 \rangle}. \tag{22}$$

The rest of the section is dedicated to solving Problem 7.1 for two general form circuits (Line 2, Algorithm 7.2). This special case is also relevant for verifying the logical action of logical operation circuits, discussed in Section 8.

7.1 Relating (un)encoding circuits

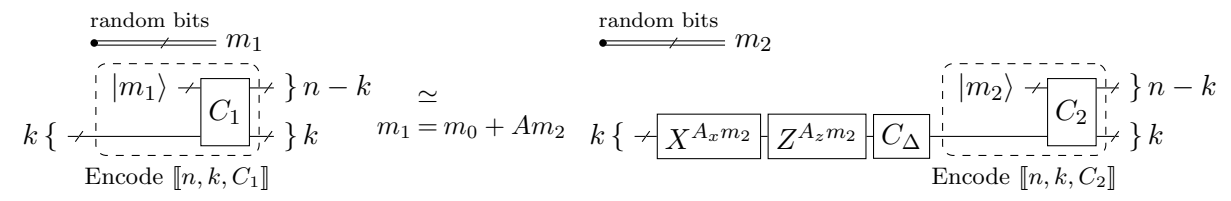
As discussed in Section 4 and highlighted in Fig. 4.1, a general form circuit consists of three steps: (1) an unencoding circuit, (2) Pauli unitaries conditioned on both random bits and the syndrome measured by the unencoding circuit and (3) an encoding circuit. To compare two general form circuits, we first consider how the encoding and unencoding circuits of one general form can be related to those of the other general form.

Recall that encoding and unencoding circuits for the code [n, k, C] are fully specified by the Clifford unitary C and integers n, k. We define the encoding circuit for $[n_1, k_1, C_1]$ to be the circuit in the left in Fig. 7.1b, similarly we define the unencoding circuit for $[n_1, k_1, C_1]$ to be the circuit in the left in Fig. 7.1b. We say that a pair of codes are equivalent⁶ if their stabilizer groups S_1 and S_2 satisfy $S_1 \subset (S_2 \cup -S_2)$ and $S_2 \subset (S_1 \cup -S_1)$. We use this notion of code equivalence to relate two encoding circuits (or two unencoding circuits) as follows.

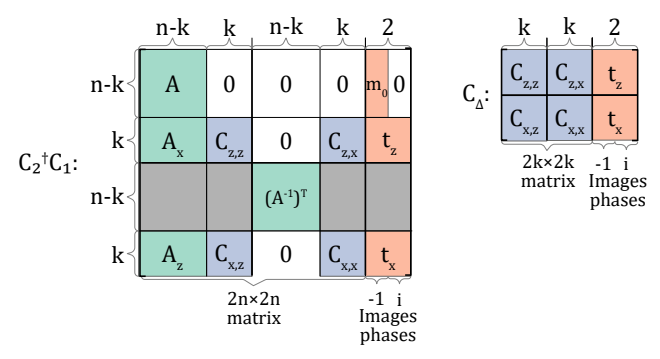
Problem 7.3 (Relating (un)encoding circuits). Consider two (un)encoding circuits defined by n_1, k_1, C_1 and n_2, k_2, C_2 respectively. First find if the (un)encoding circuits are related, which is

⁶This definition of code equivalence is motivated by stabilizer instrument equivalence since the action of any circuit that measures any complete set of generators of S_1 is equivalent to the action of any circuit that measures any complete set of generators of S_2 if and only if the two codes are equivalent under this definition.

(a) The relation between unencoding circuits for equivalent codes.



(b) The relation between encoding circuits for equivalent codes.



(c) Deriving Clifford unitary C_{Δ} , condition matrices A, A_x, A_z and vector m_0 from $C_2^{\dagger}C_1$. See Proposition A.5 for the correctness proof.

Figure 7.1: Relating (un)encoding circuits. When codes $[n, k, C_1]$, $[n, k, C_2]$ are equivalent, there exist Clifford unitary C_{Δ} , matrices A, A_x, A_z and vector m_0 such that the circuits in subfigures (a),(b) have equivalent action. The map between outcomes is $m_1 = m_0 + Am_2$.

the case if and only if the corresponding stabilizer codes $[n_1, k_1, C_1]$ and $[n_2, k_2, C_2]$ are equivalent. If the (un)encoding circuits are related, find a Clifford unitary C_L , condition matrices A_x, A_z, A and a vector m_0 that relates the second circuit to the first according to Fig. 7.1.

Note that for fixed outcomes m_1 , m_2 the equalities (up to a global phase) in Figs. 7.1a and 7.1b are equivalent. Indeed, Fig. 7.1b can be obtained from Fig. 7.1a by applying the conjugate-transpose to the product of the linear maps corresponding to the circuits, and vice versa. A solution to Problem 7.3 is given in Procedure 7.4. The correctness proof is Proposition A.5 with $C = C_2^{\dagger}C_1$, the runtime is

$$O(n^{\omega})$$
 (23)

and is dominated by computing $C_2^{\dagger}C_1$.

Procedure 7.4 (Relating (un)encoding circuits) Input:

• Unitaries C_1 and C_2 and integers n_1 , n_2 , k_1 and k_2 that specify (un)encoding circuits for $[n_1, k_1, C_1]$ and $[n_2, k_2, C_2]$.

Output: One of the following:

- Not related ($[n_1, k_1, C_1]$ and $[n_2, k_2, C_2]$ are not equivalent).
- Related ($[n_1, k_1, C_1]$ and $[n_2, k_2, C_2]$ are equivalent), Clifford unitary C_{Δ} , condition matrices A, A_x, A_z and vector m_0 which relate the circuits as in Problem 7.3 are satisfied

```
1: if n_1 \neq n_2 or k_1 \neq k_2 then return False.
                                                                                              ▶ Code dimensions do not match
 2: Set C \leftarrow C_2^{\dagger}C_1, n \leftarrow n_1, k \leftarrow k_1.
3: Set A \leftarrow 0_{(n-k)\times(n-k)}, A_x \leftarrow 0_{k\times(n-k)}, A_z \leftarrow 0_{k\times(n-k)}, m_0 = 0^{n-k}.

ightharpoonup for C_1Z_iC_1^{\dagger}, stabilizers of \llbracket n_1,k_1,C_1 \rrbracket
4: for P, j \in \{(CZ_{j'}C^{\dagger}, j') : j' \in [n-k]\} do
          if x(P) \neq 0 or z(P)_{[n-k+1,n]} \neq 0 then

ightharpoonup \pm C_1 Z_j C_1^{\dagger} is not a stabilizer of [\![n_2,k_2,C_2]\!]
               return Not related
 6:
 7:
          else
                A_i = z(P)_{[n-k]}, (m_0)_i = s(P)/2
9: Compute A_x, A_z, C_{\Delta} from the equations CZ_{j+n-k}C^{\dagger} = Z^{(A_x)_j} \otimes C_{\Delta}Z_jC_{\Delta}^{\dagger},
                    CX_{j+n-k}C^{\dagger} = Z^{(A_z)_j} \otimes C_{\Delta}X_jC_{\Delta}^{\dagger}, \ j \in [k]
10: return Related, C_{\Delta}, A, A_x, A_z, m_0
                                                        \triangleright See Fig. 7.1c for an illustration of relation to C = C_2^{\dagger} C_1
```

Procedure 7.4 is useful outside of the context of this section. For example, it can be used for general from circuit classification, that is determining if an action of the circuit corresponds to some common circuit family such as measurement of a set of commuting Pauli operators.

7.2 Comparing general form circuits

Here we provide the general form circuit comparison Algorithm 7.5 that solves the circuit comparison Problem 7.1 for general form circuits. We first give a high-level overview of the algorithm, then discuss its correctness and explain how data produced by the algorithm can be used to find a correction unitary to append to the first circuit to achieve equivalence. At the end of this section we discuss the algorithm's run time.

Algorithm 7.5 consists of two main steps. The first step checks if the left and right Clifford unitaries are consistent with the two circuits having equivalent action. If they are, the algorithm proceeds to the second step, which checks if the condition matrices are consistent with the two circuits having equivalent action. The algorithm returns True if the checks in both of these steps are passed, and False otherwise. In the next two paragraphs we give a high-level overview of these two steps.

The first step of Algorithm 7.5 makes use of the fact that equivalence of $[n_{in}, k_1, L_1]$, $[n_{in}, k_2, R_2]$ and $[n_{out}, k_1, D_1]$, $[n_{out}, k_2, D_2]$ is a necessary condition for the two general form circuits to have equivalent circuit action, so the algorithm returns False if the codes are not equivalent. If the codes are equivalent, the algorithm transforms the first general form circuit C_1 (see Fig. 7.2(a)) into an equivalent circuit C_1' (see Fig. 7.2(b)) using the relating (un)encoding Procedure 7.4 from Section 7.1. The circuit C_1' more closely resembles the second general form circuit C_2 – in particular C_1' has the same left and right Clifford unitaries as C_2 . At this point, it is clear that circuits C_1' and C_2 are equivalent up to a conditional Pauli when C_L is equal to C_R up to a Pauli. If this this the case we further transform C_1' into the general form circuit C_1'' (see Fig. 7.2(c)) by consolidating the various conditional Paulis, making use of the compression map Procedure 6.6 from Section 6.2 to do so. We then further transform C_1'' to C_1''' (see Fig. 7.2(d)) by pulling the Clifford unitary C_L^{\dagger} through the conditional Paulis to meet C_R , transforming the conditional Paulis it is pulled through.

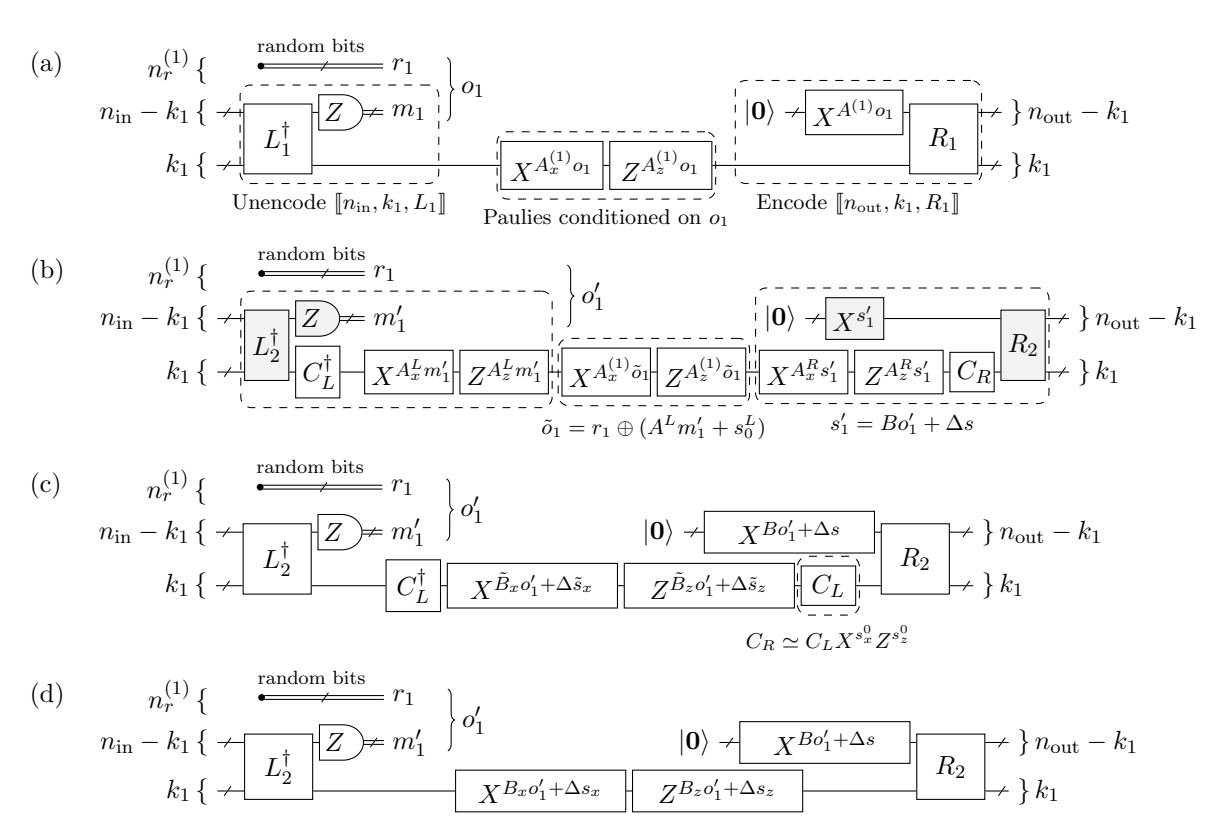


Figure 7.2: To verify that general form circuits C_1 and C_2 are equivalent, Algorithm 7.5 passes through a sequence of equivalent circuits: (a) C_1 , (b) C'_1 , (c) C''_1 and (d) C'''_1 . (b) If code pairs $[n_{\rm in}, k_1, L_1]$, $[n_{\rm in}, k_1, R_2]$ and $[n_{\rm out}, k_1, D_1]$, $[n_{\rm out}, k_1, D_2]$ are equivalent, we form the circuit C'_1 with unencoding and encoding circuits related by C_L , A^L , A^L_x , A^L_z , m_0^L (Fig. 7.1a) and C_R , A^R , A^R_x , A^R_z , m_0^R (Fig. 7.1b) respectively. The action of C'_1 matches that of C_1 when $m_1 = (m_0^L + A^L m'_1)$. (c) If $C_R \simeq C_L X^{s_0^L} Z^{s_2^0}$, we form C''_1 by consolidating the conditional Paulis in C'_1 . (d) We form C'''_1 by transforming the conditional Paulis in C''_1 by the Clifford C_L .

The second step of Algorithm 7.5, beginning on Line 16, compares the condition matrices of \mathcal{C}_1''' and \mathcal{C}_2 . To do so, we split each condition matrix into two sub-matrices for each of \mathcal{C}_1''' and \mathcal{C}_2 . The first sub-matrix determines the dependence of each conditional Pauli on the measurement outcomes, and these sub-matrices must be equal for \mathcal{C}_1''' and \mathcal{C}_2 if the circuits have equivalent action. The second sub-matrix determines the dependence of each conditional Pauli on the random bits and do not need to be equal for \mathcal{C}_1''' and \mathcal{C}_2 to have equivalent equivalent, but must satisfy a weaker equivalence condition which we check using the compression map Procedure 6.6.

In what follows, we show the correctness of Algorithm 7.5 by considering the following

Algorithm 7.5 (General form circuit comparison) Input:

• Two general form circuits C_1, C_2 with n_{in} input qubits, n_{out} output qubits, $n_r^{(1)}, n_r^{(2)}$ random bits, left Clifford unitaries L_1, L_2 , right Clifford unitaries R_1, R_2, k_1, k_2 inner qubits, condition matrices $A^{(1)}, A_x^{(1)}, A_z^{(1)}$ and $A^{(2)}, A_x^{(2)}, A_z^{(2)}$.

Output: One of the following:

- False (the general form circuits are not equivalent)
- True (the general form circuits are equivalent), matrices M_1, M_2 and vectors u_1, u_2 such that conditions in Problem 7.1 are satisfied.

ightharpoonup Check equivalence of $\llbracket n_{\mathrm{in}}, k_1, L_1 \rrbracket$, $\llbracket n_{\mathrm{in}}, k_2, R_2 \rrbracket$ and of $\llbracket n_{\mathrm{out}}, k_1, D_1 \rrbracket$, $\llbracket n_{\mathrm{out}}, k_2, D_2 \rrbracket$

1: Relate the unencoding circuits for $[n_{in}, k_1, L_1]$, $[n_{in}, k_2, R_2]$

▶ Procedure 7.4

2: if $[n_{in}, k_1, L_1]$, $[n_{in}, k_2, R_2]$ are not equivalent then return False

⊳ See Fig. 7.1a

Let $C_L, A^L, A_x^L, A_z^L, m_0^L$ relate the unencoding circuits for $[n_{\rm in}, k_1, L_1]$, $[n_{\rm in}, k_2, R_2]$ 4:

5: Relate the encoding circuits for $[\![n_{\mathrm{out}},k_1,D_1]\!],\,[\![n_{\mathrm{out}},k_2,D_2]\!]$

▶ Procedure 7.4

6: if $[n_{\text{out}}, k_1, D_1]$, $[n_{\text{out}}, k_2, D_2]$ are not equivalent then return False

7: else

 \triangleright See Fig. 7.1b

Let $C_R, A^R, A_x^R, A_z^R, m_0^R$ relate the encoding circuits for $[\![n_{\mathrm{out}}, k_1, D_1]\!], [\![n_{\mathrm{out}}, k_2, D_2]\!]$

▶ Check equivalence up to Pauli unitaries

9: if $C_R C_L^{\dagger}$ is not a Pauli unitary then return False

▶ Table 7.1

Find s_x^0, s_z^0 from equation $X^{s_x^0} Z^{s_z^0} \simeq C_L^\dagger C_R$ 11:

 \triangleright Simplify the unitary acting on the k_1 inner qubits in \mathcal{C}'_1

12: Let $\Delta s = (A^R)^{-1}(A^{(1)}(0^{n_r^{(1)}} \oplus m_0^L) + m_0^R)$ and $B = (A^R)^{-1}A^{(1)}(I_{n_r^{(1)}} \oplus A^L)$.

13: For $\sigma \in \{x, z\}$, $\tilde{B}_{\sigma} \leftarrow \left(\mathbf{0}_{k \times n_{\tau}^{(1)}} | A_{\sigma}^{L}\right) + A_{\sigma}^{(1)} \left(I_{n_{\tau}^{(1)}} \oplus A^{L}\right) + A_{\sigma}^{R}B$.

14: For $\sigma \in \{x, z\}$, let $\Delta \tilde{s}_{\sigma} \leftarrow s_{\sigma}^{0} + A_{\sigma}^{(1)}(0^{n_{r}^{(1)}} \oplus m_{0}^{L}) + A_{\sigma}^{R} \Delta s$

15: Find B_x , B_z , Δs_x , Δs_z from $X^{(B_x|\Delta s_x)s}Z^{(B_z|\Delta s_z)s} \simeq C_L X^{(\tilde{B}_x|\Delta \tilde{s}_x)s}Z^{(\tilde{B}_z|\Delta \tilde{s}_z)s}C_L^{\dagger}$, for all s

▶ Proposition A.3

▷ Check equivalence for a fixed outcome

16: Find outcome compression matrix F_1 , condition matrices B', B'_x, B'_z for a general form circuit with k input qubits, condition matrices $B_{*,[n_r^{(1)}]},(B_x)_{*,[n_r^{(1)}]},(B_z)_{*,[n_r^{(1)}]}.$

17: Let r_0 be a solution to linear equations $\left(\begin{array}{c} B' \\ \hline B'_x \\ \hline B'_z \end{array}\right) r_0 = \Delta s \oplus \Delta s_x \oplus \Delta s_z$

18: **if** there is no r_0 exists **then return False**

 \triangleright Table 7.1

20: **if**
$$B^{(m)} \neq A^{(2,m)}$$
 or $B_x^{(m)} \neq A_x^{(2,m)}$ or $B_z^{(m)} \neq A_z^{(2,m)}$ then return False \triangleright Table 7.1

▶ Check equivalence for all outcomes

21: Find outcome compression matrix F_2 , condition matrices A', A'_x, A'_z for a general form circuit with k input qubits, condition matrices $A_{*,[n_r^{(2)}]}^{(2)}, (A_x^{(2)})_{*,[n_r^{(2)}]}, (A_z^{(2)})_{*,[n_r^{(2)}]}^{*,[n_r^{(2)}]}$. \triangleright Procedure 6.6

22: if
$$\left(\frac{B'}{B'_x}\right) \neq \left(\frac{A'}{A'_x}\right)$$
 then return False \triangleright Table 7.1

23: **return** True, $M_1 = F_1 \oplus (A^L)^{-1}$, $M_2 = F_2 \oplus I_{n_{\text{in}}-k}$, $u_1 = F_1^{(-1)} r_0 \oplus s_0^L$, $u_2 = 0^{n_r^{(2)} + n_{\text{in}} - k}$

sequence of conditions which are checked in order by the algorithm:

- (A) equivalence of $[n_{\text{in}}, k_1, L_1]$, $[n_{\text{in}}, k_2, L_2]$ and of $[n_{\text{out}}, k_1, R_1]$, $[n_{\text{out}}, k_2, R_2]$ (Lines 2 and 6),
- (B) equivalence up to Pauli unitaries (Line 9),
- (C) equivalence for a fixed outcome vector (Line 18),
- (D) equivalence for all measurement outcomes but fixed random bit vector (Line 20),
- (E) equivalence (equivalence for all outcomes, including random bits (Line 22)).

We show that each condition must hold if the two input circuits have equivalent action, and that the conditions become progressively stricter down the list, with the last condition being that the circuits are equivalent. To show the correctness of Algorithm 7.5, we verify that it sequentially checks these conditions, returning False if it encounters a condition that is not satisfied, and returns True if and only if all of the conditions hold. While discussing each of these conditions, we also build up the contents of Table 7.1, which specifies a modification that can be applied to the first input circuit to make it equivalent to the second input circuit.

(A) Let us show that the circuit equivalence of C_1 and C_2 implies the code equivalence of $[n_{\rm in}, k, L_1]$ and $[n_{\rm in}, k, L_2]$. This follows from two observations. First, all the Choi states of equivalent general form circuits are equal up to Pauli unitaries and the Choi state's stabilizer groups are equal up to signs. This is because, for fixed $j \in [2]$, Fig. 4.3 implies that all the Choi states $|\Psi_{o_j}\rangle$ corresponding to C_j 's stabilizer instrument are equal up to Pauli unitaries, that is $|\Psi_{o_j}\rangle$ equals $|\Psi_{o_j'}\rangle$ up to Pauli unitaries for any outcomes o_j, o_j' . Second, the fact that the stabilizer groups of the Choi circuits of C_1 and C_2 match up to signs implies that the stabilizer groups of $[n_{\rm in}, k, L_1]$ and $[n_{\rm in}, k, L_2]$ match up to signs too (which is the defining property of code equivalence). This is because the stabilizer group of $[n_{\rm in}, k, L_j]$ is equal up to signs to the subgroup of the stabilizer group of $|\Psi_{o_j}\rangle$ supported on last $n_{\rm in}$ qubits, for all outcomes o_j (see stabilizer generators in Fig. 4.3). Similarly, the circuit equivalence of C_1 and C_2 implies the code equivalence of $[n_{\rm out}, k, R_1]$ and $[n_{\rm out}, k, R_2]$. We check the equivalence of these stabilizer groups using Procedure 7.4 in Lines 1 and 5 and the algorithm returns Fail if it is not the case.

Reason	Li	Correction unitary U to achieve equivalence
for inequivalence	Line	via appending U to general form circuit \mathcal{C}_1
Circuits differ by	9	$U = R_2 \left(I_{n_{\text{out}} - k_1} \otimes \left(C_L C_R^{\dagger} \right) \right) R_2^{\dagger}$
a Clifford unitary		$r_{\text{out}} = \kappa_1 \circ \left(\frac{\sigma_{\text{Lo}} \cdot \kappa_1}{\sigma_{\text{out}}} \right) r_{\text{out}}$
Circuits differ by	18	$U = D / (V\Delta s \otimes V\Delta s_x / Z\Delta s_z) / D^{\dagger}$
a Pauli unitary	18	$U = R_2 \left(X^{\Delta s} \otimes X^{\Delta s_x} Z^{\Delta s_z} \right) R_2^{\dagger}$
Circuits differ by	20	Let $\Delta A = B^{(m)} - A^{(2,m)}, \Delta A_{\sigma} = B_{\sigma}^{(m)} - A_{\sigma}^{(2,m)}$
a Pauli unitary		for $\sigma \in \{x, z\}, f(m_1) = (A^L)^{-1}(m_1 + s_0^L)$
conditioned on		$U(m_1) = R_2 \left(X^{\Delta A f(m_1)} \otimes X^{\Delta A_x f(m_1)} Z^{\Delta A_z f(m_1)} \right) R_2^{\dagger}$
measurements		
Circuits differ by	22	Let $\tilde{n}_r = \operatorname{ncols}(A'), \ l = n_r^{(1)} - \tilde{n}_r, \text{ for } \sigma \in \{x, z\}$
a Pauli unitary		$\Delta B = B_{*,[n_r^{(1)}]} + (A' 0_{(n_{\text{out}}-k)\times l}), \Delta B_{\sigma} = (B_{\sigma})_{*,[n_r^{(1)}]} + (A'_{\sigma} 0_{k\times l})$
conditioned on		V_{1} V_{2} V_{3} V_{4} V_{5} V_{5} V_{5} V_{5} V_{5} V_{5} V_{5}
random bits		$U(r_1) = R_2 \left(X^{\Delta B r_1} \otimes X^{\Delta B_x r_1} Z^{\Delta B_z r_1} \right) R_2^{\dagger}$

Table 7.1: Cases when the comparison of general form circuits C_1 , C_2 using Algorithm 7.5 returns False and a correction unitary exists that can be appended to C_1 to achieve circuit equivalence. We use the notation r_1 for random bit vector and m_1 for measurement outcome vector of C_1 when defining conditional correction Pauli unitaries. Variables in the equations for the correction unitaries are defined in the pseudo-code of Algorithm 7.5. Note that it is not possible to correct Pauli unitaries conditioned on random bits by modifying C_1 when number of columns $\operatorname{ncols}(A')$ of A' is greater than $n_r^{(1)}$; in this case C_2 must be modified instead.

(B) Given that $[n_{in}, k, L_1]$, $[n_{in}, k, L_2]$ are equivalent and $[n_{out}, k, R_1]$, $[n_{out}, k, R_2]$ are equivalent since condition (A) has passed, we compute the relation between the corresponding

(un)encoding circuits (Lines 3 and 7) and transform the first general form circuit C_1 into an equivalent circuit C_1' as shown in Fig. 7.2(a). If we ignore all the Pauli unitaries, C_1' is almost the same circuit as the second general form circuit C_2 , except the product $C_R C_L^{\dagger}$ on the inner qubits. The stabilizer groups of the Choi states $|\Psi_{o_1}\rangle$ and $|\Psi_{o_2}\rangle$ match up to sign (which must be the case if C_1 and C_2 are equivalent) if and only if $C_L^{\dagger} C_R$ is a Pauli unitary. We check this in Line 9, and the algorithm returns Fail if it is not the case. We can fix this by appending a correction unitary to C_1 from Table 7.1 that effectively cancels $C_R C_L^{\dagger}$ on the inner qubits.

Given that the algorithm has not yet returned False, we can assume from here onward that $C_RC_L^{\dagger}$ is a Pauli unitary. Before moving on to condition (C), we first simplify the unitary acting on the inner qubits of \mathcal{C}_1' to form the circuit \mathcal{C}_1'' as shown in Fig. 7.2(c) to make the next steps more streamlined. To see why B and Δs are set as specified in Line 12, note that their defining relation is $s_1' = Bo_1' + \Delta s$, and make use of the encoding and unencoding circuit relations in going from \mathcal{C}_1 to \mathcal{C}_1' are $s_1' = m_0^R + A^R s_1$ and $m_1' = m_0^L + A^L m_1$ respectively, where $s_1 = A^{(1)}o_1$ (and making use of the definitions $o_1 = r_1 \oplus m_1$, $o_1' = r_1 \oplus m_1'$). To see why \tilde{B}_x , \tilde{B}_z , $\Delta \tilde{s}_x$ and $\Delta \tilde{s}_z$ are set as specified on Lines 13 and 14, note that they must satisfy $\tilde{B}_\sigma o_1' + \Delta \tilde{s}_\sigma = A_\sigma^L m_1' + A_\sigma^{(1)} \tilde{o}_1 + A_\sigma^R s_1' + s_\sigma^0$ to ensure that \mathcal{C}_1'' has the same action as \mathcal{C}_1' , and then make use of the fact that $\tilde{o}_1 = r_1 \oplus (A^L m_1' + s_0^L)$ and $s_1' = Bo_1' + \Delta s$.

By the end of Line 15, we have the circuit \mathcal{C}_1''' (see Fig. 7.2(d)), which is very close to

By the end of Line 15, we have the circuit C_1''' (see Fig. 7.2(d)), which is very close to the general form circuit C_2 , except that the Paulis are conditioned on affine rather than linear outcome maps (i.e. the presence of the Δs_x , Δs_z and Δs terms). Due to these similarities, and in particular since both circuits have the same left and right Cliffords L_2 and R_2 , the stabilizer generators of the Choi states (see Fig. 4.3) of both C_1''' and C_2 can be expressed as:

$$\begin{split} R_2 Z_{j_{\text{out}}} R_2^{\dagger} \otimes (-1)^{s_{j_{\text{out}}}} I_{n_{\text{in}}}, & j_{\text{out}} \in [n_{\text{out}} - k], \\ R_2 Z_{n_{\text{out}} - k + j} R_2^{\dagger} \otimes (-1)^{s_j} (L_2 Z_{n_{\text{in}} - k + j} L_2^{\dagger})^*, & j \in [k], \\ I_{n_{\text{out}}} \otimes (-1)^{s_{j_{\text{in}}}} (L_2 Z_{j_{\text{in}}} L_2^{\dagger})^*, & j_{\text{in}} \in [n_{\text{in}} - k], \\ R_2 X_{n_{\text{out}} - k + j} R_2^{\dagger} \otimes (-1)^{s_j} (L_2 X_{n_{\text{in}} - k + j} L_2^{\dagger})^*, & j \in [k], \end{split}$$

where the only difference is captured by the sign bits,

$$s(\mathcal{C}_{1}^{""}) = \left(\frac{\frac{B}{B_{x}}}{\frac{(\mathbf{0}|I_{n_{\text{in}}-k})}{B_{z}}}\right) (r_{1} \oplus m_{2}^{\prime}) + \left(\frac{\frac{\Delta s}{\Delta s_{x}}}{\frac{0}{\Delta s_{z}}}\right), s(\mathcal{C}_{2}) = \left(\frac{\frac{A^{(2)}}{A_{x}^{(2)}}}{\frac{(\mathbf{0}|I_{n_{\text{in}}-k})}{A_{z}^{(2)}}}\right) (r_{2} \oplus m_{2}).$$
 (24)

For the linear maps enacted by C_1''' and C_2 upon outcomes o'_1 and o_2 to be equivalent⁷, the values of the sign vectors $s(C_1''')$ and $s(C_2)$ must be equal. From the third block of these matrix equations, we see that it is necessary that $m_2 = m'_2$.

(C) Next we check the equivalence for a fixed outcome. We check if there exists an outcome $m_2' \oplus r_1'$ of \mathcal{C}_1''' upon which it enacts the same linear map (up to a global phase) as \mathcal{C}_2 upon outcome $0^{n_r^{(2)}+n_{\text{in}}-k}$. By Definition 2.6 of instrument equivalence, such an outcome of \mathcal{C}_1''' must exist if \mathcal{C}_1 and \mathcal{C}_2 are equivalent. Since $m_2 = m_2'$, the equality of the sign vectors $s(\mathcal{C}_1''')$, $s(\mathcal{C}_2)$ in Eq. (24) simplifies to

$$\left(\frac{\frac{B_{*,[n_r^{(1)}]}}{(B_x)_{*,[n_r^{(1)}]}}}{(B_z)_{*,[n_r^{(1)}]}}\right)r_1' + \left(\frac{\Delta s}{\Delta s_x}\right) = 0$$
(25)

We check if such an r'_1 exists using the compression map Procedure 6.6 in Line 16. The compression map replaces the outcome vector with a compressed outcome vector, and replaces the matrix in the equation with a matrix in reduced row echelon form. We solve the resulting equation in Line 17 via back substitution. The vector r'_1 is then $F_1^{(-1)}r_0$ where $F_1^{(-1)}$ is the right

⁷Linear maps are equivalent when they are equal up to a global phase

inverse of the outcome compression matrix F_1 . The matrix $F_1^{(-1)}$ corresponds to the embedding matrix computed by the compression map Procedure 6.6. If no solution exists, the circuits are not equivalent (Line 18). The correction unitary in Table 7.1 appended to the end of C_1 has the effect of setting Δs , Δs_x , Δs_z to zero and ensuring that $r'_1 = 0$ is a solution to Eq. (25).

(D) Next we check equivalence for all measurement outcomes. Consider sign vector $s(\mathcal{C}_2)$ related to the linear map enacted by \mathcal{C}_2 upon $0^{n_r^{(2)}} \oplus m_2$. It must be equal to $s(\mathcal{C}_1''')$ upon outcome $r'_1 \oplus m_2$. Therefore, for all m_2 :

$$A^{(2,m)}m_2 = B^{(m)}m_2, \ A_x^{(2,m)}m_2 = B_x^{(m)}m_2, \ A_z^{(2,m)}m_2 = B_z^{(m)}m_2.$$
 (26)

for the above matrices defined in Line 19. We check that this is the case in Line 20. If this is not the case, correction unitary in Table 7.1 appended to the end of C_1 has the effect of setting $B^{(m)}$, $B_x^{(m)}$, $B_z^{(m)}$ to $A^{(2,m)}$, $A_z^{(2,m)}$.

(E) It remains to check equivalence for all outcomes, including random bit vectors r_1, r_2 . Assuming Eqs. (25) and (26) and introducing $r = r_1 + r'_1$, the equality of sign vectors $s(\mathcal{C}'''_1)$, $s(\mathcal{C}_2)$ simplifies to

$$\left(\frac{B_{*,[n_r^{(1)}]}}{(B_x)_{*,[n_r^{(1)}]}}\right)r = \left(\frac{A_{*,[n_r^{(1)}]}^{(2)}}{(A_x^{(2)})_{*,[n_r^{(1)}]}}\right)r_2$$

for all possible values of r, r_2 . In other words, the image spaces of the stacked matrices must be the same. We check for this by using the compression map Procedure 6.6 in Line 21. We then compare the results of applying the compression maps in Line 22. If the compression maps are applied to the general form circuits with condition matrices $B_{*,[n_r^{(1)}]}, (B_x)_{*,[n_r^{(1)}]}, (B_z)_{*,[n_r^{(1)}]}, (B_z)_{*,[n_r^{(1)}]},$

We analyze the run time of the general form circuit comparison Algorithm 7.5 in terms of $n = \max(n_{\text{in}}, n_{\text{out}})$ and the number of random bits of the general form circuits being compared $n_r^{(1)}, n_r^{(2)}$. We show below that the algorithm runtime is

$$O(n \cdot (n^{\omega - 1} + n_r^{(1)} + n_r^{(2)})). \tag{27}$$

The stabilizer group equivalence check for $[n_{\rm in}, k_1, L_1]$ and $[n_{\rm in}, k_2, R_2]$ and also for $[n_{\rm out}, k_1, D_1]$ and $[n_{\rm out}, k_2, D_2]$ relies on Procedure 7.4 and contributes $O(n^{\omega})$. The equivalence check up to Pauli unitaries Lines 9 and 11 contributes $O(n^{\omega})$.

Simplifying the unitary acting on the inner qubits contributes $O(n_r^{(1)}n^{\omega-1}+n^{\omega})$. This is because computing matrix products of rectangular and square matrices in Lines 12 and 13 contributes $O(n_r^{(1)}n^{\omega-1}+n^{\omega})$ (see Eq. (47)). The run time of Line 14 is the run time of matrix vector multiplication and is negligible in comparison with matrix-matrix multiplications. The run time of Line 15 is of finding square and rectangular matrix products and is $O(n_r^{(1)}n^{\omega-1}+n^{\omega})$.

Computing the outcome compression maps in Lines 16 and 21 is $O(n_r^{(2)}n^{\omega-1})$ and $O(n_r^{(1)}n^{\omega-1})$ according to Eq. (20). The rest of the steps are matrix comparisons Lines 20 and 22, and solving a linear equation for a matrix in reduced row echelon form Line 17, with run time negligible compared with the other steps. In summary, the run time of the general form comparison algorithm is given by Eq. (27) as required.

8 Logical action of stabilizer circuits

Given a circuit that implements a logical operation on encoded information, it can be useful to identify what that logical action is. It may also be desirable to verify that the logical action matches that of some known reference circuit. For example, one may wish to check that a circuit performs some lattice surgery operations on two patches of surface code implements the joint XX or ZZ measurement of the logical qubits.

In Section 8.1 we provide Algorithm 8.2 which finds a general form circuit with action matching the logical action of an input logical operation circuit. This algorithm also flags when the input circuit is not a logical operation circuit, and we explain how to identify a correction unitary to append to the input circuit to rectify this. Then, in Section 8.2 we provide Algorithm 8.4 which checks if an input logical operation circuit \mathcal{C} implements the same action as a given reference circuit \mathcal{C}_{ref} . This makes use of Algorithm 8.2 and Algorithm 6.2 by first finding general form circuits equivalent to \mathcal{C}_{ref} and to the logical action of \mathcal{C} , before using Algorithm 7.5 to compare these two general form circuits.

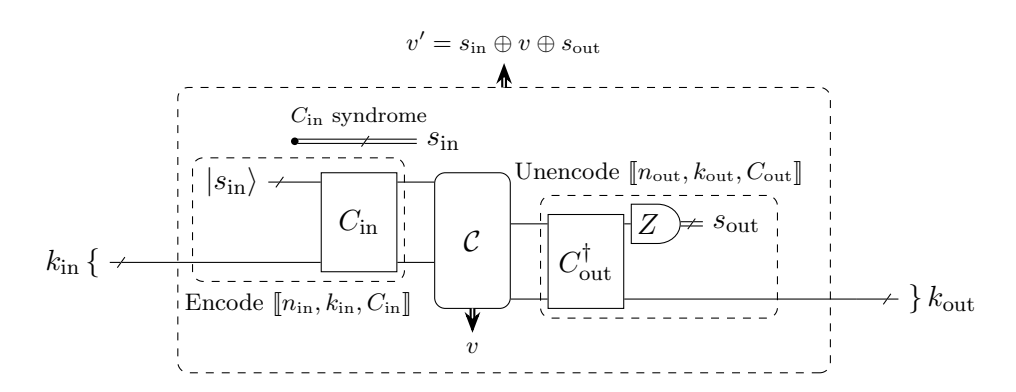
8.1 General form circuit for logical action

Building on the definitions in Section 2.3, we provide a formal definition of the problem we wish to solve:

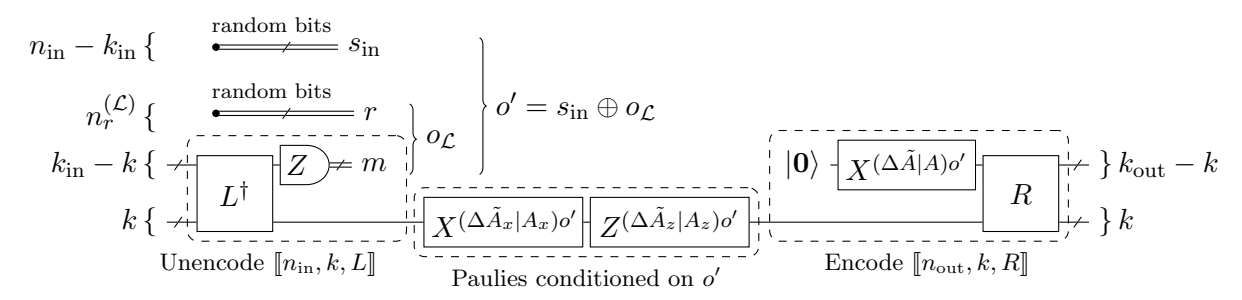
Problem 8.1 (Logical action). Consider a stabilizer circuit \mathcal{C} with outcome vector v, n_{in} input qubits and n_{out} output qubits. Further consider the stabilizer codes $[n_{in}, k_{in}, C_{in}]$ and $[n_{out}, k_{out}, C_{out}]$. Check if \mathcal{C} is a logical operation circuit with input and output codes $[n_{in}, k_{in}, C_{in}]$ and $[n_{out}, k_{out}, C_{out}]$. If \mathcal{C} is a logical operation circuit, find a general form circuit $\mathcal{C}_{\mathcal{L}}$ with outcome vector $o_{\mathcal{L}}$, full column rank matrix $M_{\mathcal{L}}$ and vector $v_{\mathcal{L},0}$ defining the equivalent outcomes such that the logical action of \mathcal{C} upon outcome $v = v_{\mathcal{L},0} + M_{\mathcal{L}}o_{\mathcal{L}}$ has the same as action as $\mathcal{C}_{\mathcal{L}}$ upon outcome $o_{\mathcal{L}}$.

Next we describe Algorithm 8.2, which solves this problem in three main steps. In the first step, the algorithm computes a general form circuit C'_{gen} for the circuit $C' = \mathcal{E}(k_{\text{in}}, C_{\text{in}}) \circ \mathcal{C} \circ \mathcal{E}^{\dagger}(k_{\text{out}}, C_{\text{out}})$, which encodes into the input code, applies the circuit, and then unencodes from the output code (see Fig. 8.1(a)). The second step analyzes C'_{gen} to check that the circuit \mathcal{C} is indeed a logical operation circuit. We show that this check can be performed by inspecting the matrix M' which specifies the map between the outcomes of \mathcal{C}' and the equivalent general form circuit C'_{gen} . At this point, it may seem that the problem has been solved since we have a general form circuit and a map specifying its equivalence to C', which above we claimed which encodes into the input code, applies the circuit, and then unencodes from the output code. However, the encoding circuit at the start of C' more precisely encodes into a code equivalent to the input code $[n_{\text{in}}, k_{\text{in}}, C_{\text{in}}]$, but with a random syndrome s_{in} . We seek a general form circuit $C_{\mathcal{L}}$ which has equivalent action to C' when s_{in} is trivial, which corresponds to the case where C' begins by encoding into precisely the code $[n_{\text{in}}, k_{\text{in}}, C_{\text{in}}]$. Below we will see that the incorporation of s_{in} strengthens the power of the Algorithm 8.2 considerably.

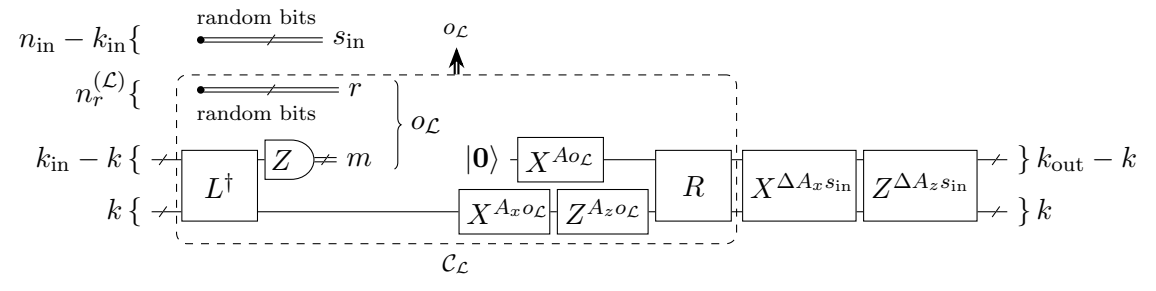
To find a general form circuit $\mathcal{C}_{\mathcal{L}}$ equivalent to the logical action of \mathcal{C} , the third step of Algorithm 8.2 is to split the matrix M' and the condition matrices A', A'_x, A'_z of $\mathcal{C}'_{\text{gen}}$ into two components (see Fig. 8.1(b)). The set of first components of these matrices specifies the matrices needed to define $\mathcal{C}_{\mathcal{L}}$, while the set of second components of these matrices specifies the difference between the action of \mathcal{C}' when the syndrome s_{in} is zero (corresponding to the logical action of \mathcal{C}) and when it is not zero (see Fig. 8.1(c)). The first two outputs of Algorithm 8.2, marked as (1) and (2), are the solution to Problem 8.1 and the last two outputs, marked as (3) and (4), describe how the action is modified when s_{in} is non-zero. Note that the information in (3) and (4) is not explicitly called for by Problem 8.1 but it can be very useful to know the logical action of a circuit for any input code syndrome s_{in} , for example to analyze its fault-tolerance properties.



(a) Circuit \mathcal{C}' , defining the logical action of \mathcal{C} for input and output codes $[n_{\text{in}}, k_{\text{in}}, C_{\text{in}}]$, $[n_{\text{out}}, k_{\text{out}}, C_{\text{out}}]$.



(b) A general form circuit C'_{gen} , equivalent to C' with outcome map $v' = M'o' + v'_0$. For convenience, we split the random bit register as $r' = s_{\text{in}} \oplus r$ and split the condition matrices as $A' = (\Delta \tilde{A}|A)$, $A'_x = (\Delta \tilde{A}_x|A_x)$ and $A'_Z = (\Delta \tilde{A}_z|A_z)$, into $(n_{\text{in}} - k_{\text{in}})$ -column and $(n_r^{(\mathcal{L})} + (k_{\text{in}} - k))$ -column components.



(c) A circuit which is equivalent to \mathcal{C}' . This circuit is built from a general form circuit $\mathcal{C}_{\mathcal{L}}$, which is equivalent to \mathcal{C}' when s_{in} is trivial, followed by Paulies conditioned on s_{in} with outcome vector $s_{\text{in}} \oplus o_{\mathcal{L}}$.

Figure 8.1: The circuits in (a) and (c) are equivalent with outcome map $s_{\text{in}} \oplus v \oplus s_{\text{out}} = s_{\text{in}} \oplus (M_{\mathcal{L}}o_{\mathcal{L}} + v_{\mathcal{L},0} + \Delta M s_{\text{in}}) \oplus \Delta A s_{\text{in}}$ provided that \mathcal{C} is a logical operation circuit.

Algorithm 8.2 (Logical action) Input:

- A stabilizer circuit C with n_{in} input qubits, n_{out} output qubits and n_M outcomes,
- Stabilizer codes $[n_{\rm in}, k_{\rm in}, C_{\rm in}]$ and $[n_{\rm out}, k_{\rm out}, C_{\rm out}]$.

Output: One of the following:

- False (the circuit C is not a logical operation circuit with input code $[n_{in}, k_{in}, C_{in}]$ and output code $[n_{\text{out}}, k_{\text{out}}, C_{\text{out}}]$).
- True (the circuit is a logical operation circuit) and the following:
 - (1) General form circuit $\mathcal{C}_{\mathcal{L}}$ equivalent to $\mathcal{C}' = \mathcal{E}(k_{\rm in}, C_{\rm in}) \circ \mathcal{C} \circ \mathcal{E}^{\dagger}(k_{\rm out}, C_{\rm out})$ when the random outcome of the encoding circuit $\mathcal{E}(k_{\rm in}, C_{\rm in})$ is $s_{\rm in} = 0$,
 - (2) Logical outcome map $o_{\mathcal{L}} \mapsto M_{\mathcal{L}} o_{\mathcal{L}} + v_{\mathcal{L},0}$ from outcomes of $\mathcal{C}_{\mathcal{L}}$ to outcomes of \mathcal{C} ,
 - (3) Difference operator: k_{out} -qubit conditional Pauli unitary $X^{(\tilde{\Delta}A_x)s_{\text{in}}}Z^{(\Delta A_z)s_{\text{in}}}$,
 - (4) Difference map: $\Delta v = \Delta M s_{\text{in}}$, output syndrome map $s_{\text{out}} = (\Delta A) s_{\text{in}}$.

Upon the output True, the outputs of the algorithm satisfy conditions in Fig. 8.1. Additionally, the matrix $M_{\mathcal{L}}$ has full column rank and is in $(n_r^{(\mathcal{L})}, n_m^{(\mathcal{L})})$ -split reduced form for $n_r^{(\mathcal{L})}, n_m^{(\mathcal{L})}$ being the number of random bit and measurement outcomes of $\mathcal{C}_{\mathcal{L}}$. The entries of $v_{\mathcal{L},0}$ corresponding to the row rank profile of the left and right parts of $M_{\mathcal{L}}$ are zero.

- 1: Construct stabilizer circuit $C' = \mathcal{E}(k_{\rm in}, C_{\rm in}) \circ \mathcal{C} \circ \mathcal{E}^{\dagger}(k_{\rm out}, C_{\rm out})$.
- 2: Find a general form \mathcal{C}'_{gen} of \mathcal{C}' (Algorithm 6.2) (that is find left and right Clifford unitaries L, R, condition matrices A', A'_x, A'_z , matrix M' in (n'_r, n'_m) -split reduced echelon form and vector v_0' which determine the mapping between outcomes of $\mathcal{C}_{\text{gen}}'$ and \mathcal{C}' .

 \triangleright Check if $\mathcal C$ is a logical operation circuit

```
3: for j \in [n_{\text{out}} - k_{\text{out}}] do
                                                  \triangleright Check if s_{\text{out}} are redundant outcomes dependent only on s_{\text{in}}
```

if $(n_{\rm in} - k_{\rm in}) + n_M + j$ is in row rank profile of $M'_{*,[n'_r]}$ then

 \triangleright Syndrome outcome $(s_{\text{out}})_j$ is a random outcome 5:

if $(n_{\rm in}-k_{\rm in})+n_M+j$ is in row rank profile of $M'_{*,[n'_r+1,n'_r+n'_m]}$ then 6:

 \triangleright Syndrome outcome $(s_{\text{out}})_j$ is an input-dependent outcome 7:

if $M'_{(n_{\text{in}}-k_{\text{in}})+n_M+j,[n'_r-(n_{\text{in}}-k_{\text{in}})+1,n'_r]} \neq 0$ then return False \triangleright Syndrome outcome (8:

 \triangleright Syndrome outcome $(s_{\text{out}})_j$ depends on random outcomes of \mathcal{C} 9:

10: **if** $(v_0')_{(n_{\text{in}}-k_{\text{in}})+n_M+[n_{\text{out}}-k_{\text{out}}]} \neq 0$ **then**

 \triangleright Syndrome s_{out} is not zero when syndrome s_{in} is zero

12:
$$\Delta A \leftarrow M'_{(n_{\text{in}}-k_{\text{in}})+n_M+[n_{\text{out}}-k_{\text{out}}],[n_{\text{in}}-k_{\text{in}}]}$$

 \triangleright Construct outputs (1)-(4)

13: Let $\mathcal{C}_{\mathcal{L}}$ be a general form circuit with left and right Clifford unitaries L, R and condition matrices $A=A'_{*,[n_{\rm in}-k_{\rm in}+1,\cdot]}, A_{\sigma}=(A'_{\sigma})_{*,[n_{\rm in}-k_{\rm in}+1,\cdot]}$ for $\sigma\in\{x,z\}$. 14: Find $\Delta A_x, \Delta A_z$ from the equality

▶ Proposition A.3

$$X^{(\Delta A_x)s}Z^{(\Delta A_z)s} \simeq R\left(X^{(\Delta \tilde{A})s}\otimes \left(X^{(\Delta \tilde{A}_x)s}Z^{(\Delta \tilde{A}_z)s}\right)\right)R^{\dagger},$$

where
$$\Delta \tilde{A} = A'_{*,[n_{\text{in}}-k_{\text{in}}]}$$
, $\Delta \tilde{A}_x = (A'_x)_{*,[n_{\text{in}}-k_{\text{in}}]}$, and $\Delta \tilde{A}_z = (A'_z)_{*,[n_{\text{in}}-k_{\text{in}}]}$.

15:
$$M_{\mathcal{L}} \leftarrow M'_{[n_{\text{in}}-k_{\text{in}}+1, n_{\text{in}}-k_{\text{in}}+n_M], [n_{\text{in}}-k_{\text{in}}+1, \cdot]}, v_{L,0} = (v'_0)_{[n_{\text{in}}-k_{\text{in}}+1, n_{\text{in}}-k_{\text{in}}+n_M]}$$

16: $\Delta M \leftarrow M'_{[n_{\text{in}}-k_{\text{in}}+1,n_{\text{in}}-k_{\text{in}}+n_M],[n_{\text{in}}-k_{\text{in}}]}$ 17: **return** True, (1) $\mathcal{C}_{\mathcal{L}}$, (2) $M_{\mathcal{L}}$, $v_{\mathcal{L},0}$, (3) ΔA_x , ΔA_z , (4) ΔA , ΔM .

Next we explain the correctness of Algorithm 8.2. While working through this explanation, we also describe how to find a correction unitary as specified in Table 8.1 which can be appended to the input circuit \mathcal{C} when the algorithm returns False (due to \mathcal{C} not being a logical operation circuit) in order to modify \mathcal{C} to form a logical operation circuit.

Let us first discuss in more detail how to check that \mathcal{C} is a logical operation circuit using the general form circuit $\mathcal{C}'_{\text{gen}}$ and the outcome mapping defined by the matrix M' for the circuit $\mathcal{C}' = \mathcal{E}(k_{\text{in}}, C_{\text{in}}) \circ \mathcal{C} \circ \mathcal{E}^{\dagger}(k_{\text{out}}, C_{\text{out}})$ (see Fig. 8.1(a)). Consider a general form circuit $\mathcal{C}''_{\text{gen}}$ of $\mathcal{C}'' = \mathcal{E}(k_{\text{in}}, C_{\text{in}}) \circ \mathcal{C}$ (which is the sub-circuit of \mathcal{C}' consisting of $\mathcal{E}(k_{\text{in}}, C_{\text{in}})$ followed by \mathcal{C}). For the circuit \mathcal{C} to be a logical operation circuit with input code $[n_{\text{in}}, k_{\text{in}}, C_{\text{in}}]$ and output code $[n_{\text{out}}, k_{\text{out}}, C_{\text{out}}]$, it is necessary that the left stabilizer group of $\mathcal{C}''_{\text{gen}}$ contains $[n_{\text{out}}, k_{\text{out}}, C_{\text{out}}]$ up to signs. In other words, it is necessary that each outcome bit in s_{out} of \mathcal{C}' is a redundant outcome. We check for this necessary condition in Lines 4 and 6 by ensuring that each outcome bit in s_{out} is neither random, nor input-dependent, making use of the fact that M' is in split reduced echelon form (see Definition 4.1 and Fig. 4.2).

The logical operation circuit Definition 2.8 requires that the circuit output is encoded in $[n_{\text{out}}, k_{\text{out}}, C_{\text{out}}]$ when the circuit input is encoded in $[n_{\text{in}}, k_{\text{in}}, C_{\text{in}}]$. To ensure this requirement, it is necessary that outcomes in s_{out} do not depend on the random outcomes of circuit \mathcal{C} . We check this in Line 8. We can also amend \mathcal{C} if this necessary condition is not satisfied by including the conditional Pauli correction at the end of \mathcal{C} as shown in Table 8.1, resulting in a new circuit which satisfies the condition.

Even when all the aforementioned necessary conditions are met, it is possible that \mathcal{C} is not a logical operation circuit as it could map states encoded in $[n_{\rm in}, k_{\rm in}, C_{\rm in}]$ to states encoded in a code which is equivalent to but not equal to $[n_{\rm out}, k_{\rm out}, C_{\rm out}]$ (i.e. with a fixed non-zero syndrome). We check that this is not the case in Line 10. It this check fails, we can correct for it by appending the Pauli unitaries shown in Table 8.1 to the end of \mathcal{C} . When all the necessary conditions we have discussed are met, it must be that \mathcal{C} is a logical operation circuit and the output code syndrome $s_{\rm out}$ must be a linear function of the input code syndrome $s_{\rm in}$, that is $s_{\rm out} = (\Delta A)s_{\rm in}$.

The matrix ΔA is extracted from M' in Line 12. This is possible because the matrix M' is in split reduced echelon form and those entries of v'_0 which correspond to random outcomes are zero and so the first $n_{\rm in} - k_{\rm in}$ bits of the outcome vector of \mathcal{C}' that are equal to the input code syndrome $s_{\rm in}$ are also equal to the first $n_{\rm in} - k_{\rm in}$ random bits of the general form circuit $\mathcal{C}'_{\rm gen}$. For the same reason, the first $n_{\rm in} - k_{\rm in}$ columns of the condition matrices A', A'_x, A'_z determine the dependence of the action of \mathcal{C}' on the input code syndrome $s_{\rm in}$. We use this to compute the difference Pauli operators in Line 14. The remaining columns of A', A'_x, A'_z are precisely the condition matrices of $\mathcal{C}_{\mathcal{L}}$ (Line 13).

The mapping between the outcomes of the general form circuit $\mathcal{C}_{\mathcal{L}}$ and the outcomes of \mathcal{C} is given by a sub-matrix M_L of M' in Line 15. This is because circuit \mathcal{C}' starts with allocating $n_{\rm in} - k_{\rm in}$ random bits and top-left $(n_{\rm in} - k_{\rm in}) \times (n_{\rm in} - k_{\rm in})$ block is identity. This structure and the fact that all outcomes in $s_{\rm out}$ are redundant also implies that the sub-matrix M_L is in split reduced echelon form. Similarly, the outcome difference map ΔM for when input code syndrome is non-trivial is captured by the first $n_{\rm in} - k_{\rm in}$ columns of M' as in Line 16.

Next we discuss the run time of Algorithm 8.2. The run time of Algorithm 8.2 is limited by the run time of Line 2:

$$O(n_{\uparrow} \cdot (N_{\text{u}} + (N_{\text{cnd}} + n_M)(n_r + n_m + (n_{\text{in}} - k_{\text{in}}) + (n_{\text{out}} - k_{\text{out}}) + 1) + n_{\uparrow}(n_{\uparrow} + n_r))). \tag{28}$$

This equation follows from Eq. (17) and the following bounds on the parameters of \mathcal{C}' . The circuit \mathcal{C}' has $n_M + n_{\text{out}} - k_{\text{out}}$ outcomes, of which at most $n_r + n_{\text{in}} - k_{\text{in}} + n_{\text{out}} - k_{\text{out}}$ are random and at most $n_m + n_{\text{out}} - k_{\text{out}}$ are input-dependent. We also include the run time $O(n_{\downarrow}^3)$ of simulating the unitaries C_{in} and C_{out}^{\dagger} when computing the general form $\mathcal{C}'_{\text{gen}}$.

Algorithm 8.2 has a number of applications. For example, we can use the additional outputs (3) and (4) of the algorithm to determine which input code syndromes do not cause logical errors

Case when \mathcal{C}		Correction unitary U to ensure
is not a logical	Line	that \mathcal{C} is a logical operation circuit
operation circuit	e	via appending U to $\mathcal C$
Output syndrome s_{out}		Let $\Delta a = M'_{(n_{\text{in}} - k_{\text{in}}) + n_M + j, [n'_r - (n_{\text{in}} - k_{\text{in}}) + 1, n'_r]}$ (Line 8)
depends on random	9	$U = C_{\text{out}}^{\dagger} X_j C_{\text{out}}$ conditioned on the random outcomes of
outcomes of \mathcal{C}		\mathcal{C} indicated by Δa
Output syndrome s_{out}		Let $\Delta v = (v_0')_{(n_{\text{in}} - k_{\text{in}}) + n_M + [n_{\text{out}} - k_{\text{out}}]}$ (Line 10)
when input syndrome	11	Let $\Delta v = (v_0')_{(n_{\text{in}} - k_{\text{in}}) + n_M + [n_{\text{out}} - k_{\text{out}}]}$ (Line 10) $U = C_{\text{out}}^{\dagger}(X^{\Delta v} \otimes I_{k_{\text{out}}})C_{\text{out}}$
$s_{\rm in}$ is zero		

Table 8.1: Cases when computing the logical action of stabilizer circuit \mathcal{C} using Algorithm 8.2 fails a check and returns False and there exists a correction unitary to append to \mathcal{C} to ensure that check is passed. Variables in the equations for the correction unitaries are defined in the pseudo-code of Algorithm 8.2.

and classify all syndromes according to the logical errors they cause. First, code syndromes that do not cause logical errors must not cause Pauli X or Z errors on the logical qubits, so such $s_{\rm in}$ must belong to the intersection of kernels of ΔA_x , ΔA_z returned as output (3). Additionally, these syndromes must not flip the logical measurement outcomes, that is they should belong to the kernel of $M_L^{(-1)}(\Delta M)s_{\rm in}$, where ΔM is returned as part of output (4) of the algorithm. The syndromes of the input code that do not cause logical errors form a linear space L_0 . Taking the quotient of the space of all possible syndromes by L_0 lets us partition syndromes into the sets that cause the same logical error.

8.2 Logical action verification

It may be desirable to verify that the logical action of given logical operation circuit matches the action of some known reference circuit. We can state the logical operation circuit comparison problem in a form that is similar to the stabilizer circuit comparison Problem 7.1:

Problem 8.3 (Logical circuit comparison). Consider:

- ullet a stabilizer circuit ${\mathcal C}$ with outcome vector v, $n_{\rm in}$ input qubits and $n_{\rm out}$ output qubits,
- an input code $[n_{in}, k_{in}, C_{in}]$ and an output code $[n_{out}, k_{out}, C_{out}]$,
- a reference stabilizer circuit C_{ref} with outcome vector v_{ref} , k_{in} input and k_{out} output qubits.

Find if C is a logical operation circuit (Definition 2.8) with input code $[n_{in}, k_{in}, C_{in}]$ and output code $[n_{out}, k_{out}, C_{out}]$. If it is, find if the logical action (Definition 2.9) of C is equivalent to the action of C_{ref} . If the actions are equivalent, find matrices M, M_{ref} and vectors u, u_{ref} such that the logical action of C upon outcome v is the same as the action of C_{ref} upon outcome v_{ref} if and only if $M(v + u) = M_{ref}(v_{ref} + u_{ref})$.

The main difference between the above problem and the stabilizer circuit comparison Problem 7.1 is that in Problem 7.1 we must first check if \mathcal{C} is a logical operation circuit and then analyze its logical action with respect to the input and output codes. Similarly to the stabilizer circuit comparison Problem 7.1, when the circuits are equivalent and the matrix M_{ref} has a left inverse, we can find a map between the outcome vector v of \mathcal{C} and the outcome vector v_{ref} of \mathcal{C}_{ref} as

$$v_{\text{ref}} = u_{\text{ref}} + M_{\text{ref}}^{(-1)} M(v + u).$$

Consider an example in which one wishes check that a circuit which performs a lattice surgery operation on two patches of surface code implements the joint XX measurement of the logical qubits encoded in the patches. In this case, the input circuit can be highly complex, producing a long output vector v containing a long list of measurement outcomes. The reference circuit

on the other hand consists of an XX measurement on a pair of qubits, which produces a single output bit v_{ref} , and as such it must be that $M_{\text{ref}} = 1$. This trivially has a left inverse $M_{\text{ref}}^{(-1)} = I_1$, and the above map will provide the lattice surgery circuit outcomes corresponding the logical XX or ZZ measurement outcome.

Below we present a logical action verification Algorithm 8.4, which solves the logical action verification Problem 8.3 in three main steps. The first step is to verify that the circuit circuit \mathcal{C} is a logical operation circuit and find a general form circuit $\mathcal{C}_{\mathcal{L}}$ equivalent to its logical action (Definition 2.9). The second step is to find a general form circuit equivalent to \mathcal{C}_{ref} using Algorithm 6.2. The third step is to compare the logical action general form circuit $\mathcal{C}_{\mathcal{L}}$ and the general form circuit equivalent to \mathcal{C}_{ref} using the general form comparison Algorithm 7.5.

Algorithm 8.4 (Logical action verification) Input:

return True, M, M_{ref} , u, u_{ref}

11:

- A stabilizer circuit C with $n_{\rm in}$ input qubits, $n_{\rm out}$ output qubits.
- Stabilizer codes $[n_{\rm in}, k_{\rm in}, C_{\rm in}], [n_{\rm out}, k_{\rm out}, C_{\rm out}].$
- A stabilizer circuit C_{ref} with k_{in} input qubits, k_{out} output qubits.

Output: One of the following:

- False (the circuit is not a logical operation circuit with input code $[n_{in}, k_{in}, C_{in}]$ and output code $[n_{out}, k_{out}, C_{out}]$ equivalent to C_{ref}).
- True (the circuit is a logical operation circuit equivalent to C_{ref}) and matrices M, M_{ref} , vectors u, u_{ref} defining the equivalent outcomes as in Problem 8.3.

```
1: Solve logical action Problem 8.1 for C, [n_{\rm in}, k_{\rm in}, C_{\rm in}], [n_{\rm out}, k_{\rm out}, C_{\rm out}]
                                                                                                                                           ▶ Algorithm 8.2
 2: if C is a not a logical operation circuit then
            return False
                                                                                                                                                    ▶ Table 8.1
 4: else
            Let \mathcal{C}_{\mathcal{L}} be a general form circuit for logical action of \mathcal{C}
                  with the outcome mapping between C and C_{\mathcal{L}} defined by M_L, v_{0,L}
 6: Let \mathcal{C}_{gen} be a general form circuit equivalent to \mathcal{C}_{ref},
                                                                                                                                           ▶ Algorithm 6.2
            with the outcome mapping defined by M_{\rm gen}, v_{0,\rm gen}.
                                                                                                                                           ▶ Algorithm 7.2
 7: Compare general form circuits \mathcal{C}_{\mathcal{L}} and \mathcal{C}_{\mathrm{gen}}
 8: if \mathcal{C}_{\mathcal{L}} and \mathcal{C}_{\mathrm{gen}} are equivalent with matrices \tilde{M}_L, \tilde{M}_{\mathrm{gen}} and vectors \tilde{u}_L, \tilde{u}_{\mathrm{gen}}
            defining the equivalent outcomes then
M \leftarrow \tilde{M}_L M_L^{(-1)}, \ u \leftarrow \tilde{u}_L + M_L^{(-1)} v_{0,L}, \ M_{\text{ref}} \leftarrow \tilde{M}_{\text{gen}} M_{\text{gen}}^{(-1)}, \ u_{\text{ref}} \leftarrow \tilde{u}_{\text{gen}} + M_{\text{gen}}^{(-1)} v_{0,\text{gen}}
10:
```

12: else
13: return False ▷ Table 7.1

Now we briefly discuss the correctness of Algorithm 8.4. The logical action of \mathcal{C} is equivalent to the action of the reference circuit if and only if corresponding general form circuits are equivalent. The expressions for the matrices M, M_{ref} and vectors u, u_{ref} follow from: (1) expressing the outcome vector o_L of $\mathcal{C}_{\mathcal{L}}$ in terms of the outcome vector v of \mathcal{C} as $o_L = M_L^{(-1)}(v + v_{0,L})$, (2) expressing the outcome vector o of \mathcal{C}_{gen} in terms of the outcome vector v_{ref} of \mathcal{C}_{ref} as $o = M_{\text{gen}}^{(-1)}(v_{\text{ref}} + v_{0,\text{gen}})$ and (3) substituting expressions for o and o_L into the condition $\tilde{M}_L(o_l + \tilde{u}_l) = \tilde{M}_{\text{gen}}(o + \tilde{u}_{\text{gen}})$ for when the action of $\mathcal{C}_{\mathcal{L}}$ upon o_L is equivalent to the action of \mathcal{C}_{gen} upon o.

The run time of our logical action verification Algorithm 8.4 is dominated by the general form circuit computation subroutines. We parameterize \mathcal{C} as specified in Section 3.1, and use the same notation to parameterize the reference circuit \mathcal{C}_{ref} but with the superscript ^(ref) on each parameter.

The run time analysis of our logical action Algorithm 8.2 presented in the previous subsection (Eq. (28)) and the run time analysis of our general form Algorithm 6.2 (Eq. (17)) and

general form comparison Algorithm 7.5 (Eq. (27)) imply that the runtime of our logical action verification Algorithm 8.4 is:

$$O\left(n_{\updownarrow} \cdot (N_{\rm u} + (N_{\rm cnd} + n_M)(n_r + n_m + (n_{\rm in} - k_{\rm in}) + (n_{\rm out} - k_{\rm out}) + 1) + n_{\updownarrow}(n_{\updownarrow} + n_r)\right) + n_{\updownarrow}^{(\rm ref)} \cdot \left(N_{\rm u}^{(\rm ref)} + (N_{\rm cnd}^{(\rm ref)} + n_M^{(\rm ref)})(n_r^{(\rm ref)} + n_m^{(\rm ref)} + 1) + n_{\updownarrow}(n_{\updownarrow}^{(\rm ref)} + n_r^{(\rm ref)})\right).$$
(29)

When the logical action verification Algorithm 8.4 fails a check and returns False, it can be useful to find a "correction" unitary that can be appended to \mathcal{C} ensure that test is passed. The algorithm returns False in two cases. In the first case (Line 3), the circuit \mathcal{C} is not a logical operation circuit. In the second case (Line 13), the logical action is not equivalent to the action of the reference circuit. In the first case, it is sometimes possible to ensure that \mathcal{C} is a logical operation by appending conditional Pauli unitaries as computed within Algorithm 8.2 and provided in Table 8.1. In the second case, it is sometimes possible to ensure the action equivalence by appending Clifford unitaries or conditional Pauli unitaries to the general form circuit $\mathcal{C}_{\mathcal{L}}$ as described in Table 7.1. These unitaries act on the logical qubits of the output code $[n_{\text{out}}, k_{\text{out}}, C_{\text{out}}]$ and are conditioned on outcomes o_L of $\mathcal{C}_{\mathcal{L}}$. They can be easily translated to unitaries to append to the end of circuit \mathcal{C} to ensure the circuit equivalence. For example, the conditional Pauli unitary $X_j^{\langle c_x, o_L \rangle} Z_j^{\langle c_z, o_L \rangle}$ becomes

$$C_{\text{out}}\left(X_j^{\langle (M_L^{(-1)})^T c_x, v + v_{0,L} \rangle} Z_j^{\langle (M_L^{(-1)})^T c_z, v + v_{0,L} \rangle}\right) C_{\text{out}}^{\dagger}. \tag{30}$$

9 Logical action of code deformation circuits (analytic)

Here we consider the logical action of the class of **code deformation circuits**, which measure a set of commuting Pauli operators and then apply conditional Paulis. Such circuits form the basis of many fault-tolerance schemes, for instance they can be used to sequentially deform stabilizer codes, to perform syndrome extraction for stabilizer and Floquet codes [32], and to implement lattice surgery operations. In this section, we first formulate a precise problem logical action of code deformation Problem 9.1. While this is a special case of the logical action Problem 8.1 which is solved by Algorithm 8.2, here we present Theorem 9.4 which provides an analytic solution to Problem 9.1. We then provide an example of how this can be applied to analyze an infinite family of lattice surgery circuits in Section 9.1. In Section 9.2, we find a general form circuit equivalent to measuring two stabilizer groups, which is a result that may be of independent interest, and which we leverage in our proof of Theorem 9.4 which is given in Section 9.3.

Problem 9.1 (Logical action of code deformation). Consider the n-qubit stabilizer group $S_{\rm in}$ and a circuit $\mathcal M$ that first measures a set of commuting Pauli operators that generate an n-qubit stabilizer group M, and then applies some Pauli unitaries conditioned on the measurement outcomes. Additionally consider stabilizer codes $[n, k_{\rm in}, C_{\rm in}]$ and $[n, k_{\rm out}, C_{\rm out}]$ with stabilizer groups $S_{\rm in}$ and $S_{\rm out} \subset M \cdot (S_{\rm in} \cap M^{\perp})$.

Check whether \mathcal{M} is a logical operation circuit with input and output codes $[n, k_{\rm in}, C_{\rm in}]$ and $[n, k_{\rm out}, C_{\rm out}]$. If so, find a general form circuit $\mathcal{M}_{\mathcal{L}}$ equivalent to the logical action of \mathcal{M} (Definition 2.9) and an associated relation between the outcomes of \mathcal{M} and $\mathcal{M}_{\mathcal{L}}$.

Let us clarify what the associated relation is between the outcomes of \mathcal{M} and $\mathcal{M}_{\mathcal{L}}$ mentioned above. When the logical action of \mathcal{M} is equivalent to a general form circuit $\mathcal{M}_{\mathcal{L}}$ there exists a relation \mathcal{R} between the outcomes v_M of \mathcal{M} and the outcomes m of $\mathcal{M}_{\mathcal{L}}$ such that the following property holds: The action of $\mathcal{E}(k_{\rm in}, C_{\rm in}) \circ \mathcal{M} \circ \mathcal{E}^{\dagger}(k_{\rm out}, C_{\rm out})$ upon outcome $\mathbf{0} \oplus v_M \oplus \mathbf{0}$ is equivalent to the action of $\mathcal{M}_{\mathcal{L}}$ upon outcome m if and only if the relation \mathcal{R} is true for v_M and m. We say that \mathcal{R} is a relation associated with the equivalence of the logical action of the circuit \mathcal{M} and the circuit $\mathcal{M}_{\mathcal{L}}$.

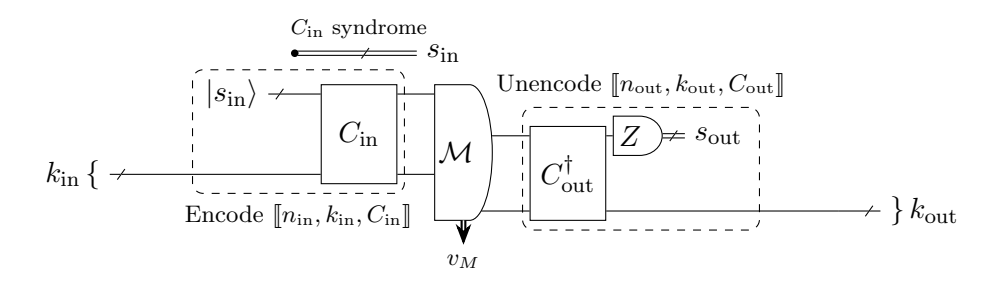
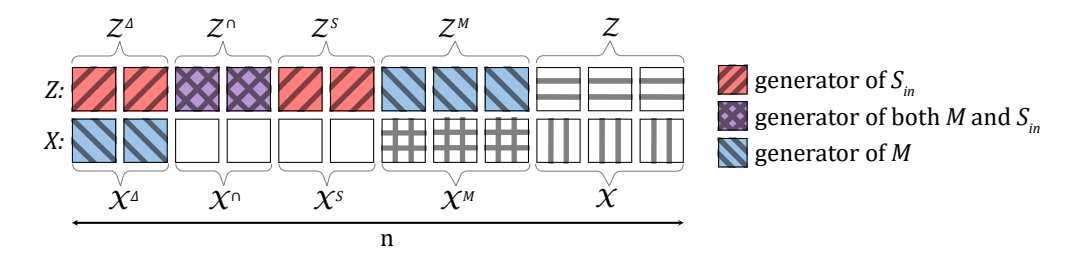


Figure 9.1: The circuit $\mathcal{E}(k_{\text{in}}, C_{\text{in}}) \circ \mathcal{M} \circ \mathcal{E}^{\dagger}(k_{\text{out}}, C_{\text{out}})$ with outcome vector $v' = s_{\text{in}} \oplus v_M \oplus s_{\text{out}}$ used for defining the logical action of a logical operation circuit \mathcal{M} with outcome vector v_M , input code $[n_{\text{in}}, k_{\text{in}}, C_{\text{in}}]$ and output code $[n_{\text{out}}, k_{\text{out}}, C_{\text{out}}]$ (Problem 9.1).

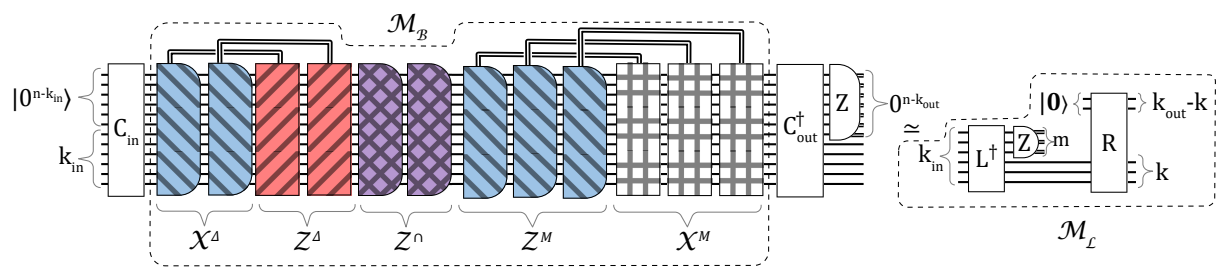
It is useful to define a symplectic basis that clarifies how any two stabilizer groups relate to each other. In Appendix E we prove any two n-qubit stabilizer groups have a common symplectic basis, defined as:

Definition 9.2 (Common symplectic basis of two stabilizer groups). A common symplectic basis \mathcal{B} for two n-qubit stabilizer groups S_{in} and M is a symplectic basis that can be grouped into ten ordered sets $\mathcal{Z}^{\Delta}, \mathcal{X}^{\Delta}, \mathcal{Z}^{\cap}, \mathcal{X}^{\cap}, \mathcal{Z}^{S}, \mathcal{X}^{S}, \mathcal{Z}^{M}, \mathcal{X}^{M}, \mathcal{Z}, \mathcal{X}$ as in Fig. 9.2a, and such that $S_{\text{in}} = \langle \mathcal{Z}^{\Delta} \cup \mathcal{Z}^{\cap} \cup \mathcal{Z}^{S} \rangle$ and $M = \langle \mathcal{X}^{\Delta} \cup \mathcal{Z}^{\cap} \cup \mathcal{Z}^{M} \rangle$.

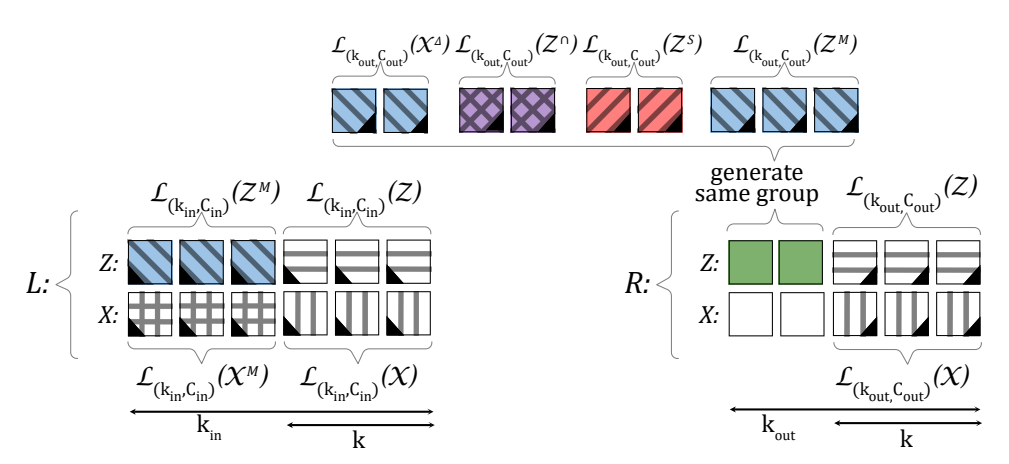
We restrict our attention in Problem 9.1 to symplectic-basis code deformation circuits defined as follows (note that any code deformation circuit \mathcal{M} that measures a group M is equivalent up to conditional Paulis to a symplectic code deformation circuit $\mathcal{M}_{\mathcal{B}}$ that measures M).



(a) A common symplectic basis \mathcal{B} of *n*-qubit stabilizer groups S_{in} and M (Definition 9.2) consists of 2n Pauli operators. Boxes correspond to basis elements of \mathcal{B} , only vertically adjacent elements anti-commute.



(b) A general form circuit $\mathcal{M}_{\mathcal{L}}$ equivalent to the logical action of circuit $\mathcal{M}_{\mathcal{B}}$ with respect to input and output codes $[n, k_{\rm in}, C_{\rm in}]$ and $[n, k_{\rm out}, C_{\rm out}]$, with stabilizer groups $S_{\rm in}$ and $S_{\rm out} \subset M \cdot (S_{\rm in} \cap M^{\perp})$ as described in Theorem 9.4. The circuit $\mathcal{M}_{\mathcal{B}}$ measures a complete set of generators of M and applies conditional Paulis determined by the common symplectic basis \mathcal{B} of $S_{\rm in}$ and M (see in Definition 9.3).



(c) The left and right Clifford unitaries L and R of the general form circuit $\mathcal{M}_{\mathcal{L}}$, where $\mathcal{M}_{\mathcal{L}}$ has k inner qubits, zero random bits and all-zero condition matrices A, A_x, A_z . To specify the k_{in} -qubit and k_{out} -qubit Clifford unitaries L and R, we show the images of the standard k_{in} -qubit and k_{out} -qubit Pauli bases under each. Most of these images correspond to images of specific elements of the symplectic basis \mathcal{B} under the logical operator maps $\mathcal{L}_{(k_{\text{in}},C_{\text{in}})}$ and $\mathcal{L}_{(k_{\text{out}},C_{\text{out}})}$ (which map n-qubit logical operators representatives for codes $[n,k_{\text{in}},C_{\text{in}}]$ and $[n,k_{\text{out}},C_{\text{out}}]$ to elements of the k_{in} -qubit and k_{out} -qubit logical Pauli group as described in Eq. (8)). Those images of Pauli basis elements under R marked in green are found however from the combination of specific elements of the symplectic basis \mathcal{B} under $\mathcal{L}_{(k_{\text{out}},C_{\text{out}})}$.

Figure 9.2: Analyzing the logical action with respect to input and output codes S_{in} and $S_{\text{out}} \subset M \cdot (S_{\text{in}} \cap M^{\perp})$ of a code deformation circuit which measures the stabilizer group M.

Definition 9.3 (Symplectic-basis code deformation circuit). Given a common symplectic basis \mathcal{B} of two n-qubit stabilizer groups S_{in} and M, we define a stabilizer circuit $\mathcal{M}_{\mathcal{B}}$ (Fig. 9.2b) with outcome vector v_M :

- measure \mathcal{X}^{Δ} , \mathcal{Z}^{\cap} , \mathcal{Z}^{M} (a full set of generators of M),
- apply Pauli unitaries \mathcal{Z}_{j}^{Δ} conditioned on measuring \mathcal{X}_{j}^{Δ} being one, for $j \in [|\mathcal{Z}^{\Delta}|]$, apply Pauli unitaries \mathcal{X}_{j}^{M} conditioned on measuring \mathcal{Z}_{j}^{M} being one, for $j \in [|\mathcal{Z}^{M}|]$.

By construction, the choice of the corrections in $\mathcal{M}_{\mathcal{B}}$ ensures that it is a logical operation circuit for any output code that satisfies the condition of Problem 9.1, that is $S_{\text{out}} \subset M$. $(S_{\rm in} \cap M^{\perp})$. To see that this is the case requires showing that $s_{\rm out} = 0$ when $s_{\rm in} = 0$ for $\mathcal{E}(k_{\rm in}, C_{\rm in}) \circ \mathcal{M}_{\mathcal{B}} \circ \mathcal{E}^{\dagger}(k_{\rm out}, C_{\rm out})$. First note that the state prior to the measurement in Fig. 9.2b, which corresponds to the state after applying the encoding circuit $\mathcal{E}(k_{\rm in}, C_{\rm in})$ with $s_{\rm in} = 0$, is stabilized by all elements of S. From the common symplectic basis Fig. 9.2a, it is clear that the expectation value of all elements of $S_{\rm in} \cap M^{\perp} = \mathcal{Z}^{\cap} \cup \mathcal{Z}^{S}$ are unchanged by measuring M and from applying corrections in $\mathcal{Z}^{\Delta} \cup \mathcal{X}^{M}$. The corrections ensure that in addition to $S_{\rm in} \cap M^{\perp}$, all elements of M are also stabilized by the state which is fed into the encoding circuit $\mathcal{E}^{\dagger}(k_{\text{out}}, C_{\text{out}})$, such that $s_{\text{out}} = 0$.

A solution to Problem 9.1 with $\mathcal{M} = \mathcal{M}_{\mathcal{B}}$ is given in Theorem 9.4 as follows:

Theorem 9.4 (Logical action of code deformation). Consider the n-qubit stabilizer groups S_{in} and M with a common symplectic basis $\mathcal{B} = \langle \mathcal{Z}^{\Delta}, \mathcal{X}^{\Delta}, \mathcal{Z}^{\cap}, \mathcal{X}^{\cap}, \mathcal{Z}^{S}, \mathcal{X}^{S}, \mathcal{Z}^{M}, \mathcal{X}^{M}, \mathcal{Z}, \mathcal{X} \rangle$ (Definition 9.2, Fig. 9.2a), and input and output codes $[n, k_{\rm in}, C_{\rm in}]$ and $[n, k_{\rm out}, C_{\rm out}]$ with stabilizer groups S_{in} and $S_{\text{out}} \subset M \cdot (S_{\text{in}} \cap M^{\perp})$.

The symplectic-basis code deformation circuit $\mathcal{M}_{\mathcal{B}}$ (Definition 9.3, Fig. 9.2b) is a logical operation circuit with input and output codes $[n, k_{\rm in}, C_{\rm in}]$ and $[n, k_{\rm out}, C_{\rm out}]$. The logical action of $\mathcal{M}_{\mathcal{B}}$ is equivalent to the general form circuit $\mathcal{M}_{\mathcal{L}}$ with zero random bits, $k = |\mathcal{Z}|$ inner qubits, left $k_{\rm in}$ -qubit Clifford unitary L, right $k_{\rm out}$ -qubit Clifford unitary R defined using using maps $\mathcal{L}_{(k_{\text{in}},C_{\text{in}})}$ and $\mathcal{L}_{(k_{\text{out}},C_{\text{out}})}$ Eq. (8), (Fig. 9.2c):

$$\langle RZ_{j}R^{\dagger}: j \in [k_{\text{out}} - k] \rangle = \langle \mathcal{L}_{(k_{\text{out}}, C_{\text{out}})}(P): P \in \mathcal{X}^{\Delta} \cup \mathcal{Z}^{\cap} \cup \mathcal{Z}^{S} \cup \mathcal{Z}^{M} \rangle$$

$$LZ_{k_{\text{in}} - k + j}L^{\dagger} = \mathcal{L}_{(k_{\text{in}}, C_{\text{in}})}(\mathcal{Z}_{j}), \qquad RZ_{k_{\text{out}} - k + j}R^{\dagger} = \mathcal{L}_{(k_{\text{out}}, C_{\text{out}})}(\mathcal{Z}_{j}), \qquad j \in [k],$$

$$LZ_{j}L^{\dagger} = \mathcal{L}_{(k_{\text{in}}, C_{\text{in}})}(\mathcal{Z}_{j}^{M}), \qquad j \in [k_{\text{in}} - k],$$

$$LX_{k_{\text{in}} - k + j}L^{\dagger} = \mathcal{L}_{(k_{\text{in}}, C_{\text{in}})}(\mathcal{X}_{j}), \qquad RX_{k_{\text{out}} - k + j}R^{\dagger} = \mathcal{L}_{(k_{\text{out}}, C_{\text{out}})}(\mathcal{X}_{j}), \qquad j \in [k],$$

$$(31)$$

All condition matrices of $\mathcal{M}_{\mathcal{L}}$ are zero. Measurement outcomes of $\mathcal{Z}_1^M, \dots, \mathcal{Z}_{k-k_{\text{in}}}^M$ in $\mathcal{M}_{\mathcal{B}}$ are input-dependent and are equal to measurement outcome vector m of $\mathcal{M}_{\mathcal{L}}$, measurement outcomes of \mathcal{X}^{Δ} in $\mathcal{M}_{\mathcal{B}}$ are random, and the measurement outcomes of \mathcal{Z}^{\cap} of $\mathcal{M}_{\mathcal{B}}$ are zero.

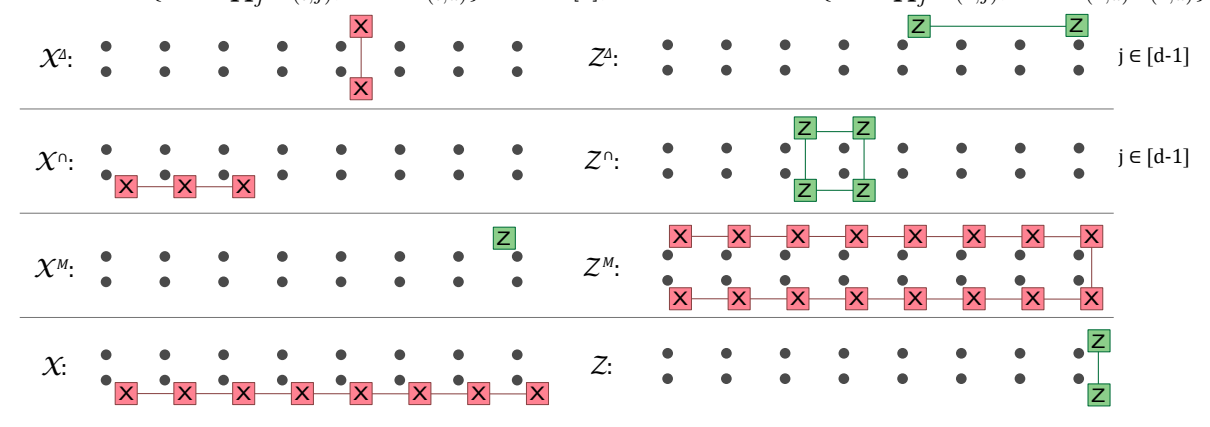
Example: lattice surgery for repetition codes

Here we provide an example demonstrating how the analytic results of Theorem 9.4 can be used to extract the logical action of an infinite family of code deformation circuits.

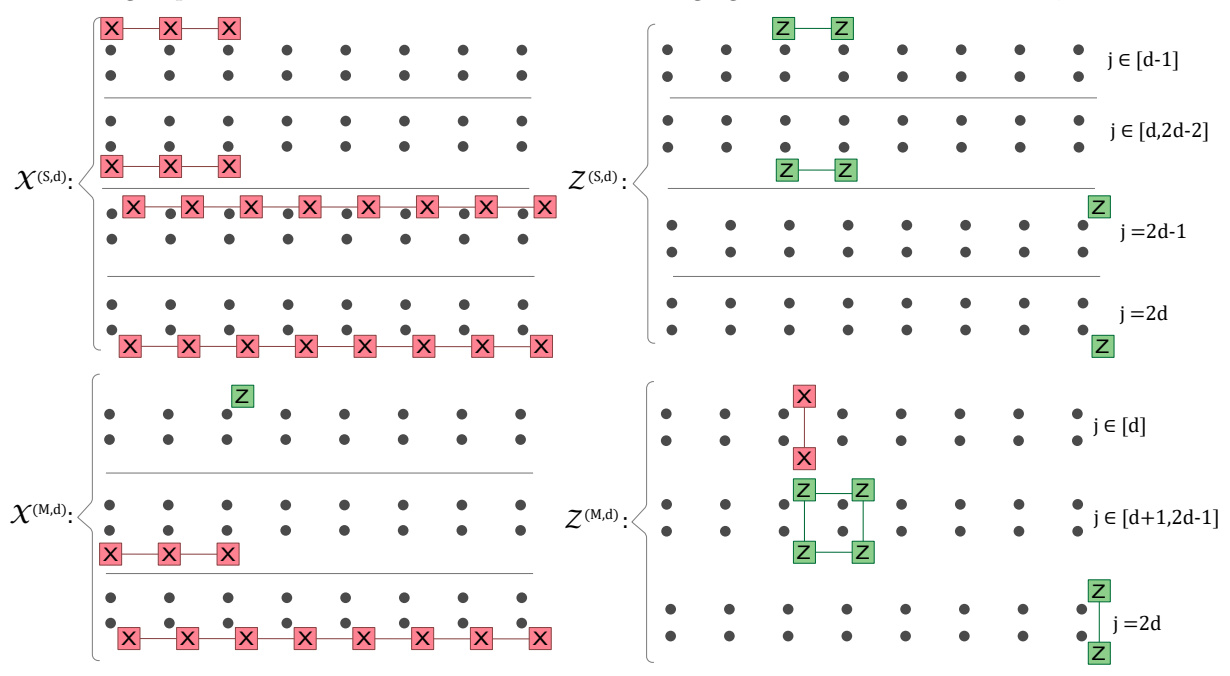
In this example, we consider 2d qubits laid out in two rows, where $d \in \mathbb{N}$. Initially two logical qubits are each encoded in a d-qubit repetition code (one code in each row of qubits) which together have the stabilizer group S_d (left of Fig. 9.3a). Then a two-step code deformation circuit \mathcal{C}_d performs lattice surgery by measuring the generators of a 2d-qubit coupled repetition code with stabilizer group M_d (right of Fig. 9.3a), before returning to the initial code by measuring the generators of S_d . We assume that there are Pauli corrections after each of the two code deformation step such that they are symplectic-basis code deformation circuits. Then \mathcal{C}_d $\mathcal{M}_{\mathcal{B}_d} \circ \mathcal{M}_{\mathcal{B}'_d}$, where \mathcal{B}_d is a common symplectic basis for S_d and M_d (see Fig. 9.3b) and \mathcal{B}'_d is a common symplectic basis for M_d and S_d . Our goal in this example is to find the logical action of \mathcal{C}_d with respect to input and output codes which are both equal to $[2d, 2, C_{S_d}]$ for an encoding unitary C_{S_d} for S_d which is specified in Fig. 9.3c.



(a) The stabilizer group S_d for a pair of d-qubit repetition codes (left) and the stabilizer group M_d of a coupled repetition code (right). S_d is generated by horizontal neighbor pairs $Z_{(i,j)}Z_{(i,j+1)}$ with $j \in [d-1]$ on each row $i \in [2]$. M_d is generated by vertical neighbor pairs $X_{(1,j)}X_{(2,j)}$ with $j \in [d]$, and squares $Z_{(1,j)}Z_{(1,j+1)}Z_{(2,j)}Z_{(2,j+1)}$ with $j \in [d-1]$. Logical operator representatives are fixed by subfigure (c) for S_d to be $\{\bar{X}_i = \prod_j X_{(i,j)}, \bar{Z}_i = Z_{(i,d)}\}$ for $i \in [2]$, and for M_d to be $\{\bar{X} = \prod_j X_{(1,j)}, \bar{Z} = Z_{(1,d)}Z_{(2,d)}\}$.



(b) The common symplectic basis \mathcal{B}_d for stabilizer groups S_d and M_d , where $|\mathcal{Z}^{\Delta}| = |\mathcal{X}^{\Delta}| = |\mathcal{Z}^{\cap}| = |\mathcal{X}^{\cap}| = |\mathcal{X}^{\cap}| = d-1$, $|\mathcal{Z}^S| = |\mathcal{X}^S| = 0$, $|\mathcal{Z}^M| = |\mathcal{X}^M| = |\mathcal{Z}| = |\mathcal{X}| = 1$. The common symplectic basis \mathcal{B}'_d for stabilizer groups M_d and S_d is obtained from \mathcal{B}_d interchanging $\mathcal{Z}^{\Delta} \leftrightarrow \mathcal{X}^{\Delta}$ and $\mathcal{Z}^S \leftrightarrow \mathcal{Z}^M$, $\mathcal{X}^S \leftrightarrow \mathcal{X}^M$.



(c) Encoding unitaries C_{S_d} , C_{M_d} for codes $[2d, 2, C_{S_d}]$, $[2d, 1, C_{M_d}]$ with stabilizer groups S_d and M_d , specified by their action on basis Paulis such that $\mathcal{X}_j^{\text{in}} = C_{S_d} X_j (C_{S_d})^{\dagger}$, $\mathcal{Z}_j^{\text{in}} = C_{S_d} Z_j (C_{S_d})^{\dagger}$ and $\mathcal{X}_j^{\text{out}} = C_{M_d} X_j (C_{M_d})^{\dagger}$, $\mathcal{Z}_j^{\text{out}} = C_{M_d} Z_j (C_{M_d})^{\dagger}$. Note that for $j \in [2d-2]$, the images under C_{S_d} are stabilizers of S_d , while for j = 2d-1, 2d they are logical operators of 2d. Similarly, for 2d images under 2d are stabilizers of 2d while for 2d they are logical operators of 2d.

Figure 9.3: Stabilizer groups, symplectic Pauli basis and encoding unitaries to analyze the example of lattice surgery for repetition codes on 2d qubits arranged in two rows using Theorem 9.4. To clarify any ambiguity in this figure, explicit definitions are provided in Appendix F.

To find the logical action of C_d , we first find and then compose the logical actions of the circuits $\mathcal{M}_{\mathcal{B}_d}$ and $\mathcal{M}_{\mathcal{B}'_d}$. To do so, we define encoding unitaries C_{S_d} and C_{M_d} for codes $[2d, 2, C_{S_d}]$ and $[2d, 1, C_{M_d}]$ with stabilizer groups S_d and M_d as specified in Fig. 9.3c. Applying Theorem 9.4 to the first step yields a general form circuit $\mathcal{M}_{\mathcal{L}}$ with action equivalent to the logical action of $\mathcal{M}_{\mathcal{B}_d}$ with respect to input and output codes $[2d, 2, C_{S_d}]$ and $[2d, 1, C_{M_d}]$. The circuit $\mathcal{M}_{\mathcal{L}}$ has k = 1 inner qubit, a $k_{\rm in} = 2$ -qubit left Clifford L and a $k_{\rm out} = 1$ -qubit right Clifford R which are defined by the equations:

$$LZ_1L^{\dagger} = X_1X_2,$$
 $LZ_2L^{\dagger} = Z_1Z_2,$ $LX_2L^{\dagger} = X_2,$ $RZ_1R^{\dagger} = Z_1,$ $RX_1R^{\dagger} = X_1.$ (32)

These equations can be identified from the specification of L and R in terms of the logical operator maps $\mathcal{L}_{(k_{\text{in}},C_{S_d})}(P)$ and $\mathcal{L}_{(k_{\text{out}},C_{M_d})}(P)$ (according to Theorem 9.4), which in turn can be read off Fig. 9.3c by considering the pre-images of the logical representatives given by the common symplectic basis of S_d and M_d under C_{S_d} and C_{M_d} respectively (according to Eq. (8)). We can check that R = I and $L = H_1CX_{1,2}$.

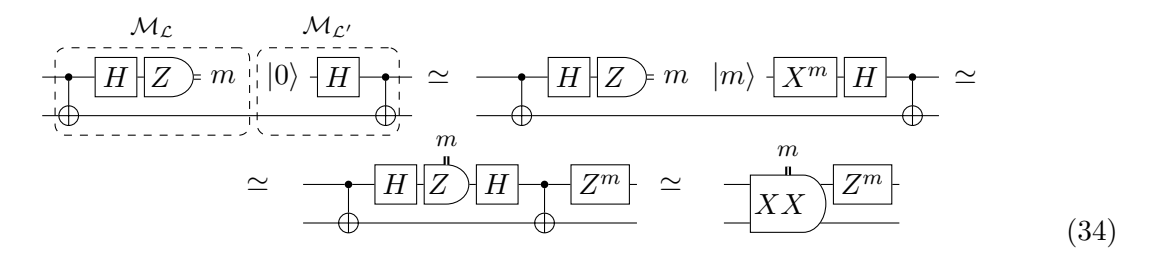
Similarly, applying Theorem 9.4 to the second step yields a general form circuit $\mathcal{M}_{\mathcal{L}'}$ with action equivalent to the logical action of $\mathcal{M}_{\mathcal{B}'_d}$ with respect to input and output codes $[2d, 1, C_{M_d}]$ and $[2d, 2, C_{S_d}]$. The circuit $\mathcal{M}_{\mathcal{L}'}$ has k' = 1 inner qubit, a $k'_{\text{in}} = 1$ -qubit left Clifford L' and a $k'_{\text{out}} = 2$ -qubit right Clifford R' which are defined by the equations:

$$R'Z_{1}(R')^{\dagger} = X_{1}X_{2}, \qquad R'Z_{2}(R')^{\dagger} = Z_{1}, \qquad L'X_{1}(L')^{\dagger} = X_{1}.$$

$$R'Z_{1}(R')^{\dagger} = X_{1}X_{2}, \qquad R'Z_{2}(R')^{\dagger} = Z_{1}Z_{2}, \qquad R'X_{2}(R')^{\dagger} = X_{2},$$
(33)

We have L' = I and $R' = H_1CX_{1,2}$.

Using these results, we see that circuit $\mathcal{C}_d = \mathcal{M}_{\mathcal{B}_d} \circ \mathcal{M}_{\mathcal{B}'_d}$ has logical action $\mathcal{M}_{\mathcal{L}} \circ \mathcal{M}_{\mathcal{L}'}$ of measuring $X \otimes X$ followed by $Z \otimes I$ conditioned on the outcome 1 of $X \otimes X$ with input and output code S_d . This follows from the following circuit identities:



The outcome m of the logical XX measurement is equal to the outcome of \mathcal{Z}_1^M in $\mathcal{M}_{\mathcal{B}_d}$. The rest of the outcomes in the circuits $\mathcal{M}_{\mathcal{B}_d}$ and $\mathcal{M}_{\mathcal{B}_d'}$ are either zero or random. The actions of the circuits $\mathcal{M}_{\mathcal{B}_d}$ and $\mathcal{M}_{\mathcal{B}_d'}$ do not depend on the random outcomes because of the choice of conditional Pauli unitaries.

9.2 General form for measuring two stabilizer groups

Here we consider a circuit which sequentially measures two stabilizer groups, and find an equivalent general form circuit (Lemma 9.6) and find the stabilizers of the circuit's Choi states (Corollary 9.7). To state these results more precisely, it is useful to first define the syndrome extraction circuit in Definition 9.5.

Definition 9.5 (Syndrome extraction circuit). Given a common symplectic basis \mathcal{B} of two n-qubit stabilizer groups S_{in} and M, we define the circuit $S_{\mathcal{B}}$ with outcome vector v_S :

(i) measure
$$\mathcal{Z}^{\Delta}$$
, \mathcal{Z}^{\cap} , \mathcal{Z}^{S} (a full set of generators of $S_{\rm in}$).

In Lemma 9.6, we derive a general form circuit equivalent to $\mathcal{S}_{\mathcal{B}} \circ \mathcal{M}_{\mathcal{B}}$, where the syndrome extraction circuit $\mathcal{S}_{\mathcal{B}}$ (Definition 9.5) measures stabilizer group S_{in} and symplectic-basis code deformation circuit $\mathcal{M}_{\mathcal{B}}$ (Definition 9.3) measures stabilizer group M, and where \mathcal{B} is a common symplectic basis \mathcal{B} of S_{in} and M.

Lemma 9.6 (General form circuit for measuring two stabilizer groups). Consider two n-qubit stabilizer groups $S_{\rm in}$ and M with a common symplectic basis \mathcal{B} . Additionally, consider circuits $S_{\mathcal{B}}$ and $\mathcal{M}_{\mathcal{B}}$ defined from \mathcal{B} in Definitions 9.3 and 9.5.

Then the circuit $S_B \circ M_B$ is equivalent to a general form circuit C_{gen} with:

- $k = |\mathcal{Z}|$ inner qubits and zero random bits.
- Left and right Clifford unitaries $L = C_{\mathcal{B}}$ and $R = C_{\mathcal{B}}$ $(H^{\otimes |\mathcal{Z}^{\Delta}|} \otimes I_{n-|\mathcal{Z}^{\Delta}|})$, where is the Clifford unitary that maps the standard Pauli basis to \mathcal{B} .
- Condition matrices A_x and A_z are zero, while A is an $(n-k) \times (n-k)$ matrix equal to $\mathbf{0}_{|\mathcal{Z}^{\Delta}| \times |\mathcal{Z}^{\Delta}|} \oplus I_{|\mathcal{Z}^{\cap}| + |\mathcal{Z}^{S}|} \oplus \mathbf{0}_{|\mathcal{Z}^{M}| \times |\mathcal{Z}^{M}|}.$

Circuits $S_{\mathcal{B}}$ and C_{gen} have the same action when their outcome vectors $v_S \oplus v_M$ and m satisfy:

$$m = (v_S(\mathcal{Z}_j^{\Delta}))_{j \in |\mathcal{Z}^{\Delta}|} \oplus (v_S(\mathcal{Z}_j^{\cap}))_{j \in |\mathcal{Z}^{\cap}|} \oplus (v_S(\mathcal{Z}_j^S))_{j \in |\mathcal{Z}^S|} \oplus (v_M(\mathcal{Z}_j^M))_{j \in |\mathcal{Z}^M|}.$$

The outcomes $(v_M(\mathcal{X}_j^M))_{j\in|\mathcal{Z}^M|}$ are random and the action of $\mathcal{S}_{\mathcal{B}} \circ \mathcal{M}_{\mathcal{B}}$ does not depend on them. The outcomes $(v_M(\mathcal{Z}_j^{\cap}))_{j\in|\mathcal{Z}^{\cap}|}$ are redundant and equal to $(v_S(\mathcal{Z}_j^{\cap}))_{j\in|\mathcal{Z}^{\cap}|}$.

Proof. The proof strategy is to transform the circuit $\mathcal{S}_{\mathcal{B}} \circ \mathcal{M}_{\mathcal{B}}$ to the general form circuit \mathcal{C}_{gen} via a series of equivalence-preserving transformations. The first step is to replace both $\mathcal{S}_{\mathcal{B}}$ and $\mathcal{M}_{\mathcal{B}}$ with equivalent circuits that use the Clifford unitary $C_{\mathcal{B}}$, single-qubit non-destructive X and Z measurements and conditional Paulis as shown in Fig. 9.4a. The second step is to remove the adjacent $C_{\mathcal{B}}$ and $C_{\mathcal{B}}^{\dagger}$ from the right circuit in Fig. 9.4b to obtain the left circuit in Fig. 9.4b. The third step is to replace all non-destructive single-qubit measurements with equivalent destructive measurements and qubit allocations as in Fig. 9.4b. Finally, we see that the right circuit in Fig. 9.4b is equivalent to C_{gen} with the required outcome relation.

For our proof of Lemma 9.6 in Section 9.3 we will find the following Corollary 9.7 of Lemma 9.6 useful:

Corollary 9.7 (Choi state of measuring two stabilizer groups). Consider n-qubit stabilizer groups $S_{\rm in}$ and M with a common symplectic basis \mathcal{B} (Definition 9.2, Fig. 9.2a). Additionally, consider stabilizer circuit $\mathcal{M}_{\mathcal{B}}$ (Definition 9.3, Fig. 9.2b) that measures a full set of generators of M and applies conditional Pauli unitaries (defined by \mathcal{B}), and stabilizer circuit $\mathcal{S}_{\mathcal{B}}$ (Definition 9.5) that measures a full set of generators of $S_{\rm in}$ (defined by \mathcal{B}). The stabilizers of the Choi circuit of $\mathcal{S}_{\mathcal{B}} \circ \mathcal{M}_{\mathcal{B}}$ upon outcome $v_{\mathcal{S}} \oplus v_{M}$ are:

$$P \otimes (-1)^{v_{S}(P)}I, \qquad P \in \mathcal{Z}^{\cap} \cup \mathcal{Z}^{S}, \qquad (output \ stabilizers),$$

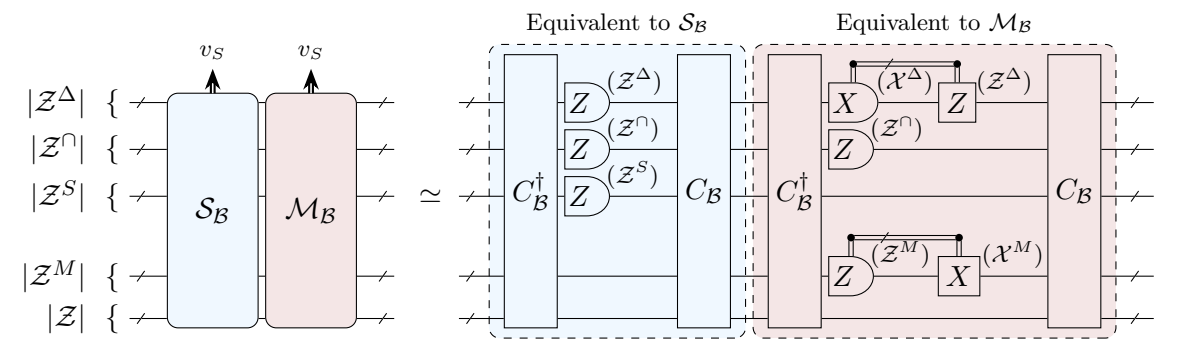
$$P \otimes I, \qquad P \in \mathcal{X}^{\Delta} \cup \mathcal{Z}^{M}, \qquad (output \ stabilizers),$$

$$I \otimes (-1)^{v_{S}(P)}P^{*}, \qquad P \in \mathcal{Z}^{\Delta} \cup \mathcal{Z}^{\cap} \cup \mathcal{Z}^{S}, (measured \ observables),$$

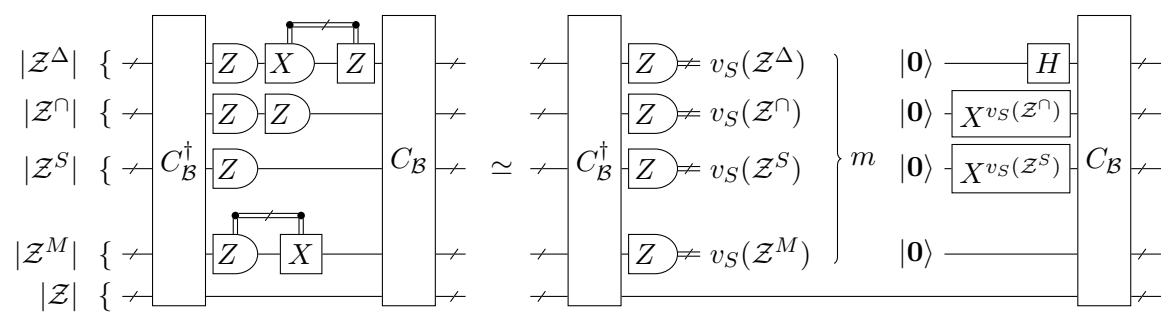
$$I \otimes (-1)^{v_{M}(P)}P^{*}, \qquad P \in \mathcal{Z}^{M}, \qquad (measured \ observables),$$

$$P \otimes P^{*}, \qquad P \in \mathcal{X} \cup \mathcal{Z}, \qquad (preserved \ observables).$$

$$(35)$$



(a) Replacing $S_{\mathcal{B}}$ and $\mathcal{M}_{\mathcal{B}}$ by equivalent circuits using Clifford unitary $C_{\mathcal{B}}$ and single-qubit measurements. Clifford unitary $C_{\mathcal{B}}$ is the Clifford unitary that maps the standard Pauli basis to \mathcal{B} .



(b) Replacing non-destructive measurements with destructive measurements and qubit allocations.

Figure 9.4: The circuit $\mathcal{S}_{\mathcal{B}} \circ \mathcal{M}_{\mathcal{B}}$ and equivalent circuits, for syndrome extraction circuit $\mathcal{S}_{\mathcal{B}}$ (Definition 9.5) and symplectic-basis code deformation circuit $\mathcal{M}_{\mathcal{B}}$ (Definition 9.3) given a common symplectic basis \mathcal{B} of groups S_{in} and M. Other than $C_{\mathcal{B}}$, all operations in the equivalent circuits act on single qubits. On Z measurements, the superscript (\mathcal{Z}^{Δ}) indicates that the outcomes are those that would be obtained for measuring \mathcal{Z}^{Δ} , while on conditional Pauli $Z_{\mathcal{S}}$, the superscript (\mathcal{Z}^{Δ}) indicates they are equivalent to conditionally applying elements of \mathcal{Z}^{Δ} .

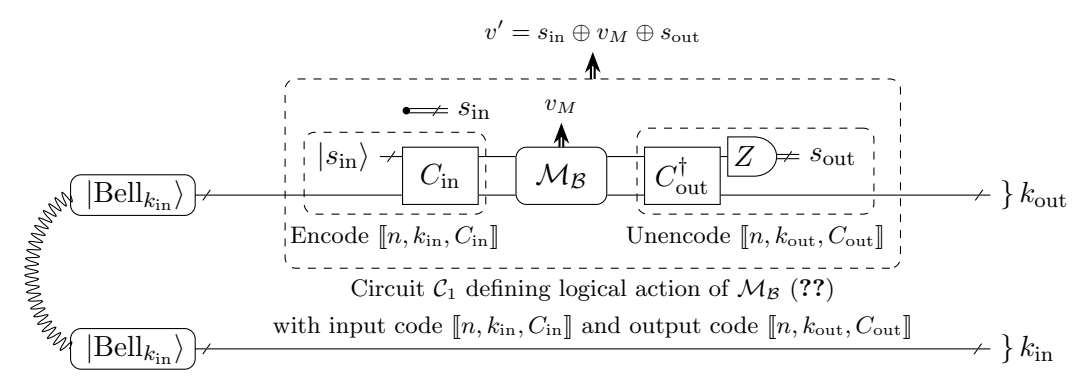
The action of the circuit $\mathcal{S}_{\mathcal{B}} \circ \mathcal{M}_{\mathcal{B}}$ and the signs of the Choi state stabilizers do not depend on the outcomes $v_M(P)$ for $P \in \mathcal{X}^{\Delta}$, these outcomes are random.

9.3 Proof of logical action theorem

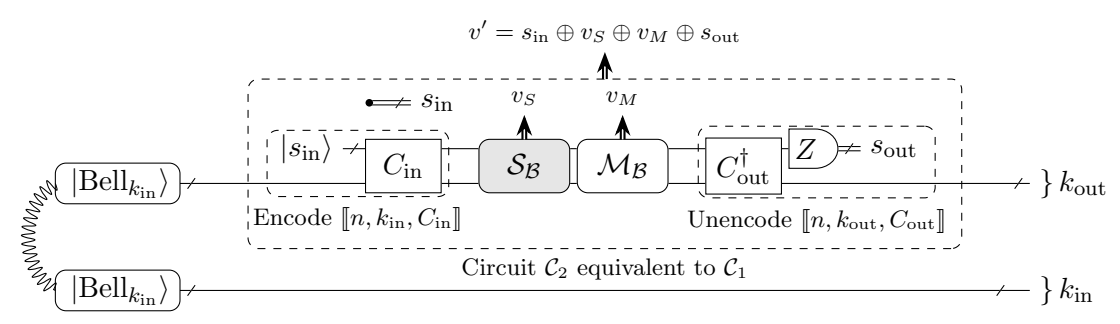
Here we prove Theorem 9.4.

Proof of Theorem 9.4. Our goal is to prove that $C_1 = \mathcal{E}(k_{\rm in}, C_{\rm in}) \circ \mathcal{M}_{\mathcal{B}} \circ \mathcal{E}^{\dagger}(k_{\rm out}, C_{\rm out})$ (with trivial input syndrome) is equivalent to the general form circuit $\mathcal{M}_{\mathcal{L}}$ with the parameters claimed in Theorem 9.4. To achieve this goal, our strategy is to derive complete sets of stabilizer generators of $\text{Choi}(C_1)$ (Fig. 9.5a) and compare these with the complete sets of stabilizer generators of $\text{Choi}(\mathcal{M}_{\mathcal{L}})$, which we know in terms of the parameters of the general form circuit $\mathcal{M}_{\mathcal{L}}$ from our earlier analysis in Fig. 4.3. There is freedom in the choice of generator sets. Given the set of Choi states produced by $\text{Choi}(C_1)$, to aid comparison we seek sets of generators which differ only by their phase for different Choi states in the set, and where the generators of the set fall into three disjoint subsets: (1) generators supported on the first $k_{\rm out}$ qubits, (2) generators supported on the last $k_{\rm in}$ qubits, and (3) generators which form a symplectic basis when restricted to first $k_{\rm out}$ qubits.

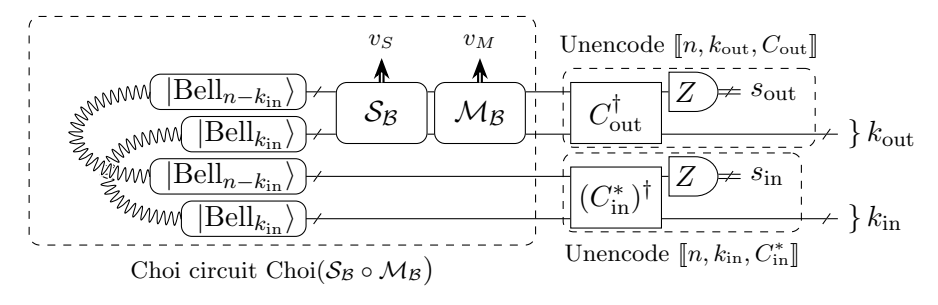
The key to finding stabilizers of $Choi(C_1)$ in satisfying conditions (1), (2) and (3) is to relate them to the stabilizers of $Choi(S_{\mathcal{B}} \circ \mathcal{M}_{\mathcal{B}})$ shown in Fig. 9.5c, described in Corollary 9.7. The relation between the stabilizers of $Choi(C_1)$ and $Choi(S_{\mathcal{B}} \circ \mathcal{M}_{\mathcal{B}})$ follows from the fact that circuits $Choi(C_1)$ (Fig. 9.5a) and C_3 (Fig. 9.5c) are equivalent as specified in Fig. 9.5. Let us postpone



(a) Choi circuit Choi(\mathcal{C}_1) of circuit \mathcal{C}_1 defining logical action of $\mathcal{M}_{\mathcal{B}}$ (Fig. 9.2b).



(b) Choi circuit Choi(\mathcal{C}_2) of circuit \mathcal{C}_2 . Circuits Choi(\mathcal{C}_2) and Choi(\mathcal{C}_1) are equivalent.



(c) Circuit C_3 , which is equivalent to circuits $Choi(C_1)$ and $Choi(C_2)$.

Figure 9.5: Equivalent circuits $Choi(C_1)$ (a), $Choi(C_2)$ (b) and C_3 (c) used to derive the logical action (Fig. 9.2c) of the circuit $\mathcal{M}_{\mathcal{B}}$ (Fig. 9.2b) specified by the common symplectic basis \mathcal{B} (Fig. 9.2a) of stabilizer groups S_{in} and M. The codes $[n, k_{in}, C_{in}]$ and $[n, k_{out}, C_{out}]$ have stabilizer groups S_{in} and S_{out} , where S_{out} is a subgroup of $M \cdot (S \cap M^{\perp})$. Given \mathcal{B} , the circuit $S_{\mathcal{B}}$ (Definition 9.5) measures a full set of generators of S_{in} , while the circuit $\mathcal{M}_{\mathcal{B}}$ (Definition 9.3) measures a full set of generators of M and applies conditional Paulies.

for now the proof that $Choi(C_1)$ and C_3 are equivalent (which we will see holds for all syndromes) and first prove that the theorem is true given that this equivalence holds.

Now let us derive the stabilizer generators of $Choi(C_1)$ upon the outcome $s_{in} = 0$ to find the general form circuit $\mathcal{M}_{\mathcal{L}}$. By the equivalence of $Choi(C_1)$ and C_3 , we can do this by finding the stabilizer generators of C_3 upon the outcome $s_{in} = 0$. The circuit C_3 is constructed by first applying $Choi(S_{\mathcal{B}} \circ \mathcal{M}_{\mathcal{B}})$ (for which we know the stabilizer generators from Corollary 9.7) and then applying the unencoding circuits for $[n, k_{in}, C_{in}]$ and $[n, k_{out}, C_{out}]$. Recall that Eq. (9) specifies the action of an unencoding map given a specific outcome, which implies that when $s_{in} = s_{out} = 0$, the state output by C_3 is stabilized by:

$$\mathcal{L}_{\llbracket n,k_{\text{out}},C_{\text{out}}\rrbracket}(P)\otimes I, \qquad P\in\mathcal{Z}^{\cap}\cup\mathcal{Z}^{S}, \qquad \text{(output stabilizers)},$$

$$\mathcal{L}_{\llbracket n,k_{\text{out}},C_{\text{out}}\rrbracket}(P)\otimes I, \qquad P\in\mathcal{X}^{\Delta}\cup\mathcal{Z}^{M}, \qquad \text{(output stabilizers)},$$

$$I\otimes\mathcal{L}_{\llbracket n,k_{\text{in}},C_{\text{in}}^{*}\rrbracket}(P^{*}), \qquad P\in\mathcal{Z}^{\Delta}\cup\mathcal{Z}^{\cap}\cup\mathcal{Z}^{S}, \text{(measured observables)},$$

$$(-1)^{v_{M}(P)}I\otimes\mathcal{L}_{\llbracket n,k_{\text{in}},C_{\text{in}}^{*}\rrbracket}(P^{*}), \qquad P\in\mathcal{Z}^{M}, \qquad \text{(measured observables)},$$

$$\mathcal{L}_{\llbracket n,k_{\text{out}},C_{\text{out}}\rrbracket}(P)\otimes\mathcal{L}_{\llbracket n,k_{\text{in}},C_{\text{in}}^{*}\rrbracket}(P^{*}), \qquad P\in\mathcal{X}\cup\mathcal{Z}, \qquad \text{(preserved observables)}.$$

It is not hard to check that the map $\mathcal{L}_{\llbracket n,k_{\text{in}},C_{\text{in}}^* \rrbracket}$ is applied to Paulies in its domain S_{in}^{\perp} and that $\mathcal{L}_{\llbracket n,k_{\text{in}},C_{\text{in}}^* \rrbracket}(P^*) = I$ for $P \in \mathcal{Z}^{\Delta} \cup \mathcal{Z}^{\cap} \cup \mathcal{Z}^S \subset S_{\text{in}}$. We need to check that $\mathcal{L}_{\llbracket n,k_{\text{out}},C_{\text{out}} \rrbracket}$ is applied to Paulies in its domain S_{out}^{\perp} . For the stabilizer group $S_{\text{out}} \subset M \cdot (S_{\text{in}} \cap M^{\perp})$ we have $(M \cdot (S_{\text{in}} \cap M^{\perp}))^{\perp} \subset S_{\text{out}}^{\perp}$. Note that $\langle \mathcal{Z}^{\cap} \cup \mathcal{Z}^S \cup \mathcal{X}^{\Delta} \cup \mathcal{Z}^M \rangle = M \cdot (S_{\text{in}} \cap M^{\perp})$ and so $(M \cdot (S_{\text{in}} \cap M^{\perp}))^{\perp} = (M \cdot (S_{\text{in}} \cap M^{\perp})) \cdot \langle \mathcal{X} \cup \mathcal{Z} \rangle$, and therefore $\langle \mathcal{Z}^{\cap} \cup \mathcal{Z}^S \cup \mathcal{X}^{\Delta} \cup \mathcal{Z}^M \cup \mathcal{X} \cup \mathcal{Z} \rangle \subset S_{\text{out}}^{\perp}$, where the equalities can be seen to be true from the symplectic basis definition in Fig. 9.2a. We conclude that $\mathcal{L}_{\llbracket n,k_{\text{out}},C_{\text{out}} \rrbracket}$ is applied to Paulies in its domain. Note that map \mathcal{L} preserves the commutation:

$$\llbracket \mathcal{L}_{\llbracket n,k,C\rrbracket}(P),\mathcal{L}_{\llbracket n,k,C\rrbracket}(Q) \rrbracket = \llbracket P,Q \rrbracket.$$

The Paulis in Eq. (36) are stabilizer generators of C_3 , and by equivalence are also stabilizer generators of $Choi(C_1)$. Moreover, they satisfy conditions (1), (2) and (3) such that they can be matched to the stabilizer generators of a general form circuit with appropriate choices of the left and the right Clifford unitaries L and R. We use Fig. 4.3 to find the expression for the left and the right Clifford unitaries of $\mathcal{M}_{\mathcal{L}}$ in Eq. (31) from Eq. (36). This also shows that measurement outcome vector m of $\mathcal{M}_{\mathcal{L}}$ is $(v(\mathcal{Z}_j^M))_{j\in[\mathcal{Z}^M]}$. The outcomes v(P) for $P \in \mathcal{X}^{\Delta}$ of $\mathcal{M}_{\mathcal{B}}$ in \mathcal{C}_1 and \mathcal{C}_3 according to Corollary 9.7.

It remains to prove that $Choi(\mathcal{C}_1)$ and \mathcal{C}_3 are equivalent, which we do in two steps by showing that both $Choi(\mathcal{C}_1)$ and \mathcal{C}_3 are equivalent to another circuit $Choi(\mathcal{C}_2)$ (Fig. 9.5b).

Circuits $Choi(C_1)$ and $Choi(C_2)$ are equivalent because their sub-circuits C_1 and C_2 are equivalent. Indeed C_2 is obtained from C_1 by inserting S_B (highlighted in grey) between $\mathcal{E}(k_{\rm in}, C_{\rm in})$ and \mathcal{M}_B . Before S_B is applied the state is already stabilized by a stabilizer group equal to $S_{\rm in}$ up to signs. The measurement outcome v_S is redundant and is a linear function of $s_{\rm in}$ and the action of S_B on the state is trivial.

Circuit C_3 is equivalent to $\operatorname{Choi}(C_2)$ because it is obtained from $\operatorname{Choi}(C_2)$ via a series of three circuit transformations preserving the circuit equivalence $\operatorname{Choi}(C_2) \to C_{3,1} \to C_{3,2} \to C_3$. First we obtain $C_{3,1}$ by replacing the part of $\operatorname{Choi}(C_2)$ which allocates the random bits s_{in} and initializes the $(n-k_{\text{in}})$ -qubit register in $|s_{\text{in}}\rangle$ with the initialization of a pair of $(n-k_{\text{in}})$ -qubit registers in $|\operatorname{Bell}_{(n-k_{\text{in}})}\rangle$ and performing destructive Z measurements on the second $(n-k_{\text{in}})$ -qubit register with the outcome s_{in} . Second we obtain $C_{3,2}$ by pulling the unitary C_{in} through the Bell state $|\operatorname{Bell}_{(n)}\rangle$ it is acting on, using the identity $(C_{\text{in}} \otimes I_n)|\operatorname{Bell}_{(n)}\rangle = (I_n \otimes C_{\text{in}}^T)|\operatorname{Bell}_{(n)}\rangle$. Third, we change the order in which the destructive Z measurements with outcome s_{in} and the sub-circuit $S_{\mathcal{B}}$ appear in the circuit to obtain C_3 . We move the destructive Z measurements with outcome s_{in} to the end of the circuit such that the outcome s_{in} becomes redundant and the outcome s_{in} becomes random.

Theorem 9.4 can be extended to apply to the case when $s_{\rm in}$ is non-zero, resulting in the inclusion of $s_{\rm in}$ -dependent condition matrices in the equivalent general form circuit. In the proof, we derived Eq. (36) assuming that $s_{\rm in}$ and $s_{\rm out}$ are zero, resulting in simplified expressions for the phases of stabilizers, but relaxing this assumption will result in additional phases from the maps $\mathcal{G}_{\llbracket n,k_{\rm in},C_{\rm in}\rrbracket}$, $\mathcal{G}_{\llbracket n,k_{\rm out},C_{\rm out}\rrbracket}$ (Eq. (8)).

Acknowledgements

Special thanks to Aarthi Sundaram and Nicolas Delfosse for helpful feedback, and guidance regarding existing literature.

List of Algorithms

3.6	Algorithm (Outcome-specific stabilizer circuit simulation)		19
5.2	Algorithm (Outcome-complete via outcome-specific stabilizer		2
5.3	Algorithm (Outcome-complete stabilizer circuit simulation)	/	30
6.2	Algorithm (Stabilizer circuit general form)		33
7.2	Algorithm (Stabilizer circuit comparison)		41
7.5	Algorithm (General form circuit comparison)		46
8.2	Algorithm (Logical action)		52
8.4	Algorithm (Logical action verification)		55
D.1	Algorithm (Pauli propagation)		87
E.1	Algorithm (Common symplectic basis)		88
1.1	Algorithm (Common Symplectic basis)		00
List o	of Problems		
2.11	Problem (Bipartite normal form of a stabilizer state)		11
3.5	Problem (Outcome-specific stabilizer circuit simulation)		18
5.1	Problem (Outcome-complete stabilizer circuit simulation)		27
6.1	Problem (Bipartite normal form of a family of stabilizer states)		33
7.1	Problem (Stabilizer circuit comparison)		41
7.3	Problem (Relating (un)encoding circuits)		42
8.1	Problem (Logical action)		50
8.3	Problem (Logical circuit comparison)		54
9.1	Problem (Logical action of code deformation)		57
List o	of Definitions		
2.1	Definition (Symplectic basis)		7
2.3	Definition (Stabilizer circuit)		7
2.4	Definition (Quantum instrument)		8
2.5	Definition (Outcome compression map)		8
2.6	Definition (Quantum instrument equivalence)		9
2.7	Definition (Choi states)		9
2.8	Definition (Logical operation circuit)		10
2.9	Definition (Logical action)		10
3.1	Definition (Pauli unitary data structure)		14
3.2	Definition (Clifford unitary data structure)		15
4.1	Definition (Split (reduced) echelon form)		21
9.2	Definition (Common symplectic basis of two stabilizer groups)		57
9.3	Definition (Symplectic-basis code deformation circuit)		59
9.5	Definition (Syndrome extraction circuit)		62
A.6	Definition (Linear family of stabilizer states)		76
A.7	Definition (Phase-complete family of stabilizer states)		76
List o	of Theorems and Lemmas		
2.10	Theorem (Theorem II.24 from [29])		11
4.2	Theorem (General form stabilizer circuit)		21
4.3	Lemma (Induction step for Theorem 4.2)		22
9.4	Theorem (Logical action of code deformation)		59
9.6	Lemma (General form circuit for measuring two stabilizer groups) .		62

	9.7	Corollary (Choi state of measuring two stabilizer groups)	62
	A.8	Lemma (Phase completeness)	76
		Lemma (General form equivalence)	79
Γ.	ist o	of Figures	
ш.	ist C	of Figures	
	1.1	Stabilizer and general form circuits (high-level)	3
	1.2	Stabilizer circuits and general form	4
	2.1	Choi state of a circuit	ç
	2.2	Encoding and unencoding circuits	10
	2.3	Circuit defining logical action	10
	$\frac{2.0}{2.4}$	Stabilizer state bipartition	11
	3.1	Description of Pauli and Clifford unitaries	14
	4.1	General form	21
	4.2	Split echelon form	$\frac{21}{22}$
	4.3	General form's Choi state	26
	5.1	Outcome mapping example for outcome-complete simulation	28
	6.1		$\frac{2}{3}$
		Bipartite normal form for a family of stabilizer states	
	6.2	Block structure of a Clifford unitary related to bipartite normal form	38
	7.1	Comparing encoding and unencoding circuits	43
	7.2	General form circuit comparison. Transformation step	45
	8.1	Logical action general form circuit	51
	9.1	Circuit defining logical action of measuring a stabilizer group	57
	9.2	Common symplectic basis and logical action of code deformation	58
	9.3	Common symplectic basis example	60
	9.4	Reducing the measurement of two stabilizer groups to a special case	63
	9.5	Deriving logical action of measuring M from common symplectic basis	64
Ŀ	ist c	of Tables	
	3.1	Data structure requirements	
	5.1	Complexity of outcome-complete stabilizer simulation	
	7.1	General form circuit comparison recovery from fails	
	8.1	Logical operation general form recovery from fails	54
	B.1	Bit-wise operations	80
Ŀ	ist c	of Procedures	
	3.3	Procedure (preimage*)	16
	3.4	Procedure (disentangle)	16
	6.3	Procedure (support-restricted subgroup)	35
	6.4	Procedure (symplectic basis)	36
	6.5	Procedure (Bipartite normal form of a family of stabilizer states)	36
	6.6	Procedure (compression map)	38
	7.4	Procedure (Relating (un)encoding circuits)	44
	B.1	Procedure (block-reshape)	80
	B.2	Procedure (left_mult_exp* (C, P))	84

List of Propositions

2.2	Proposition	(Measurement as unitary)
A.1	Proposition	(Preimage and sign)
A.2	Proposition	(CSS Clifford action)
A.3	Proposition	(Batch Pauli conjugation)
A.4	Proposition	(Generalized controlled Pauli conjugation)
A.5	Proposition	(Encoding circuit decomposition)
A.9	Proposition	(Outcome relabelling for phase complete sets of stabilizer states) 78
A.10	Proposition	(Product of split reduced echelon form matrices)
B.3	Proposition	(disentangle correctness)
E.2	Proposition	(Group's induced symplectic space)

References

- [1] Scott Aaronson and Daniel Gottesman. Improved simulation of stabilizer circuits. *Physical Review A*, 70(5):052328, 2004.
- [2] David Aasen, Zhenghan Wang, and Matthew B. Hastings. Adiabatic paths of hamiltonians, symmetries of topological order, and automorphism codes. *Phys. Rev. B*, 106:085122, Aug 2022.
- [3] Martin Albrecht, Gregory Bard, and William Hart. Algorithm 898: Efficient Multiplication of Dense Matrices over GF(2). ACM Trans. Math. Softw., 37(1), jan 2010.
- [4] Martin R. Albrecht, Gregory V. Bard, and Clément Pernet. Efficient dense gaussian elimination over the finite field with two elements.
- [5] Matthew Amy. Towards large-scale functional verification of universal quantum circuits. arXiv preprint arXiv:1805.06908, 2018.
- [6] Simon Anders and Hans J. Briegel. Fast simulation of stabilizer circuits using a graph-state representation. *Phys. Rev. A*, 73:022334, Feb 2006.
- [7] Koenraad M R Audenaert and Martin B Plenio. Entanglement on mixed stabilizer states: normal forms and reduction procedures. *New Journal of Physics*, 7:170–170, aug 2005.
- [8] Ryan Babbush, Craig Gidney, Dominic W. Berry, Nathan Wiebe, Jarrod McClean, Alexandru Paler, Austin Fowler, and Hartmut Neven. Encoding electronic spectra in quantum circuits with linear t complexity. *Phys. Rev. X*, 8:041015, Oct 2018.
- [9] Miriam Backens. The zx-calculus is complete for stabilizer quantum mechanics. *New Journal of Physics*, 16(9):093021, sep 2014.
- [10] Niel de Beaudrap and Steven Herbert. Fast Stabiliser Simulation with Quadratic Form Expansions. *Quantum*, 6:803, September 2022.
- [11] Michael Beverland, Earl Campbell, Mark Howard, and Vadym Kliuchnikov. Lower bounds on the non-clifford resources for quantum computations. *Quantum Science and Technology*, 5(3):035009, jun 2020.
- [12] Michael Beverland, Vadym Kliuchnikov, and Eddie Schoute. Surface code compilation via edge-disjoint paths. *PRX Quantum*, 3:020342, May 2022.
- [13] Héctor Bombín, Chris Dawson, Ryan V. Mishmash, Naomi Nickerson, Fernando Pastawski, and Sam Roberts. Logical blocks for fault-tolerant topological quantum computation. PRX Quantum, 4:020303, Apr 2023.

- [14] Hector Bombin, Isaac H. Kim, Daniel Litinski, Naomi Nickerson, Mihir Pant, Fernando Pastawski, Sam Roberts, and Terry Rudolph. Interleaving: Modular architectures for faulttolerant photonic quantum computing, 2021.
- [15] Parsa Bonderson, Michael Freedman, and Chetan Nayak. Measurement-only topological quantum computation. *Phys. Rev. Lett.*, 101:010501, Jun 2008.
- [16] Lukas Burgholzer and Robert Wille. Advanced equivalence checking for quantum circuits. IEEE Transactions on Computer-Aided Design of Integrated Circuits and Systems, 40(9):1810–1824, 2020.
- [17] Lukas Burgholzer and Robert Wille. Handling non-unitaries in quantum circuit equivalence checking. In *Proceedings of the 59th ACM/IEEE Design Automation Conference*, DAC '22, page 529–534, New York, NY, USA, 2022. Association for Computing Machinery.
- [18] E. B. Davies and J. T. Lewis. An operational approach to quantum probability. *Communications in Mathematical Physics*, 17:239–260, 9 1970.
- [19] Margarita Davydova, Nathanan Tantivasadakarn, and Shankar Balasubramanian. Floquet codes without parent subsystem codes, 2022.
- [20] Jeroen Dehaene and Bart De Moor. Clifford group, stabilizer states, and linear and quadratic operations over GF(2). *Phys. Rev. A*, 68:042318, Oct 2003.
- [21] Austin G. Fowler and Craig Gidney. Low overhead quantum computation using lattice surgery, 2019.
- [22] Héctor J. García, Igor L. Markov, and Andrew W. Cross. On the geometry of stabilizer states. *Quantum Info. Comput.*, 14(7 & 8):683–720, may 2014.
- [23] Craig Gidney. Stim: a fast stabilizer circuit simulator. Quantum, 5:497, July 2021.
- [24] Craig Gidney, Michael Newman, Austin Fowler, and Michael Broughton. A Fault-Tolerant Honeycomb Memory. *Quantum*, 5:605, December 2021.
- [25] Craig Gidney, Michael Newman, and Matt McEwen. Benchmarking the Planar Honeycomb Code. *Quantum*, 6:813, September 2022.
- [26] David Gosset, Daniel Grier, Alex Kerzner, and Luke Schaeffer. Fast simulation of planar clifford circuits, 2020.
- [27] Daniel Gottesman. The heisenberg representation of quantum computers. arXiv preprint quant-ph/9807006, 1998.
- [28] Chaowen Guan and Kenneth W. Regan. Stabilizer circuits, quadratic forms, and computing matrix rank, 2019.
- [29] Jeongwan Haah. Algebraic methods for quantum codes on lattices. Revista Colombiana de Matemáticas, 50(2):299, jan 2017.
- [30] Jeongwan Haah and Matthew B. Hastings. Boundaries for the Honeycomb Code. *Quantum*, 6:693, April 2022.
- [31] Matthew B. Hastings and Jeongwan Haah. Dynamically Generated Logical Qubits. *Quantum*, 5:564, October 2021.
- [32] Matthew B. Hastings and Jeongwan Haah. Dynamically Generated Logical Qubits. *Quantum*, 5:564, October 2021.

- [33] Xin Hong, Xiangzhen Zhou, Sanjiang Li, Yuan Feng, and Mingsheng Ying. A tensor network based decision diagram for representation of quantum circuits. *ACM Transactions on Design Automation of Electronic Systems (TODAES)*, 27(6):1–30, 2022.
- [34] Dominic Horsman, Austin G Fowler, Simon Devitt, and Rodney Van Meter. Surface code quantum computing by lattice surgery. New Journal of Physics, 14(12):123011, dec 2012.
- [35] Thomas Häner, Vadym Kliuchnikov, Martin Roetteler, and Mathias Soeken. Space-time optimized table lookup, 2022.
- [36] Dominik Janzing, Pawel Wocjan, and Thomas Beth. "non-identity-check" is qma-complete. *International Journal of Quantum Information*, 3(03):463–473, 2005.
- [37] Claude-Pierre Jeannerod, Clément Pernet, and Arne Storjohann. Rank-profile revealing gaussian elimination and the cup matrix decomposition, 2012.
- [38] Richard Jozsa and Marrten Van Den Nest. Classical simulation complexity of extended clifford circuits. *Quantum Info. Comput.*, 14(7 & 8):633–648, may 2014.
- [39] Daniel Litinski. A Game of Surface Codes: Large-Scale Quantum Computing with Lattice Surgery. *Quantum*, 3:128, March 2019.
- [40] Philipp Niemann, Robert Wille, and Rolf Drechsler. Equivalence checking in multi-level quantum systems. In *Reversible Computation: 6th International Conference*, *RC* 2014, *Kyoto*, *Japan*, *July* 10-11, 2014. *Proceedings* 6, pages 201–215. Springer, 2014.
- [41] Adam Paetznick, Christina Knapp, Nicolas Delfosse, Bela Bauer, Jeongwan Haah, Matthew B. Hastings, and Marcus P. da Silva. Performance of planar floquet codes with majorana-based qubits. PRX Quantum, 4:010310, Jan 2023.
- [42] Tefjol Pllaha, Kalle Volanto, and Olav Tirkkonen. Decomposition of clifford gates. In 2021 IEEE Global Communications Conference (GLOBECOM), pages 01–06, 2021.
- [43] Robert Rand, Jennifer Paykin, and Steve Zdancewic. QWIRE practice: Formal verification of quantum circuits in coq. *Electronic Proceedings in Theoretical Computer Science*, 266:119–132, feb 2018.
- [44] Kenneth Rudinger, Guilhem J. Ribeill, Luke C.G. Govia, Matthew Ware, Erik Nielsen, Kevin Young, Thomas A. Ohki, Robin Blume-Kohout, and Timothy Proctor. Characterizing midcircuit measurements on a superconducting qubit using gate set tomography. *Phys. Rev. Appl.*, 17:014014, Jan 2022.
- [45] Kaitlin N Smith and Mitchell A Thornton. A quantum computational compiler and design tool for technology-specific targets. In *Proceedings of the 46th International Symposium on Computer Architecture*, pages 579–588, 2019.
- [46] Aarthi Sundaram, Robert Rand, Kartik Singhal, and Brad Lackey. A rich type system for quantum programs, 2022.
- [47] George F. Viamontes, Igor L. Markov, and John P. Hayes. Checking equivalence of quantum circuits and states. In *Proceedings of the 2007 IEEE/ACM International Conference on Computer-Aided Design*, ICCAD '07, page 69–74. IEEE Press, 2007.
- [48] Shiou-An Wang, Chin-Yung Lu, I-Ming Tsai, and Sy-Yen Kuo. An xqdd-based verification method for quantum circuits. *IEICE transactions on fundamentals of electronics, communications and computer sciences*, 91(2):584–594, 2008.
- [49] Shigeru Yamashita and Igor L. Markov. Fast equivalence-checking for quantum circuits. In 2010 IEEE/ACM International Symposium on Nanoscale Architectures, pages 23–28, 2010.

A Additional mathematical material

Clifford and Pauli unitaries

We have a more efficient algorithm for composing a Clifford unitary with a Pauli exponent $\exp(i\pi/4)$ because of the following equation:

$$e^{i\pi/4P}Qe^{-i\pi/4P} = \frac{I+iP}{\sqrt{2}} \cdot Q \cdot \frac{I-iP}{\sqrt{2}} = \begin{cases} Q, & \text{when } [P,Q] = 0\\ iPQ, & \text{when } [P,Q] = 1 \end{cases}$$
 (37)

The following proposition allows us to further reduce amount of calculations we need to perform to compose a Clifford unitary with a Pauli exponent $\exp(i\pi P/4)$ and are used to justify correctness of Procedure B.2.

Proposition A.1 (Preimage and sign). Let C be a Clifford unitary and P a Pauli operator described as in Definition 3.1, then $s(P \cdot CZ_kC^{\dagger}) = s(P) + s(CZ_kC^{\dagger}) + 2[C^{\dagger}X^{x(P)}C, Z_k]$ and $s(P \cdot CX_kC^{\dagger}) = s(P) + s(CX_kC^{\dagger}) + 2[C^{\dagger}X^{x(P)}C, X_k]$.

Proof. The result follows from the following equations:

$$\begin{split} P \cdot C Z_k C^\dagger &= i^{s(P)} Z^{z(P)} X^{x(P)} C Z_k C^\dagger = \\ &= i^{s(P)} (-1)^{ [\![X^{x(P)}, CZ_k C^\dagger]\!]} Z^{z(P)} C Z_K C^\dagger X^{x(P)} = \\ &= i^{s(P) + s(CZ_k C^\dagger)} (-1)^{ [\![C^\dagger X^{x(P)} C, Z_k]\!]} Z^{z(P) + z(CZ_k C^\dagger)} X^{x(P) + x(CZ_k C^\dagger)} \end{split}$$

We conclude that $s(P \cdot CZ_kC^{\dagger}) = s(P) + s(CZ_kC^{\dagger}) + 2[\![C^{\dagger}X^{x(P)}C, Z_k]\!]$. Result for $s(P \cdot CX_kC^{\dagger})$ follows similarly.

The proposition below is used to justify correctness of Algorithm 6.2.

Proposition A.2 (CSS Clifford action). Let A be an invertible $n \times n$ matrix over \mathbb{F}_2 . For any computational basis state $|a\rangle$ defined by n-bit vector a, let unitary $U_A|a\rangle = |Aa\rangle$. Then the following identities hold

$$U_A Z^a U_A^{\dagger} = Z^{A^{-T}a} \tag{38}$$

$$U_A X^a U_A^{\dagger} = X^{Aa} \tag{39}$$

and U_A is a Clifford unitary with description described by the following $(2n+2) \times (2n+2)$ matrix as discussed in Definition 3.2 and Fig. 3.1:

$$\left(\begin{array}{c|cc|c}
A^{-1} & 0 & 0 \\
\hline
0 & A^T & 0 \\
\hline
0 & 0 & 0
\end{array}\right)$$

Proof. Let us start with notation:

$$Z = |0\rangle\langle 0| + (-1)|1\rangle\langle 1| = \sum_{z \in \{0,1\}} (-1)^z |z\rangle\langle z|, \quad X = |0\rangle\langle 1| + |1\rangle\langle 0| = \sum_{z \in \{0,1\}} |z\rangle\langle z + 1|,$$

$$Z^b = Z_1^{b_1} \otimes \ldots \otimes Z_l^{b_l} = \sum_{c \in \{0,1\}^l} (-1)^{\langle c,b\rangle} |c\rangle\langle c|, \quad X^b = X_1^{b_1} \otimes \ldots \otimes X_l^{b_l} = \sum_{c \in \{0,1\}^l} |c\rangle\langle c + b|.$$

We observe that the image $U_A Z^b U_A^{\dagger}$ is:

$$\begin{split} &\sum_{c\in\{0,1\}^l} (-1)^{\langle c,b\rangle} |Ac\rangle \langle Ac| = \sum_{c'\in\{0,1\}^l} (-1)^{\langle A^{-1}c',b\rangle} |c'\rangle \langle c'| = \\ &= \sum_{c'\in\{0,1\}^l} (-1)^{\langle c',A^{-T}b\rangle} |c'\rangle \langle c'| = Z^{A^{-T}b} \text{ where } A^{-T} = (A^{-1})^T. \end{split}$$

Similarly we observe that image of $U_A X^b U_A^{\dagger}$ is:

$$\sum_{c \in \{0,1\}^l} |Ac\rangle \langle A(c+b)| = \sum_{c' \in \{0,1\}^l} |c'\rangle \langle c' + Ab| = X^{Ab}.$$

The following is useful for general form circuit comparison Algorithm 7.5:

Proposition A.3 (Batch Pauli conjugation). Let C be a Clifford unitary, denote the top-left $2n \times 2n$ binary-symplectic part of the description M(C) (Definition 3.2) as

$$\left(\begin{array}{c|c} A_{z,x} & A_{x,x} \\ \hline A_{z,z} & A_{x,z} \end{array}\right).$$

Then for any vector v and matrix \hat{A} we have $CX^{\hat{A}v}C^{\dagger} \simeq X^{\hat{A}_xv}Z^{\hat{A}_zv}$ where $\hat{A}_x = A_{x,z}^T\hat{A}$, $\hat{A}_z = A_{z,z}^T\hat{A}$. Similarly for any vector v and matrix \tilde{A} we have $CZ^{\tilde{A}v}C^{\dagger} \simeq X^{\tilde{A}_xv}Z^{\tilde{A}_zv}$ where $\tilde{A}_x = A_{x,x}^T\tilde{A}$ and $\tilde{A}_z = A_{z,x}^T\tilde{A}$.

Proof. Recall that for the standard basis vectors e_j we have $Z^{e_j} = Z_j$. According to Definition 3.2 we have

$$CZ^{e_j}C^{\dagger} = CZ_jC^{\dagger} \simeq X^{(A_{x,x})_j}Z^{(A_{z,x})_j} = X^{A_{x,x}^Te_j}Z^{(A_{z,x}^T)e_j}$$

By linearity, for any \tilde{v} we have:

$$CZ^{\tilde{v}}C^{\dagger} \sim X^{A_{x,x}^T\tilde{v}}Z^{(A_{z,x}^T)\tilde{v}}$$

Now using $\tilde{v} = \tilde{A}v$ we have $\tilde{A}_x = A_{x,x}^T \tilde{A}$ and $\tilde{A}_z = A_{z,x}^T \tilde{A}$. Similarly, according to Definition 3.2 we have

$$CX^{e_j}C^{\dagger} = CX_jC^{\dagger} \simeq X^{(A_{x,z})_j}Z^{(A_{z,z})_j} = X^{A_{x,z}^Te_j}Z^{(A_{z,z}^T)e_j}$$

and therefore $\hat{A}_x = A_{x,z}^T \hat{A}$ and $\hat{A}_z = A_{z,z}^T \hat{A}$.

The following proposition helps establish correctness of deallocation step in Algorithm 5.3.

Proposition A.4 (Generalized controlled Pauli conjugation). For integer j, matrix A, vectors a, r with entries in \mathbb{F}_2 such that $a_j = 0$ the following identity holds:

$$\Lambda(X_j, Z^a) X^{Ar} \Lambda(X_j, Z^a) = X^{(I + e_j a^T)Ar}.$$

Multiplying A by $I + e_j a^T$ is equivalent to adding the sum of rows of A indicated by a to row j.

Proof. Recall that according to Eq. (6) we have:

$$\Lambda(X_j,Z^a)X^{Ar}\Lambda(X_j,Z^a) = X^{Ar}X_j^{\llbracket Z^a,X^{Ar}\rrbracket} = X^{Ar}X_j^{\langle Ar,a\rangle} = X^{Ar+e_j\langle A^Ta,r\rangle}$$

Now, using identity $v\langle u, w \rangle = \langle vu^T, w \rangle$ for column vectors v, u, W we have

$$e_j\langle A^T a, r \rangle = \langle e_j(A^T a)^T, r \rangle = \langle (I + e_j a^T)A \rangle.$$

Finally, note that $(A^T a)$ is the sum of rows of A indicated by a and $e_j(A^T a)^T$ is a matrix with all rows being zero, except row j that is equal to $A^T a$.

Encoding and unencoding circuits

The following proposition helps establish correctness of encoding and unencoding circuit comparison algorithm Procedure 7.4.

Proposition A.5 (Encoding circuit decomposition). Let C be a Clifford unitary such that code [n, k, C] has a stabilizer group equivalent to the stabilizer group of $[n, k, I_n]$, that is C maps Z_j for $j \in [n-k]$ to products of Z_j for $j \in [n-k]$ up to a sign.

Then images under conjugation by C are of the following form:

$$CZ_j C^{\dagger} = (-1)^{(m_0)_j} Z^{A_j} \otimes I_k, \ j \in [n-k],$$
 (40)

$$CZ_{j+n-k}C^{\dagger} = Z^{(A_x)_j} \otimes C_{\Delta}Z_jC_{\Delta}^{\dagger}, \quad j \in [k], \tag{41}$$

$$CX_{j+n-k}C^{\dagger} = Z^{(A_z)_j} \otimes C_{\Delta}X_jC_{\Delta}^{\dagger}, \quad j \in [k]$$

$$\tag{42}$$

for some vector m_0 , matrices A, A_x, A_z and Clifford unitary C_{Δ} . Additionally, the Choi state of an encoding circuit with syndrome m implementing the linear map $|\phi\rangle \mapsto C(|m\rangle \otimes |\phi\rangle)$ (parameterized by m) is equal to the Choi state of the map $|\phi\rangle \mapsto |m'\rangle \otimes C_{\Delta} X^{A_x m'} Z^{A_z m'} |\phi\rangle$ (parameterized by m') for $m' = A^{-1}(m_0 + m)$.

Proof. We first establish that images of X and Z under conjugation by C have required form. Images $CZ_{j+n-k}C^{\dagger}$, $CX_{j+n-k}C^{\dagger}$ for $j \in [k]$ must commute with Z_j for $j \in [n-k]$ and are, therefore, products of Pauli Z over qubits [n-k] up to signs. This is because images CZ_jC^{\dagger} for $j \in [n-k]$ generate $\langle Z_1, \ldots, Z_{n-k} \rangle$ up to signs, by the equivalence of the stabilizer groups of [n,k,C] and $[n,k,I_n]$.

Next we establish the following equations for the Choi state stabilizer generators:

$$(-1)^{\langle m', e_j \rangle} Z_j \otimes I_k \otimes I_k, \quad j \in [n-k], \tag{43}$$

$$(-1)^{\langle A_x m', e_j \rangle} I_{n-k} \otimes \left(C_{\Delta} Z_j C_{\Delta}^{\dagger} \right) \otimes Z_j, \quad j \in [k], \tag{44}$$

$$(-1)^{\langle A_z m', e_j \rangle} I_{n-k} \otimes \left(C_{\Delta} X_j C_{\Delta}^{\dagger} \right) \otimes X_j, \quad j \in [k].$$
 (45)

We gradually replace stabilizer generators with equivalent ones to arrive at the required result. By the definition of the Choi state for linear map $|\phi\rangle \mapsto C(|m\rangle \otimes |\phi\rangle)$ the stabilizer generators consist of the three sets:

$$\{(-1)^{m_j}CZ_jC^{\dagger}\otimes I_k, \ j\in[n-k]\},$$
$$\{CX_{j+n-k}C^{\dagger}\otimes X_j, \ j\in[k]\},$$
$$\{CZ_{j+n-k}C^{\dagger}\otimes Z_j, \ j\in[k]\}$$

We first multiply the generators from the first set with each other, so that after the modifications the stabilizers from the first set are Z_1, \ldots, Z_{n-k} up to phases. Using inner-product notation, the first set of generators can be rewritten as

$$(-1)^{\langle m+m_0,e_j\rangle}Z^{A^Te_j}\otimes I_k, \quad j\in[n-k].$$

This is because when syndrome is m, we have stabilizer $(-1)^{m_j}CZ_jC^{\dagger} = (-1)^{(m_0+m)_j}Z^{A_j}$, using $CZ_jC^{\dagger} = (-1)^{(m_0)_j}Z^{A_j}\otimes I_k$. Now we use $(m_0+m)_j = \langle m_0+m,e_j\rangle$ and $A_j=A^Te_j$. This implies that the Choi state is stabilized by

$$(-1)^{\langle m+m_0, (A^T)^{-1}e_j \rangle} Z^{A^T(A^T)^{-1}e_j} \otimes I_k = (-1)^{\langle A^{-1}(m+m_0), e_j \rangle} Z^{e_j} \otimes I_k, \quad j \in [n-k],$$

because each $(A^T)^{-1}e_j$ is just a sum of $e_{j'}$ for some set of j'. The above stabilizer are the same as those in Eq. (43) because $m' = A^{-1}(m_0 + m)$.

Next we multiply the stabilizers from the second and third sets by the generators from the first set, so the generators from the second and third sets are now supported on the last k qubits.

The generators from the second set must be multiplied by $Z^{(A_x)_j}$ up to phases, so $Z^{(A_x)_j}$ gets replaced by the phase

$$(-1)^{\langle m',(A_x)_j\rangle} = (-1)^{\langle m',A_x^T e_j\rangle} = (-1)^{\langle A_x m',e_j\rangle}$$

Similarly, $Z^{(A_z)_j}$ in the generators from the third set is replaced by phase

$$(-1)^{\langle m', (A_z)_j \rangle} = (-1)^{\langle A_z m', e_j \rangle}$$

The phase dependent on m' appears in Eqs. (44) and (45). Equations Eqs. (43) to (45) match the Choi state stabilizer generators of $|\phi\rangle \mapsto |m'\rangle \otimes C_{\Delta} X^{A_x m'} Z^{A_z m'} |\phi\rangle$, as required.

To connect Proposition A.5 to Procedure 7.4, set the unitary C in Proposition A.5 to be $C = C_2^{\dagger} C_1$.

Stabilizer instruments

Given a set of stabilizer states $\{|\psi\rangle_r\}_{r\in R}$ we say that Pauli operator P is a **phase operator** of $\{|\psi\rangle_r\}_{r\in R}$ when $P \neq \pm I$ and for all $r \in R$: $P|\psi\rangle_r = \pm |\psi\rangle_r$. For any phase operator P we define the corresponding **phase function** f_P via $P|\psi\rangle_r = (-1)^{f_P(r)}|\psi\rangle_r$. The set of Choi states corresponding to a stabilizer circuit and the related quantum instrument motivates the following:

Definition A.6 (Linear family of stabilizer states). Consider a family of n-qubit stabilizer states $\{|\psi\rangle_r\}_{r\in R}$, we say that it is a linear family of stabilizer states if

- (i) there exist a set of n independent commuting phase operators of $\{|\psi\rangle_r\}_{r\in R}$
- (ii) for any m phase operators P_1, \ldots, P_l set $\{(f_{P_1}(r), \ldots, f_{P_l}(r)) : r \in R\}$ is a coset⁸ of \mathbb{F}_2^l

A corollary of Theorem 4.2 and Fig. 4.3 is that the set of Choi states of any stabilizer circuit is a linear family. A natural question to ask is that if any linear family of stabilizer states corresponds to a stabilizer circuit. We will show that to answer this question affirmatively, the linear family must have an additional property. To state this property we need the following definition:

Definition A.7 (Phase-complete family of stabilizer states). Consider a linear family of n-qubit stabilizer states $\{|\psi_r\rangle\}_{r\in R}$ and set $K\subset [n]$. Consider the set \mathcal{F}_K of all phase operators of $\{|\psi_r\rangle\}_{r\in R}$ supported on K. We call $\{|\psi_r\rangle\}_{r\in R}$ phase-complete with respect to K when $-I\in \langle \mathcal{F}_K\rangle$ and for any P_1,\ldots,P_l such that $-I,P_1,\ldots,P_l$ are independent generators of $\langle \mathcal{F}_K\rangle$ set $\{(f_{P_1}(r),\ldots,f_{P_l}(r)):r\in R\}=\mathbb{F}_2^l$.

The following describes which sets of stabilizer states correspond to stabilizer circuits:

Lemma A.8 (Phase completeness). A set of n-qubit stabilizer states $\{|\psi_r\rangle\}_{r\in R}$ is a set of Choi states of some stabilizer circuit C with $n_{\rm in}$ input qubits and $n_{\rm out}=n-n_{\rm in}$ output qubits if and only if $\{|\psi_r\rangle\}_{r\in R}$ is phase-complete linear family of stabilizer states with respect to set $K=[n_{\rm out}+1,n_{\rm out}+n_{\rm in}].$

Before we proceed with the proof of Lemma A.8 note that it allows us to give an alternative definition of a stabilizer instrument without the need to mention a quantum circuit: a quantum instrument is a stabilizer instrument if its Choi states are a phase-complete linear family of stabilizer states. When completing this work we became aware of an equivalent definition of a stabilizer instrument, the Definition 6 in [13]. Results of this section can be re-derived using this alternative definition.

Proof of Lemma A.8. We first show that the set of Choi states of any stabilizer circuit \mathcal{C} is a phase-complete linear family of stabiliser states. This is achieved in three steps: (A1) construct independent commuting phase operators (A2) show that image of several phase functions together is an image of an affine map, which is a coset of a linear space (A3) show phase completeness property by expressing image of the related phase functions as an image of a full row rank linear operator. Second, we show that any phase-complete linear family of stabilizer states $\{|\psi_r\rangle\}_{r\in R}$ can be associated with a general form circuit. This is also achieved in three steps: (B1) show that the set of outcomes R can be replaced by $R' = \mathbb{F}_2^{n'_r}$ for some integer n'_r , (B2) show that all $|\psi_r\rangle \simeq C|A'r'\rangle$ for $r' \in \mathbb{F}_2^{n'_r}$ for some Clifford unitary C and matrix A' (B3) use the second stage of Algorithm 6.2 to construct the general form circuit.

(A1) Theorem 4.2 and Fig. 4.3 imply that the set of Choi state of \mathcal{C} is $\{|\phi_o\rangle\}_{o\in\mathbb{F}_2^{n_O}}$, where $|\phi_o\rangle$ is a Choi state of a linear map enacted by the general form circuit upon outcome o described

⁸Coset of a vector space V is a subset $v + L \subset V$ where $v \in V$ is a vector and $L \subset V$ is a subspace of V.

in Fig. 4.3. Removing phases from the stabiliser generators in the right half of Fig. 4.3 gives us a set of $n = n_{\text{out}} + n_{\text{in}}$ independent commuting phase operators Q_1, \ldots, Q_n of $|\phi_o\rangle$:

$$RZ_{j_{\text{out}}}R^{\dagger} \otimes I_{n_{\text{in}}}, \qquad j_{\text{out}} \in [n_{\text{out}} - k]$$

$$RZ_{n_{\text{out}}-k+j}R^{\dagger} \otimes (LZ_{n_{\text{in}}-k+j}L^{\dagger})^{*}, \qquad j \in [k]$$

$$I_{n_{\text{out}}} \otimes (LZ_{j_{\text{in}}}L^{\dagger})^{*}, \qquad j_{\text{in}} \in [n_{\text{in}} - k]$$

$$RX_{n_{\text{out}}-k+j}R^{\dagger} \otimes (LX_{n_{\text{in}}-k+j}L^{\dagger})^{*}, \qquad j \in [k]$$

(A2) We start by relating a phase function to an image affine map. Every phase operator P of $\{|\phi_o\rangle\}_{o\in\mathbb{F}_2^{n_O}}$ is the product of these operators up to a sign, that is for every phase operator P there exist vector a_P and constant s_P such that:

$$P = (-1)^{s_P} Q_1^{(a_P)_1} \dots Q_n^{(a_P)_n}.$$

Phase function f_P is then given by

$$f_P = s_P + (a_P)_1(f_{Q_1}) + \dots + (a_P)_n f_{Q_n} = s_P + (a_P)^T (f_{Q_1}, \dots, f_{Q_n})$$

We introduce matrix A' to relate $(f_{Q_1}, \ldots, f_{Q_n})$ to outcome o of the general form:

$$A' = \left(\frac{\frac{A}{A_x}}{\frac{(\mathbf{0}_{n_{\text{in}} - k \times n_r} | I_{n_{\text{in}} - k})}{A_z}}\right),$$

and have $(f_{Q_1}(o), \ldots, f_{Q_n}(o)) = A'o$. For any l phase functions we have:

$$(f_{P_1}(o), \dots, f_{P_l}(o)) = (s_{P_1}, \dots, s_{P_l}) + \left(\frac{a_{P_1}^T}{\vdots a_{P_l}^T} \right) Ao,$$

which immediately implies that image of $(f_{P_1}, \ldots, f_{P_l})$ is a coset of \mathbb{F}_2^l .

(A3) We show the phase-completeness property for a convenient set of phase operators P_1, \ldots, P_l

$$I_{n_{\mathrm{out}}} \otimes (LZ_{j_{\mathrm{in}}}L^{\dagger})^*, j_{\mathrm{in}} \in [n_{\mathrm{in}} - k]$$

first, and then use an argument similar to one in (A2) to show that the phase complete property holds for any set of phase operators $-I, P'_1, \ldots, P'_l$ such that $-I, P'_1, \ldots, P'_l$ generate $\mathcal{F}_{[n_{\text{out}}+1,n]}$ (see Definition A.7). For the chosen P_1, \ldots, P_l we have

$$(f_{P_1}(o), \dots, f_{P_l}(o)) = (\mathbf{0}_{n_{\text{in}} - k \times n_r} | I_{n_{\text{in}} - k}) o,$$

and so the image is \mathbb{F}_2^l . Similarly to the argument in (A2), we have

$$(f_{P'_1}(o), \dots, f_{P'_l}(o)) = (s_{P_1}, \dots, s_{P_l}) + \hat{A}(\mathbf{0}_{(n_{\text{in}}-k)\times n_r}|I_{n_{\text{in}}-k})o, \quad \hat{A} = \begin{pmatrix} \underline{(a_{P'_1})_{[n_{\text{out}}+1,n-k]}^T} \\ \vdots \\ \underline{(a_{P'_l})_{[n_{\text{out}}+1,n-k]}^T} \end{pmatrix}$$

Matrix \hat{A} is an invertible matrix because $-I, P'_1, \ldots, P'_l$ generate $\mathcal{F}_{[n_{\text{out}}+1,n]}$, therefore matrix $\hat{A}(\mathbf{0}_{(n_{\text{in}}-k)\times n_r}|I_{n_{\text{in}}-k})$ has column rank l and the image of $(f_{P'_1}(o), \ldots, f_{P'_l}(o))$ is \mathbb{F}_2^l .

Now we show that any phase-complete linear family of stabilizer states corresponds to a general form circuit following the approach outlined above. (B1) Let Q_1, \ldots, Q_n be some independent commuting phase operators of $\{|\psi_r\rangle\}_{r\in R}$. Image of (f_{Q_1},\ldots,f_{Q_n}) is a coset v+L. We first replace Q_1,\ldots,Q_n by $(-1)^{v_1}Q_1,\ldots,(-1)^{v_n}Q_n$ so that image of the corresponding phase

functions is L. Let us now set n'_r to the rank of L and let A' be a basis matrix of L, so that $L = A' \mathbb{F}_2^{n'_r}$. We can label $|\psi\rangle_r$ by $r' = (A')^{(-1)}r$ and define relabelled set of states $\{|\phi\rangle_{r'}\}_{r' \in \mathbb{F}_2^{n'_r}}$. (B2) Let C be any Clifford unitary such that $CZ_jC^{\dagger} = Q_j$. Note that $|\phi\rangle_{r'}$ is stabilized by $(-1)^{(A'r')_j}CZ_jC^{\dagger}$ and so $|\phi\rangle_{r'} \simeq C|A'r'\rangle$. (B3) We apply the second part of Algorithm 6.2 to the set of states $\{|\phi\rangle_{r'}\}_{r' \in \mathbb{F}_2^{n'_r}}$ described by Clifford unitary C and matrix A'. We can always find matrix \tilde{A}_m in Line 5 according to Proposition A.9 (discussed below) because $\{|\phi\rangle_{r'}\}_{r' \in \mathbb{F}_2^{n'_r}}$ is phase-complete with respect to $[n_{\text{out}} + 1, n_{\text{out}} + n_{\text{in}}]$.

The following proposition is used in the proof above and is also used to justify correctness of Algorithm 6.2.

Proposition A.9 (Outcome relabelling for phase complete sets of stabilizer states). Consider $(n_{\text{out}} + n_{\text{in}})$ -qubit s set of stabilizer state $\{\tilde{C}|Ar\rangle\}_{r\in\mathbb{F}_2^{n_r}}$, where \tilde{C} has a property described by Fig. 6.2a for integer k, Clifford unitaries B, D and $n_1 = n_{\text{out}}, n_2 = n_{\text{in}}$. Suppose that the set of stabilizer states is phase-complete with respect to $[n_{\text{out}} + 1, n_{\text{out}} + n_{\text{in}}]$, then there exist invertible matrix \tilde{A} such that $(A\tilde{A})_{[n_{\text{out}}+1, n_{\text{out}}-k]} = (\mathbf{0}_{(n_{\text{in}}-k)\times n_r}|I_{n_{\text{in}}-k})$.

Proof. First note that Phase operators

$$I_{n_{\text{out}}} \otimes (LZ_j L^{\dagger})^*, j \in [n_{\text{in}} - k]$$

generate $\mathcal{F}_{[n_{\text{out}}+1,n_{\text{i}}]}$ (see Definition A.7). The image of the corresponding phase functions is $A_{[n_{\text{out}}+1,n_{\text{out}}+n_{\text{in}}-k]}r$ and is $\mathbb{F}_2^{n_{\text{in}}-k}$ according to the phase-completeness. For this reason, $A_{[n_{\text{out}}+1,n_{\text{out}}+n_{\text{in}}-k]}$ must have rank $n_{\text{in}}-k$ and so Procedure B.1 described below can be applied to $A_{[n_{\text{out}}+1,n_{\text{out}}+n_{\text{in}}-k]}$.

Linear algebra

The following is used to justify correctness of Algorithm 6.2.

Proposition A.10 (Product of split reduced echelon form matrices). Consider $n \times n$ matrix R in (n_r, n_m) -split reduced echelon form (Definition 4.1) and $m \times n$ matrix M in (n, 0)-split echelon form, then the product MR is in (n_r, n_m) -split reduced echelon form.

Proof. The result follows from two observations. First, row j of MR is equal to the linear combination of rows of R with the coefficients given by row j of M. Second, matrix B is in reduced row echelon form if and only if it consists of leading one columns and all other column are linear combinations of previous leading one columns.

First check that $(MR)_{[n_r]}^T$ is in reduced row echelon form. We derive locations of leading one columns of $(MR)_{[n_r]}^T$. For $j \in [n]$, let s_j be maximum index of a non-zero entry of first j rows of $R_{[n_r]}$. Sequence s_j is monotonically non-decreasing, because $R_{[n_r]}$ is in row reduced echelon form. Additionally, $s_{j-1}+1=s_j$ when j is a leading one column of $R_{[n_r]}^T$ and $s_{j-1}=s_j$ otherwise. Similarly, for $j \in [n]$, let l_j be maximum index of a non-zero entry of first j rows of $M_{[n_r]}$. The maximum index of a non-zero entry of row j of $(MR)_{[n_r]}$ is at most s_{l_j} because the row $(MR)_{j,[n_r]}$ is a linear combination of first l_j rows of $R_{n[r]}$.

Leading one columns of $(MR)_{[n_r]}^T$ are exactly those j' for which $s_{l_{j'-1}}+1=s_{l_{j'}}$. This is because equality $s_{l_{j'-1}}+1=s_{l_{j'}}$ is true if and only if $l_{j'-1}+1=l_{j'}$ and $s_{l_{j'}-1}+1=s_{l_{j'}}$. In other words, $l_{j'}$ and $s_{l_{j'}}$ are leading one columns of $M_{[n_r]}^T$ and $R_{[n_r]}^T$ and so $(MR)_{j'}=0^{s_{l_{j'}-1}}10^{n-s_{l_{j'}}}$. Rows j'' of $(MR)_{[n_r]}$ for which $s_{l_{j''-1}}=s_{l_{j''}}$ are linear combinations of previous leading one rows of $(MR)_{[n_r]}$.

Observation $(MR)_{j'} = 0^{s_{l_{j'}-1}} 10^{n-s_{l_{j'}}}$ implies that $(MR)_{j',[n_r+1,n_m]}$ is 0^{n_m} for j' being leading one columns of $(MR)_{[n_r]}^T$. Finally, matrix $(MR)_{[n_r+1,n_m+n_r]}^T$ is in reduced row echelon form similarly to how $(MR)_{[n_r]}^T$ is in reduced row echelon form because $(MR)_{[n_r+1,n_m+n_r]}^T = (MR_{[n_r+1,n_m+n_r]})^T$.

General form circuits

A corollary of the general circuit comparison Algorithm 7.5 is the following

Lemma A.11 (General form equivalence). Let C_1 , C_2 be two equivalent general form circuits with $n_{\rm in}$ inputs, $n_{\rm out}$ outputs and $n_r^{(1)}, n_r^{(2)}$ random bits, then the general form circuits have the same number of inner qubits k. Additionally, there exist:

- full row rank matrices F₁, F₂ with n_r⁽¹⁾, n_r⁽²⁾ columns
 an invertible (n_{in} k) × (n_{in} k) matrix A_m
 vectors Δr, Δm of sizes n_r⁽¹⁾, n_{in} k

such that the general form circuits C_1, C_2 implement the same linear map upon outcomes o_1, o_2 if and only if

$$(F_1 \oplus A_m)(o_1 + \Delta r \oplus \Delta m) = (F_2 \oplus I_{n_{in}-k})o_2.$$

B Additional algorithmic material

Here we provide a description of some procedures that we make use of.

Bit-level procedures

In Table B.1, we list procedures involving bit strings directly.

Procedure	Mathematical action	Run time	Bit-string run time
xor(a,b)	a+b	O(n)	O(1)
$\mathtt{and}(a,b)$	$a \wedge b$	O(n)	O(1)
weight(a)	$\operatorname{wt}(a)$	O(n)	O(1)
$\mathtt{set_bit}(a,c,j)$	$a_j \leftarrow c$	O(1)	O(1)
$ exttt{check_bit}(a,j)$	Is $a_j = 1$?	O(1)	O(1)
nonzero_bit(a)	j where $a_j = 1$	O(n)	O(1)
is_zero(a)	Is $a = 0 \dots 0$?	O(n)	O(1)

Table B.1: Mathematical action and run time complexities of basic bit string procedures. Note that the bit-string run time is O(1) for all. The procedure inputs are as follows: a, b are bit strings of size n. c is an individual bit and j is a bit index.

Linear algebra

The following procedure is used in Algorithm 6.2 in Line 5.

Procedure B.1 (block-reshape)

Input: $m \times n$ matrix A over \mathbb{F}_2 with rank m

Output: $n \times n$ invertible matrix R, $m \times m$ invertible matrix F such that $AR = (\mathbf{0}_{m \times (n-m)}|F)$ and R is in (n-m,m)-split reduced echelon form (Definition 4.1).

- 1: Find $m \times m$ invertible matrix F' such that $(F')^{-1}A'$ is in reduced row echelon form
- 2: Set R to $I_{n\times n}$, let $L=l_1,\ldots,l_m$ be the increasing sequence of leading one columns of F'A'
- 3: for $j \in [n]$ do
- 4: **if** column j of $((F')^{-1}A')$ does not contain leading 1 **then**
- 5: **for** $k \in [m]$ **do** $R_{n+1-l_k,n+1-j} \leftarrow ((F')^{-1}A')_{k,j}$
- 6: Permute columns of R so that columns $n+1-l_m,\ldots,n+1-l_1$ become last m columns, that is for increasing sequence j_1,\ldots,j_{n-m} of integers in $[n]\setminus L$ apply column permutation σ defined as

$$\sigma(k) = n + 1 - j_{n-m+1-k}, k \in [n-m], \ \sigma(k+m) = n + 1 - l_{m+1-k}, k \in [m]$$

- 7: $F \leftarrow \text{matrix } F' \text{ with reversed columns}$
- 8: **return** R, F

The key idea behind Procedure B.1 is to pick m linear-independent columns of A with an additional property that every other column that is linear dependent, is linear dependent only on the columns to the right from it. To illustrate the procedure, consider an example matrix A of rank m=3 with columns 1, 4, 7 being the linear independent ones:

$$\begin{pmatrix} \mathbf{k_1} & ef_1 + gh_1 & cf_1 + dh_1 & \mathbf{h_1} & bf_1 & af_1 & \mathbf{f_1} & 0 \\ \mathbf{k_2} & ef_2 + gh_2 & cf_2 + dh_2 & \mathbf{h_2} & bf_2 & af_2 & \mathbf{f_2} & 0 \\ \mathbf{k_3} & ef_3 + gh_3 & cf_3 + dh_3 & \mathbf{h_3} & bf_3 & af_3 & \mathbf{f_3} & 0 \end{pmatrix}$$

Finding such set of column is achieved by computing row-reduced echelon form in Line 1 of matrix A' equal to matrix A with reversed columns:

$$A' = F'B, \ F' = \begin{pmatrix} f_1 & h_1 & k_1 \\ f_2 & h_2 & k_2 \\ f_3 & h_3 & k_3 \end{pmatrix}, \ B = \begin{pmatrix} 0 & \mathbf{1} & a & b & \mathbf{0} & c & e & \mathbf{0} \\ & & & & \mathbf{1} & d & g & \mathbf{0} \\ & & & & & \mathbf{1} \end{pmatrix}$$

Columns with leading ones correspond to the m=3 linear independent columns of A, and the values in the other columns of B give the coefficients to express linear dependent columns using the linear independent ones. Sequence L in Line 2 is 2,5,8 in our example. Before the column permutation in Line 6, matrix R constructed by the procedure is lower-triangular and product RA consist of reversed columns of F separated by some zero columns

$$R = \begin{pmatrix} \mathbf{1} & & & & & & \\ & 1 & & & & & \\ & 0 & 1 & & & & \\ & g & d & \mathbf{1} & & & & \\ & 0 & 0 & & 1 & & & \\ & 0 & 0 & & 0 & 1 & & \\ & e & c & & b & a & \mathbf{1} & \\ & 0 & 0 & & 0 & 0 & & 1 \end{pmatrix}, AR = \begin{pmatrix} k_1 & 0 & 0 & h_1 & 0 & 0 & f_1 & 0 \\ k_2 & 0 & 0 & h_2 & 0 & 0 & f_2 & 0 \\ k_3 & 0 & 0 & h_3 & 0 & 0 & f_3 & 0 \end{pmatrix}$$

Column j of R can be interpreted as coefficients of a linear combinations of columns of A needed to obtain column j of AR. Matrix R is lower-triangular because each linear dependent column of A depends on the linear independent columns to the right of it. After the column permutation in Line 6 matrix R becomes:

and has the required shape.

Runtime of the Procedure B.1 is

$$O(nm^{\omega-1}) \tag{46}$$

dominated by reduced echelon form computation and is $O(nm^{\omega-1})$ using Algorithm 8 in [37].

Complexity of basic linear algebra operations

Matrix multiplication This is used to analyze many cases when matrix multiplications are required, for example, to derive Eq. (57) used in complexity analysis of Algorithm 5.3. Complexity of matrix multiplication of square $n \times n$ matrices over \mathbb{F}_2 is a well-studied problem. In practical implementations, such as [3], the complexity of matrix multiplication is $O(n^{\omega})$ for $\omega = \log_2 7$. Note that multiplication of matrices over \mathbb{F}_2 has been optimized taking into account the architecture of modern CPUs and is very efficient in practice, see benchmark results in [3]. We reduce the multiplication of rectangular matrices to multiplication of square matrices by subdividing rectangular matrices into square blocks. For example, complexity of multiplying $m \times n$ by $n \times n$ matrix is

$$O(n \max(m, n) \min(m, n)^{\omega - 2}) = O(n(m + n) \min(m, n)^{\omega - 2})$$
(47)

Indeed, if m > n, we multiply $\lceil m/n \rceil$ $n \times n$ blocks in $O(n \cdot m \cdot n^{\omega-2})$. If n > m, we multiply $1 \times \lceil n/m \rceil$ matrix of $n \times n$ blocks by $\lceil n/m \rceil \times \lceil n/m \rceil$ matrix of $n \times n$ blocks in $O(\lceil n/m \rceil^2 m^{\omega}) = O(n \cdot n \cdot m^{\omega-2})$. We use naive matrix multiplication for matrices of $n \times n$ blocks.

Reduced row echelon form This is a core subroutine to solve many linear algebra problems and its complexity used for complexity analysis of Procedure B.1 in Line 1, that is used in Algorithm 6.2. Additionally it is indirectly used in Procedure 6.3, Procedure 6.5. Given a matrix $m \times n$ matrix A of rank r, we can represent A = BR for invertible square matrix B and matrix R in reduced-row echelon form. Using Algorithm 8 in [37] we can find B and B in $O(mnr^{\omega-2})$. Matrix B constructed by Algorithm 8 in [37] has certain block structure up to column permutations, and so finding its inverse requires only $O(r^{\omega})$ operations. For this reason, we can find B, B^{-1} and R in

$$O(mnr^{\omega-2}) \tag{48}$$

Multiplication by a matrix in reduced and split reduced echelon forms Multiplication of an $m \times n$ matrix A by a $n \times (l_1 + l_2)$ matrix B in (l_1, l_2) -split reduced echelon form (Definition 4.1) is used in Algorithm 6.2 in Line 7. A matrix in split reduced echelon form is sparse, with first l_1 columns of weight at most $n - l_1 + 1$ and the last l_2 columns of weight one. Multiplying $m \times n$ matrix by a column of weight w has run time O(mw), so runtime of AB is

$$O(m \cdot (l_1(n - l_1) + l_2)) \tag{49}$$

When A^T is in reduced row-echelon form matrix A is equal to $(\frac{I}{A'})$ up to row permutations, for some dense matrix A'. In this case complexity of computing the product is even lower and equals to

$$O((m-n) \cdot (l_1(n-l_1) + l_2)) \tag{50}$$

Above equation is also useful for complexity analysis of Line 7 in Algorithm 6.2.

Finding a basis of the kernel of a matrix This is used to justify runtime of Procedure 6.3. Kernel of the matrix A can be computed by first decomposing matrix into product BR of a square invertible matrix B and matrix R in reduced row-echelon form. Kernel basis of R can be easily constructed as illustrated by an example below. We show how basis $b_{(2)}, b_{(4)}, b_{(5)}, b_{(7)}$ of the kernel of a 3×7 matrix R in reduced row-echelon form.

$$R = \begin{vmatrix} \mathbf{1} & a_{1,2} & \mathbf{0} & a_{1,4} & a_{1,5} & \mathbf{0} & a_{1,7} \\ \mathbf{0} & 0 & \mathbf{1} & a_{2,4} & a_{2,5} & \mathbf{0} & a_{2,7} \\ \mathbf{0} & 0 & \mathbf{0} & 0 & 0 & \mathbf{1} & a_{3,7} \end{vmatrix}$$

$$b_{(2)} = \begin{vmatrix} \mathbf{a}_{1,2} & 1 & \mathbf{0} & 0 & 0 & \mathbf{0} & \mathbf{0} \\ a_{1,4} & 0 & a_{2,4} & 1 & 0 & \mathbf{0} & \mathbf{0} \\ b_{(5)} = \begin{vmatrix} \mathbf{a}_{1,5} & 0 & a_{2,5} & 0 & 1 & \mathbf{0} & \mathbf{0} \\ a_{1,7} & 0 & a_{2,7} & 0 & 0 & a_{3,7} & 1 \end{vmatrix}$$

$$(51)$$

Kernel bases of A and R are the same, therefore for $m \times n$ matrix A of rank r, the complexity of finding kernel basis is

$$O(mnr^{\omega-2} + nr). (52)$$

This is because kernel basis matrix found in this way is has n-r columns of weight one and only has an $(n-r) \times r$ dense sub-matrix.

Completing a matrix to a full rank matrix This is used to justify runtime of Procedure 6.5 in Line 4. An $m \times n$ matrix A can be completed to a full rank matrix by decomposing matrix into product BR of a square invertible matrix B and matrix R in reduced row-echelon form. Next matrix R can be easily completed to a full-rank matrix:

$$R = \begin{vmatrix} \mathbf{1} & a_{1,2} & \mathbf{0} & a_{1,4} & a_{1,5} & \mathbf{0} & a_{1,7} \\ \mathbf{0} & 0 & \mathbf{1} & a_{2,4} & a_{2,5} & \mathbf{0} & a_{2,7} \\ \mathbf{0} & 0 & \mathbf{0} & 0 & \mathbf{0} & \mathbf{1} & a_{3,7} \end{vmatrix}$$

$$\hat{R} = \begin{vmatrix} 0 & 1 & 0 & 0 & 0 & 0 & 0 \\ 0 & 0 & 0 & 1 & 0 & 0 & 0 \\ 0 & 0 & 0 & 0 & 1 & 0 & 0 \\ 0 & 0 & 0 & 0 & 0 & 0 & 1 \end{vmatrix}$$
(53)

The full-rank completion of A is $\tilde{A}=(\frac{A}{\tilde{R}})$. The bottleneck for the completion procedure is computing row-echelon form in $O(mn\min(m,n)^{\omega-2})$ using estimate $\min(m,n)$ for rank of A and Eq. (48). Because completion matrix is 1-sparse we conclude that full-rank completion complexity is

$$O(mn\min(m,n)^{\omega-2})\tag{54}$$

Procedures for Pauli and Clifford unitary manipulation

Here we justify run time and bit-string run time for procedures in Table 3.1. We omit justification of run time of the following procedures:

- init_pauli, x_bits, z_bits, xz_phase,
- set_x_bits, set_z_bits, mult_phase,
- copy_cliff, num_qubits, image,
- right_mult_swap, tensor_prod, add_qubits, remove_qubits.

The run time and bit-string run time of disentange and preimage has been justified in Section 3.4.

Hermitian conjugate, commutator and product of Pauli unitaries

The run time and bit-string run time of is_hermitian, commutator and prod_pauli in Table 3.1 follows from three key observations below and Table B.1 of run time of bit string procedures. First, the Hermitian conjugate of a Pauli unitary can be written as:

$$P^{\dagger} = (i^{s(P)}Z^{x(P)}X^{x(P)})^{\dagger} = i^{s(P)}(-1)^{1 + \operatorname{wt}(x(P) \wedge z(P))}Z^{x(P)}X^{x(P)}$$

So checking if P is hermitian requires checking if $\operatorname{wt}(x(P) \wedge z(P)) = 0 \mod 2$. Second, the commutator of two Pauli unitaries can be written as

Third, the product of two Pauli unitaries can be written as:

$$PQ = i^{s(P)}Z^{x(P)}X^{x(P)}i^{s(Q)}Z^{x(Q)}X^{x(Q)} = i^{s(P)+s(Q)}(-1)^{\operatorname{wt}(x(P) \wedge z(Q))}Z^{z(P)+z(Q)}X^{x(P)+x(Q)} = i^{s(P)}Z^{x(Q)}X^{x(Q)} = i^{s(P)+s(Q)}(-1)^{\operatorname{wt}(x(P) \wedge z(Q))}Z^{z(P)+z(Q)}X^{x(P)+x(Q)} = i^{s(P)+s(Q)}(-1)^{\operatorname{wt}(x(P) \wedge z(Q))}Z^{x(P)+z(Q)} = i^{s(P)+s(Q)}Z^{x(Q)} = i^{s(P)+s(Q)}Z^{x($$

Initialization, product and inverse for Clifford unitaries

In this subsection we discuss run time and bit-string run time of initialization procedures, product and inverse as they are closely related.

init_cliff During the initialization we are given images and their phases. Those just get stored in M(C) in $O(n^2)$. Additionally we need to compute phases of pre-images, which can be achieved by computing the inverse of C without using the pre-image phases information. The inverse can also be computed by using matrix-matrix and matrix-vector multiplications [20]. For this reason, the run time is $O(n^{\omega})$ and bit-string run time is $O(n^2)$.

init_cliff_css Initialization of a CCS Clifford is essentially copying entries of inputs A and B into appropriate locations in M(C). The exact relation between A, B and C is described by Proposition A.2. For this reason run time and bit-string run time are $O(n^2)$.

inverse_cliff The inverse of Clifford unitary has run time and bit-string run time of $O(n^2)$ because it consists of two simple steps: rearranging of binary symplectic part of M(C) as in Eq. (13) and exchanging image phases for preimage phases. Both of the steps can be done in $O(n^2)$ in both complexity models.

prod_cliff The run time for the product of Clifford unitaries is $O(n^{\omega})$. This is because binary symplectic part of $M(C_1C_2)$ and phases of images can be found using matrix-matrix and matrix-vector multiplications [20]. The fact that computing inverses is $O(n^2)$, implies that phases of preimages can also be computed in $O(n^{\omega})$ be relating them to phases of images of $C_2^{\dagger}C_1^{\dagger}$.

The bit-string run time for the product of Clifford unitaries is $O(n^{\omega})$. This is because bitstring run time of matrix-matrix multiplication is $O(n^2)$ and bit-string run time of matrix-vector multiplication is O(n) when matrix columns or rows are stored as bit strings.

Left multiplication of Clifford unitaries left_mult_*

```
Procedure B.2 (left_mult_exp*(C, P))
Input: Clifford unitary C, Pauli operator P.
Output: C \leftarrow e^{i\pi/4P}C
 1: Let K be indices of qubits on which P is supported, k = |K|
 2: \tilde{P} = C^{\dagger}PC, \tilde{P}_x = C^{\dagger}X^{x(P)}C.
                                       \triangleright Update image phases in Clifford unitary representation M(C)
 3: for j in [n] do
                                          ▷ Below we interpret integers mod 4 as bit vectors of length 2
        if x(\tilde{P})_j = 1 then M(C)_{j,[2n+1,2n+2]} \leftarrow s(CZ_kC^{\dagger}) + 1 + s(P) + 2x(\tilde{P}_x)_j \mod 4
        if z(\tilde{P})_j = 1 then M(C)_{n+j,[2n+1,2n+2]} \leftarrow s(CX_kC^{\dagger}) + 1 + s(P) + 2z(\tilde{P}_x)_j \mod 4
                                          \triangleright Update pre-images in Clifford unitary representation M(C)
 6: for j in [k] do
                                   \triangleright Below we interpret Pauli unitaries as bit vectors of length 2n+2
         if [\![Z_{K(i)}, P]\!] = 1 then M(C)_{*,n+K(i)} \leftarrow i(C^{\dagger}Z_{K(i)}C)\tilde{P}
 7:
        if [X_{K(i)}, P] = 1 then M(C)_{*,K(i)} \leftarrow i(C^{\dagger}Z_{K(i)}C)\tilde{P}
 8:
```

In this subsection we first focus on implementing left_mult_exp*(C, P) (Procedure B.2). Left and right multiplication by any other Clifford unitary can be built using this procedure. This is because any n-qubit Clifford unitary can be written as product of O(n) exponents $e^{i\pi/4P}$ [42]. For example, $CZ = \exp(i\pi|11\rangle\langle11|) \simeq e^{-i\pi Z_1/4}e^{i\pi Z_1/4}e^{\pi Z_1Z_2/4}$ and similarly generalized Controlled-Pauli $\Lambda(P,Q) \simeq e^{-i\pi P/4}e^{i\pi Q/4}e^{\pi PQ/4}$. Procedures

- left_mult_swap
- left_mult_pauli,
- left_mult_ctrl_pauli,

can be implemented by using a constant number of calls to left_mult_exp*. Using identity $Ce^{i\pi P/4}C = e^{i\pi CPC^{\dagger}/4}C$ right multiplication my $e^{i\pi/4P}$ can be implemented using the left multiplication by Pauli exponent. In practice, more efficient implementations the reduction to left_mult_exp* (C, P) are possible and preferable. In the remainder of this section we discuss correctness of Procedure B.2, analyse its run time and bit-string run time. We conclude with the correctness proof of the procedure disentangle (Procedure 3.4).

Next we briefly discuss correctness of the above Procedure B.2. First consider how images CX_kc^{\dagger} and CZ_kC^{\dagger} change after left-multiplication by $e^{i\pi P/4}$. Using Eq. (37) and $[\![CPC^{\dagger},Q]\!] = [\![P,C^{\dagger}Q,C]\!]$ we have:

$$e^{i\pi P/4}CZ_kC^{\dagger}e^{-i\pi P/4} = (iP)^{\llbracket C^{\dagger}PC,Z_k\rrbracket}CZ_kC^{\dagger}$$

$$e^{i\pi P/4}CX_kC^{\dagger}e^{-i\pi P/4} = (iP)^{\llbracket C^{\dagger}PC,X_k\rrbracket}CX_kC^{\dagger}$$
(55)

In Line 4, condition $x(\tilde{P})_j = 1$ is equivalent to $\llbracket C^{\dagger}PC, Z_k \rrbracket = 1$. Similarly, in Line 5, condition $z(\tilde{P})_j = 1$ is equivalent to $\llbracket C^{\dagger}PC, X_k \rrbracket = 1$. We see that we update exactly those image phases that change after composing with $e^{i\pi P/4}$. The equation for updating the image phases follows from Proposition A.1 and observation that $x(\tilde{P}_x)_j = \llbracket \tilde{P}_x, Z_j \rrbracket, z(\tilde{P}_x)_j = \llbracket \tilde{P}_x, X_j \rrbracket$.

Second we consider how preimages $C^{\dagger}X_kC$ and $C^{\dagger}Z_kC$ change after left-multiplication by $e^{i\pi P/4}$. Using Eq. (37) we have:

$$C^{\dagger} e^{-i\pi P/4} Z_k e^{i\pi P/4} C = C^{\dagger} Z_k C (iC^{\dagger} PC)^{\llbracket P, Z_k \rrbracket}$$

$$C^{\dagger} e^{-i\pi P/4} X_k e^{i\pi P/4} C = C^{\dagger} X_k C (iC^{\dagger} PC)^{\llbracket P, X_k \rrbracket}$$

$$(56)$$

In Line 7, condition $x(P)_{K(j)} = 1$ is equivalent to $[\![P, Z_{K(j)}]\!] = 1$. Similarly, in Line 8, condition $z(P)_{K(j)} = 1$ is equivalent to $[\![P, X_{K(j)}]\!] = 1$. We see that we update exactly those preimages that change after composing C with $e^{i\pi P/4}$.

Next we analyze run time and bit-string run time of Procedure B.2 in terms of number of qubits n on which |C| is defined and weight |P| of P. We show that the run time is $O(n \cdot |P|)$. The run time of computing preimage of P and $X^x(P)$ is $O(n \cdot |P|)$. The run time of updating phases of images is O(|C|). The run time of updating preimages is $O(n \cdot |P|)$.

Next we show that bit-string run time of Procedure B.2 is O(|P|). Recall that bit-string run time of a product of two Pauli unitaries is O(1). For this reason, the bit-string run time of computing preimage of P and $X^x(P)$ is O(|P|). Similarly, the bit-string run time of updating preimages is O(|P|). Next lest us show that bit-string run time of updating phases of images is O(1). Instead of updating image phases in a for loop we can use bit-wise operations as follows:

- 1: $s_{\pm 1}, s_{(i)} = s(P) + 1 \mod 4$
- 2: $\Delta_{\pm 1} \leftarrow (x(\tilde{P}_x) \oplus z(\tilde{P}_x)) + s_{(i)} \cdot M(C)_{[2n], 2n+2} + (s_{\pm 1})^{2n}$ \triangleright + is bit-wise XOR
- 3: $M(C)_{[2n],2n+2} \leftarrow M(C)_{[2n],2n+2} + s_{(i)} \cdot (x(\tilde{P}) \oplus z(\tilde{P}))$
- 4: $M(C)_{[2n],2n+1} \leftarrow M(C)_{[2n],2n+1} + \Delta_{\pm 1} \wedge (x(\tilde{P}) \oplus z(\tilde{P}))$ \triangleright \wedge is bit-wise AND

The correctness of above lines follows from separately considering cases $s_{(i)} = 0$ and $s_{(i)} = 1$ and the following expression for adding two two-bit integers modulo four:

$$(a_1 \cdot 2^1 + a_0) + (b_1 \cdot 2^1 + b_0) \mod 4 = ((a_1 + b_1 + a_0 b_0) \mod 2) \cdot 2^1 + (a_0 + b_0 \mod 2).$$

Correctness of disentangle

Proposition B.3 (disentangle correctness). Procedure disentangle (Procedure 3.4) is correct.

Proof. To avoid confusion arising from the Clifford unitary C being modified throughout the algorithm, we define the static Clifford unitary C_0 as the initial Clifford unitary that is fed into the algorithm, and other static Clifford unitaries throughout. Note that $Z_jC_0|0^n\rangle=C_0|0^n\rangle$ implies $x(C_0^{\dagger}Z_jC_0)=0$. At the end of step 2, C is replaced by C_1 , where $C_1=\Lambda(C_0X_{j'}C^{\dagger},C_0Z_{j'}C^{\dagger}_0Z_j)$ C_0 SWAP_{j,j'}. To see that $C_1|0^n\rangle=C_0|0^n\rangle$, note that $C_0Z_{j'}C^{\dagger}_0Z_j$ stabilizes C_0 SWAP_{j,j'} $|0^n\rangle$ (using $x(C_0^{\dagger}Z_jC_0)=0$ and SWAP_{j,j'} $|0^n\rangle=|0^n\rangle$), and then apply Eq. (5). Moreover, we see using Eq. (6) that $C_1Z_jC_1^{\dagger}$ is now C_0 SWAP_{j,j'} Z_j SWAP_{j,j'} C_0^{\dagger} · $C_0Z_{j'}C_0^{\dagger}$ $Z_j=Z_j$ since C_0 SWAP_{j,j'} Z_j SWAP_{j,j'} C_0^{\dagger} commutes with $C_0Z_{j'}C_0^{\dagger}$ Z_j (because $x(C_0^{\dagger}Z_jC_0)=0$) but anticommutes with $C_0X_{j'}C_0^{\dagger}$. Note that $C_1Z_jC_1^{\dagger}=Z_j$ implies the jth bit of $x(C_1^{\dagger}X_jC_1)$ is one (since $C_1^{\dagger}X_jC_1$ anticommutes with $C_1^{\dagger}Z_jC_1$).

In the second part of the algorithm, there are two cases. The first case is when the jth bit of $z(C_1^{\dagger}X_jC_1)$ is zero, triggering the if condition and C is then set to $C_2 = \Lambda(C_1Z_jC_1^{\dagger}, C_1X_jC_1^{\dagger}X_j)$ C_1 . To see that $C_2|0^n\rangle = C_1|0^n\rangle$ note that $C_1Z_jC_1^{\dagger}$ stabilizes $C_1|0^n\rangle$, and make use of Eq. (5). To see that the image of Z_j is unchanged, i.e., that $C_2Z_jC_2^{\dagger}=Z_j$, apply Eq. (6) making use of the fact that the jth bit of $x(C_1^{\dagger}X_jC_1)$ is one. Moreover, by Eq. (6), image of X_j becomes $C_2X_jC_2^{\dagger}=C_1X_jC_1^{\dagger}$ $C_1X_jC_1^{\dagger}X_j=X_j$ since $C_1X_jC_1^{\dagger}$ commutes with $C_1X_jC_1^{\dagger}X_j$ (by the if condition) but anticommutes with $C_1Z_jC_1^{\dagger}$.

The second case is when the jth bit of $z(C_1^{\dagger}X_jC_1)$ is one, triggering the else condition and C is set to $C_3 = \Lambda(C_1Z_jC_1^{\dagger},X_j \ C_1 \ iZ_jX_j \ C_1^{\dagger}) \ e^{i\frac{\pi}{4}C_1Z_jC_1^{\dagger}} \ C_1$. To see that $C_3|0^n\rangle = C_1|0^n\rangle$, first note that since $C_1Z_jC_1^{\dagger}$ has $C_1|0^n\rangle$ as an eigenstate, so too does $e^{i\frac{\pi}{4}C_1Z_jC_1^{\dagger}}$, such that $e^{i\frac{\pi}{4}C_1Z_jC_1^{\dagger}}C_1|0^n\rangle = e^{i\frac{\pi}{4}}C_1|0^n\rangle$. This implies that the state $e^{i\frac{\pi}{4}C_1Z_jC_1^{\dagger}}C_1|0^n\rangle$ is stabilized by $C_1Z_jC_1^{\dagger}$, which (using Eq. (5)) tells us that $C_3|0^n\rangle = e^{i\frac{\pi}{4}}C_1|0^n\rangle$, and thus $C_3|0^n\rangle = C_1|0^n\rangle$ (up to an unimportant phase). To see that the image of Z_j is unchanged, i.e., that $C_3Z_jC_3^{\dagger}=Z_j$, one can implement a direct calculation making use of Eq. (1), Eq. (6), and that $C_1Z_jC_1^{\dagger}=Z_j$. To see that the image of X_j becomes $C_3X_jC_3^{\dagger}=X_j$, one can implement a direct calculation making use of Eq. (1), Eq. (6), and that $C_1Z_jC_1^{\dagger}=Z_j$ and that the jth bit of $z(C_1^{\dagger}X_jC_1)$ are both one.

C Bulk deallocation of qubits in stabilizer simulation algorithms

We discuss how to reduce the cost of deallocation in outcome-complete stabilizer simulation, a similar idea applies to outcome-specific stabilizer simulation. Table 5.1 shows that qubit deallocation is an expensive operation. Instead of deallocating qubits every time the deallocation is requested, we can delay deallocation to the end of the simulation algorithm. Next we describe an efficient approach to a bulk deallocation of qubits.

To deallocate many qubits in a stabilizer circuit that requires n_{max} qubits, has n_{out} output qubits and n_r random outcomes we use bipartite normal form for a family of stabilizer states described in Section 6.1. We apply the bipartite normal form Procedure 6.5 to the family of states $D|Ar\rangle$ describing the result of outcome complete simulation for bipartition of n_{max} qubits into n_{out} and $n_{\text{max}} - n_{\text{out}}$ qubits. Because the output qubits should be disentangled by the end of the simulation, the number of Bell pairs across the partition is zero. The bipartite normal form procedure finds Clifford unitaries D_1 , D_2 on n_{out} and $n_{\text{max}} - n_{\text{out}}$ qubits such that $DU_F|a\rangle \simeq (D_1 \otimes D_2)|a\rangle$ for all computational basis states $|a\rangle$, and so the family $D|Ar\rangle$ can be expressed as $(D_1 \otimes D_2)|F^{-1}Ar\rangle$. Last $n_{\text{max}} - n_{\text{out}}$ rows of $F^{-1}A$ must be zero and D_2 must map Pauli Z to products of Pauli Z operators, because the qubits being deallocated must all be in zero state. The result of outcome complete simulation is the family of states $D_1|(F^{-1}A)_{[n_{\text{out}}]}r\rangle$.

We conclude with runtime analysis of the bulk deallocation. Complexity of computing basis change matrix F, its inverse and bipartite normal form is n_{\max}^{ω} because the number of Bell pairs across partition is zero. Computing product $F^{-1}A$ is the complexity of multiplying $n_{\max} \times n_{\max}$ matrix by $n_{\max} \times n_r$ matrix over \mathbb{F}_2 and is $O(n_{\max}(n_{\max} + n_r) \min(n_{\max}, n_r)^{\omega-2})$ according to Eq. (47). The overall complexity of the algorithm is

$$O(n_{\max}^{\omega - 1}(n_r + n_{\max})). \tag{57}$$

D Pauli propagation

Algorithm D.1 (Pauli propagation)
Input:

• A stabilizer circuit \mathcal{C} with n_M outcomes and n_{out} output qubits

Output:

- A stabilizer circuit C' with n_M outcomes and n_{out} output qubits that has no conditional Pauli unitaries
- An $n_M \times n_M$ matrix M and n_M -dimensional vector v_0
- An $n_{\text{out}} \times n_M$ condition matrices A_x , A_z , n_{out} dimensional vectors v_x, v_z

such that \mathcal{C} upon outcome vector v followed by $X^{A_xv+v_x}Z^{A_zv+v_z}$ enacts the same (up to a global phase) linear map as \mathcal{C}' upon outcome vector $v'=Mv+v_0$. Circuit \mathcal{C}' is the circuit \mathcal{C} with conditional Pauli unitaries removed. Matrix M is a unit lower-triangular matrix and is the identity matrix when restricted to rows and columns corresponding to the random bit allocation operations.

```
1: C_{\text{rem}} \leftarrow C,
 2: C' \leftarrow \text{empty circuit}, n'_O \leftarrow 0
 3: Let A_x, A_z be n \times n_O matrix, v_x, v_z are n-dimensional zero vectors
 4: Let M be n'_O \times n'_O matrix, and v_0 be n'_O dimensional zero vector
 5: while C_{\text{rem}} is not empty do
         Let g be the first operation in C_{\text{rem}}, remove g from C_{\text{rem}}
                                                                                                            ▶ allocation
 7:
         if g allocates qubit j, then
             Append zero row to A_x, A_z and zero entry to v_x, v_z
 8:
             Append g to C'
 9:
         else if g deallocates qubit j then
                                                                             ▶ Assumes that the qubit is in zero
10:
             Remove row j from A_x, A_z and entry j from v_x, v_z
11:
             Append q to C'
12:
         else if g allocates a random bit then
13:
             Append zero column to A_x, A_z, M, add zero row to M, n'_O \leftarrow n'_O + 1, M_{n'_O, n'_O} \leftarrow 1
14:
             Append g to \mathcal{C}'
15:
                                                                                                             ▶ unitaries
         else if g is a unitary U then
16:
             Find A'_x, A'_z, v'_x, v'_z from X^{A'_xv+v'_x}Z^{A'_zv+v'_z} \simeq U\left(X^{A_xv+v_x}Z^{A_zv+v_z}\right)U^{\dagger} for all v
17:
             Replace A_x, A_z, v_x, v_z by A'_x, A'_z, v'_x, v'_z
18:
             Append g to \mathcal{C}'
19:
         else if g applies a Pauli unitary P if \langle c \rangle = c_0,
20:
                    where \langle c \rangle is the parity of outcomes indicated by c \in \mathbb{F}_2^{n_M}, then
21:
             A_x \leftarrow A_x + x(P)c^T, \ A_z \leftarrow A_z + z(P)c^T
22:
             v_x \leftarrow v_x + (c_0 + 1) \cdot x(P), \ v_z \leftarrow v_z + (c_0 + 1) \cdot z(P)
23:
                                                                                                       ▷ measurements
         else if q measures Pauli P then
24:
             Append row A_x^T z(P) + A_z^T x(P) to M
25:
             Append zero column to M, n'_O \leftarrow n'_O + 1, M_{n'_O, n'_O} \leftarrow 1
26:
             Append \langle x(P), v_z \rangle + \langle z(P), v_x \rangle to v_0, append g to \mathcal{C}'
27:
28: return C', A_x, A_z, v_x, v_z, M, v_0
```

E Common symplectic basis of two stabilizer groups

We show that any two stabilizer groups S and M have a common symplectic basis (Definition 9.2) by providing an efficient Algorithm E.1. Correctness of the algorithm is established by three

Algorithm E.1 (Common symplectic basis)

Input: n-qubit stabilizer groups S, M

Output: Common symplectic basis $\mathcal{B} = \langle \mathcal{Z}^{\Delta}, \mathcal{X}^{\Delta}, \mathcal{Z}^{\cap}, \mathcal{X}^{\cap}, \mathcal{Z}^{S}, \mathcal{X}^{S}, \mathcal{Z}^{M}, \mathcal{X}^{M}, \mathcal{Z}, \mathcal{X} \rangle$ of S, M, that is $S = \langle \mathcal{Z}^{\Delta} \cup \mathcal{Z}^{\cap} \cup \mathcal{Z}^{S} \rangle$, $M = \langle \mathcal{X}^{\Delta} \cup \mathcal{Z}^{\cap} \cup \mathcal{Z}^{M} \rangle$

- 1: Let $\bar{g}_1, \ldots, \bar{g}_{k_{\Lambda}}$ be independent generators of $S/(S \cap M^{\perp})$
- 2: Let $\bar{h}_1, \ldots, \bar{h}_{k_{\Delta}}$ be independent generators of $M/(M \cap S^{\perp})$
- 3: Let g_j, h_j be representatives of cosets \bar{g}_j, \bar{h}_j for $j \in [k_{\Delta}]$
- 4: Let $A_{i,j} = \llbracket h_i, g_j \rrbracket$, let $\mathcal{Z}_j^{\Delta} = g_j$, $\mathcal{X}_j^{\Delta} = \prod_{i \in [k_{\Delta}]} h_i^{A_{j,i}^{-1}}$ 5: Let \mathcal{Z}^{\cap} be independent generators of $S \cap M$
- 6: Let $\bar{e}_1, \ldots, \bar{e}_{k_S}$ be independent generators of $(S \cap M^{\perp})/(S \cap M)$
- 7: Let \mathcal{Z}_{j}^{S} be a representative of coset \bar{e}_{j} for $j \in k_{S}$

- 8: Let $\bar{f}_1, \ldots, \bar{f}_{k_M}$ be independent generators of $(M \cap S^{\perp})/(S \cap M)$ 9: Let \mathcal{Z}_j^M be a representative of coset \bar{f}_j for $j \in k_M$ 10: Find $\mathcal{X}^{\cap}, \mathcal{X}^S, \mathcal{X}^M, \mathcal{Z}, \mathcal{X}$ by completing the partially specified symplectic basis $\mathcal{Z}^{\Delta}, \mathcal{X}^{\Delta}, \mathcal{Z}^{\cap}, \mathcal{Z}^{S}, \mathcal{Z}^{M}$ to a full symplectic basis.
- 11: **return** $\langle \mathcal{Z}^{\Delta}, \mathcal{X}^{\Delta}, \mathcal{Z}^{\cap}, \mathcal{X}^{\cap}, \mathcal{Z}^{S}, \mathcal{X}^{S}, \mathcal{Z}^{M}, \mathcal{X}^{M}, \mathcal{Z}, \mathcal{X} \rangle$

key properties. First, the number of independent generators of $S/(S \cap M^{\perp})$ and $M/(M \cap S^{\perp})$ computed in Lines 1 and 2 are the same. Second, matrix A constructed in Line 4 is indeed invertible. Third, M and S are isomorphic to the direct sum of $S \cap M$ and some quotient groups as follows:

$$\begin{array}{rcl} M & \simeq & \left(M/(M\cap S^\perp)\right) \oplus \left((M\cap S^\perp)/(S\cap M)\right) \oplus S\cap M, \\ S & \simeq & \left(S/(S\cap M^\perp)\right) \oplus \left((S\cap M^\perp)/(S\cap M)\right) \oplus S\cap M, \end{array}$$

so that $S = \langle \mathcal{Z}^{\Delta} \cup \mathcal{Z}^{S} \cup \mathcal{Z}^{\cap} \rangle$ and $M = \langle \mathcal{X}^{\Delta} \cup \mathcal{Z}^{M} \cup \mathcal{Z}^{\cap} \rangle$.

The first and the second properties follow from the following proposition:

Proposition E.2 (Group's induced symplectic space). Let M and S be two stabilizer groups, then $M/(M\cap S^{\perp})$ and $S/(S\cap M^{\perp})$ are commutative groups of the same size. For \bar{g} from $M/(M\cap S^{\perp})$ and \bar{h} from $S/(S\cap M^{\perp})$ the map $[\bar{q},\bar{h}]$ is well-defined as

$$[\![\bar{g}, \bar{h}]\!] = [\![g, h]\!]$$
 for any representatives g, h of cosets \bar{g}, \bar{h} .

The map $[\bar{q}, \bar{h}]$ is non-degenerate, that is:

if
$$\bar{h} \in S/(S \cap M^{\perp})$$
 is such that $\forall \bar{g} \in M/(M \cap S^{\perp}) : [\![\bar{g}, \bar{h}]\!] = 0$, then $\bar{h} = M \cap S^{\perp}$ if $\bar{g} \in M/(M \cap S^{\perp})$ is such that $\forall \bar{h} \in S/(S \cap M^{\perp}) : [\![\bar{g}, \bar{h}]\!] = 0$, then $\bar{g} = S \cap M^{\perp}$.

Before proceeding with the proof, let us clarify how above proposition implies that matrix A constructed in Line 4 is indeed invertible. If square $k_{\Delta} \times k_{\Delta}$ matrix A were not invertible, then there would exist $\alpha_1, \ldots, \alpha_{k_{\Delta}}$ from \mathbb{F}_2 that are not all zero but yield a trivial row sum

$$\sum_{i\in[k_{\Delta}]}\alpha_iA_i=\mathbf{0}.$$

In other words, following definition of A in Line 4, for all $j \in k_{\Delta}$ we have

$$\sum_{i \in [k_{\Delta}]} \alpha_i \llbracket h_i, \mathcal{Z}_j^{\Delta} \rrbracket = \llbracket \sum_{i \in [k_{\Delta}]} \alpha_i h_i, \mathcal{Z}_j^{\Delta} \rrbracket = 0.$$

Then for $h=\sum_{i\in[k_{\Delta}]}\alpha_ih_i\notin M\cap S^{\perp}$ and for all $j\in k_{\Delta}$ we have $[\![h,\mathcal{Z}_j^{\Delta}]\!]=0$ which is a contradiction to $[\bar{q}, \bar{h}]$ being non-degenerate.

Proof of Proposition E.2. Let us first show that for \bar{g} from $M/(M \cap S^{\perp})$ and for \bar{h} from $S/(S \cap M^{\perp})$ the map $[\![\bar{g}, \bar{h}]\!]$ is well-defined. Let g and h be representatives of cosets \bar{g}, \bar{h} . Then any other representative of the same coset can be written as gr and hs for r from $M \cap S^{\perp}$ and s from $S \cap M^{\perp}$. We have:

$$[gr, hs] = [g, hs] + [r, hs] = [g, h] + [g, s] + [r, h] + [r, s]$$

Now $\llbracket g,s \rrbracket = 0$ because g is from M and s from $S \cap M^{\perp} \subset M^{\perp}$. Analogously, $\llbracket h,r \rrbracket = 0$ because $h \in S, \ r \in M \cap S^{\perp}$, and $\llbracket r,s \rrbracket = 0$ because $r \in M \cap S^{\perp} \subset M$, $s \in S \cap M^{\perp}$. We see that $\llbracket gr,hs \rrbracket = \llbracket g,h \rrbracket$.

Next we show that $M/(M\cap S^{\perp})$ and $S/(S\cap M^{\perp})$ have the same size. First note that $M/(M\cap S^{\perp})$ has zero generators if and only if $S/(S\cap M^{\perp})$ has zero generators. Indeed, $M/(M\cap S^{\perp})$ has zero generators if and only if $M\subset S^{\perp}$; $M\subset S^{\perp}$ if and only if $S\subset M^{\perp}$; $S\subset M^{\perp}$ if and only if $S/(S\cap M^{\perp})$ has zero generators.

Now we show that if $M/(M \cap S^{\perp})$ has $k \geq 1$ generators, then $S/(S \cap M^{\perp})$ has at least k generators. Suppose $\bar{g}_1, \bar{g}_2, \ldots, \bar{g}_k$ are some generators of $M/(M \cap S^{\perp})$. Let \bar{h}_1 be an element of $S/(S \cap M^{\perp})$ that anti-commutes with \bar{g}_1 . Such an \bar{h}_1 must exist because \bar{g}_1 represents a non-trivial coset of $M/(M \cap S^{\perp})$, so it is not equal to $(M \cap S^{\perp})$. Adjust generators $\bar{g}_2, \ldots, \bar{g}_k$ so they commute with \bar{h}_1 , multiplying anti-commuting generators by \bar{g}_1 . Let \bar{h}_2 be an element of $S/(S \cap M^{\perp})$ that anti-commutes with \bar{g}_2 . It must exist, because \bar{g}_2 represents a non-trivial coset of $M/(M \cap S^{\perp})$. Coset \bar{h}_2 is not equal to \bar{h}_1 , because \bar{h}_1 commutes with \bar{g}_2 and the commutator map $[\![,]\!]$ is well-defined on the cosets. We can also adjust \bar{h}_2 to commute with \bar{g}_1 , by multiplying it with by \bar{h}_1 , if necessary.

Suppose that we have constructed independent $\bar{h}_1, \ldots, \bar{h}_l$ such that $[\![\bar{h}_i, \bar{g}_j]\!] = \delta_{i,j}$ for $i = 1, \ldots, l$ and $j = 1, \ldots, k$. Let \bar{h}_{l+1} be an element of $S/(S \cap M^{\perp})$ that anti-commutes with \bar{g}_{l+1} . It must exist, because \bar{g}_{l+1} represents a non-trivial coset of $M/(M \cap S^{\perp})$. It must be independent of \bar{h}_1, \ldots, h_l , because they all commute with \bar{g}_{l+1} and so does the product of any of their subset. Finally, multiply \bar{h}_{l+1} by some of \bar{h}_1, \ldots, h_l so $[\![h_i, g_j]\!] = \delta_{i,j}$ for $i = 1, \ldots, l+1$ and $j = 1, \ldots, l+1$. Adjust $\bar{g}_{l+2}, \ldots, \bar{g}_k$ so they all commute with h_{k+1} . By induction we see that $|S/(S \cap M^{\perp})| \geq |M/(M \cap S^{\perp})|$. Using the same argument we see that the number of generators of $|M/(M \cap S^{\perp})| \geq |S/(S \cap M^{\perp})|$.

Finally we can show that $[\![\bar{h}, \bar{g}]\!]$ is non-degenerate. Let us fix \bar{h} and assume that for any \bar{g} , $[\![\bar{h}, \bar{g}]\!] = 0$. For this reason all h from \bar{h} commute with all $g \in M$ and so $\bar{h} = (M \cap S^{\perp})$. A similar argument applies to \bar{g} for which $[\![\bar{h}, \bar{g}]\!] = 0$ for all possible \bar{h} .

F Equations for common symplectic basis example

Consider groups S_d , M_d defined on 2d qubits (Fig. 9.3a). For convenience we index qubits with two indices (i, j), $i \in [2]$ and $j \in d$, with i corresponding to the row index and j corresponding to a column index j of a qubit in Fig. 9.3.

$$S_d = \langle Z_{(i,j)} Z_{(i,j+1)} : i \in [2], j \in [d-1] \rangle$$
(58)

$$M_d = \langle Z_{(1,j)} Z_{(1,j+1)} Z_{(2,j)} Z_{(2,j+1)}, X_{(1,j')} X_{(2,j')} : i \in [2], j \in [d-1], j' \in [d] \rangle$$

$$(59)$$

A common symplectic basis \mathcal{B}_d (Fig. 9.3b) for S_d , M_d is given by the following equations:

$$\mathcal{X}_{j}^{\Delta} = X_{(1,j)}X_{(2,j)}, j \in [d-1], \qquad \mathcal{Z}_{j}^{\Delta} = Z_{(1,j)}Z_{(1,d)}, j \in [d-1]
\mathcal{X}_{j}^{\cap} = \prod_{i \in [j]} X_{(2,i)}, j \in [d-1], \qquad \mathcal{Z}_{j}^{\cap} = Z_{(1,j)}Z_{(1,j+1)}Z_{(2,j)}Z_{(2,j+1)}, j \in [d-1]
\mathcal{X}^{S} = \varnothing \qquad \qquad \mathcal{Z}^{S} = \varnothing \qquad \qquad (60)
\mathcal{X}^{M} = \{Z_{1,d}\} \qquad \qquad \mathcal{Z}^{M} = \{\prod_{j \in d} X_{(1,j)}X_{(2,j)}\}
\mathcal{X} = \{\prod_{j \in d} X_{(2,j)}\} \qquad \mathcal{Z} = \{Z_{1,d}Z_{2,d}\}$$

We consider Clifford unitaries $C_{\text{in}}^{(d)}$ such that $[2d, 2, C_{\text{in}}^{(d)}]$ has stabilizer group S_d are given by the following equations, via corresponding symplectic basis \mathcal{X}^{in} , \mathcal{Z}^{in} Fig. 9.3c:

$$\mathcal{X}_{j}^{\text{in}} = \prod_{i \in [j]} X_{(1,i)}, j \in [d-1], \quad \mathcal{Z}_{j}^{\text{in}} = Z_{(1,j)} Z_{(1,j+1)}, j \in [d-1]
\mathcal{X}_{(d-1)+j}^{\text{in}} = \prod_{i \in [j]} X_{(2,i)}, j \in [d-1], \quad \mathcal{Z}_{(d-1)+j}^{\text{in}} = Z_{(2,j)} Z_{(2,j+1)}, j \in [d-1]
\mathcal{X}_{2d-1}^{\text{in}} = \prod_{i \in [d]} X_{(1,i)}, \quad \mathcal{Z}_{2d-1}^{\text{in}} = Z_{(1,d)}
\mathcal{X}_{2d}^{\text{in}} = \prod_{i \in [d]} X_{(2,i)}, \quad \mathcal{Z}_{2d}^{\text{in}} = Z_{(2,d)}$$
(61)

Clifford unitaries $C_{\text{out}}^{(d)}$ such that $[2d, 1, C_{\text{out}}^{(d)}]$ has stabilizer group M_d are given by the following equations via corresponding symplectic basis \mathcal{X}^{out} , \mathcal{Z}^{out} Fig. 9.3c:

$$\mathcal{X}_{j}^{\text{out}} = Z_{(1,j')}, j' \in [d], \qquad \mathcal{Z}_{j}^{\text{out}} = X_{(1,j)} X_{(2,j)}, j' \in [d]
\mathcal{X}_{d+j}^{\text{out}} = \prod_{i \in [j]} X_{(2,i)}, j' \in [d], \qquad \mathcal{Z}_{d+j}^{\text{out}} = Z_{(1,j)} Z_{(1,j+1)} Z_{(2,j)} Z_{(2,j+1)}, j \in [d-1]
\mathcal{Z}_{2d}^{\text{out}} = Z_{(1,d)} Z_{(2,d)}$$
(62)